DOE/SF/11563--T1

DE83 011632

FINAL TECHNICAL REPORT

Geothermal-Brine Modeling

Prediction of Mineral Solubilities in Natural Waters: The Na-K-Mg-Ca-H-Cl-SO_4-OH-HCO_3-CO_3-CO_2-H_2O System to High Ionic Strengths at 25°C.

John H. Weare
Department of Chemistry
University of California, San Diego
La Jolla, CA 92093

Los Alamos 4X21-8556U-1: support period - 10/1/80 to 12/31/81
Los Alamos 4-X29-905M-1: support period - 9/15/79 to 9/30/80

DISCLAIMER

ABSTRACT

The mineral solubility model of Harvie and Weare (1980) is extended to the eight component system, Na-K-Ca-Mg-H-Cl-SO_4-OH-HCO_3-CO_3-CO_2-H_2O at 25°C to high concentrations. The model is based on the semi-empirical equations of Pitzer (1973) and co-workers for the thermodynamics of aqueous electrolyte solutions. The model is parameterized using many of the available isopiestic, electromotive force, and solubility data available for many of the subsystems. The predictive abilities of the model are demonstrated by comparison to experimental data in systems more complex than those used in parameterization. The essential features of a chemical model for aqueous electrolyte solutions and the relationship between pH and the equilibrium properties of a solution are discussed.

I. INTRODUCTION

Geochemical models based on equilibrium thermodynamics have been widely used to interpret field data and to provide theoretical descriptions for the origin and evolution of natural systems. Early applications of this approach include the work of Van't Hoff (1912) and co-workers who analyzed with considerable success the German Zechstein marine evaporites in terms of the theoretical mineral succession resulting from the evaporation of seawater. Methods similar to that of Van't Hoff were introduced by Bowen (1928) to study magma differentiation. Since this work there have been many similar applications utilizing phase diagrams to study the evolution of chemical systems. More recently, theoretical models have been based on numerical solutions to the mass action equations defining chemical equilibrium. Garrels and Thompson (1962) introduced general equilibrium models to analyze rock-water environments. Their approach has been adopted by many workers and has been successfully applied to a broad range of geochemical systems. The most comprehensive effort to model equilibrium properties has been that of Helgeson (1978) and co-workers. Other aqueous solution models for a large number of components have been developed. These models have been described and compared in a recent review (Nordstrom et al. (1979), Kerrisk (1981)). Because of the inherently complicated nature of concentrated aqueous solutions, these models are limited in their application primarily to the dilute solution range ($I<.1$). Such limitations have been discussed earlier (Harvie and Weare (1980), Kerrisk (1981)).

Recently Harvie and Weare (1980) (cited hereafter as HW) developed a chemical equilibrium model for calculating mineral solubilities in the $Na-K-Mg-Ca-Cl-SO_4-H_2O$ system at 25°C. This model, which was based on the Pitzer (1973) equations for aqueous electrolyte solutions, is accurate to high ionic strengths (20m). We have applied this model to several problems in marine evaporite geochemistry. (Harvie et al. (1980); Eugster et al. (1980)). However, since this model did not include carbonate species, its application was limited.

In this article, we extend the HW model to include the carbonate system and acid-base equilibria. This generalized model accurately predicts mineral solubilities in the $Na-K-Mg-Ca-H-Cl-SO_4-OH-HCO_3-CO_3-CO_2-H_2O$ system at 25°C to high concentration and variable CO_2 pressure. This model can be used in the study of geochemical processes which are influenced by mineral precipitation or dissolution (e.g. evaporation, brine mixing, fluid infiltration through reacting media). Applications of the mineral solubility model can now be extended to complex geochemical systems ranging from the high carbonate concentrations of many continental evaporites to the low carbonate concentrations of seawater.

In section II, we define the phenomenological equations used for mineral solubility prediction, and discuss several extensions to the equations used by HW. In section V, we describe the parameterization of the model. In this section, model calculations are compared to experimental data in numerous systems including seawater. The prediction of data not utilized in the parameterization suggests that mineral solubilities can be calculated to within 10% of the experimental results in concentrated multicomponent systems.

For some systems where a large amount of experimental data is available (e.g. gypsum) solubility predictions are more accurate.

In section III and IV, details related to the construction of models for concentrated aqueous solutions are discussed. When necessary, ion complex species are included (e.g. HCO_3^-, HSO_4^-) within the virial expansion model to describe the observed solution behavior. Guidelines for incorporating these species are discussed in section III. In section IV, the approximations in calculating the pH are assessed, and the method for utilizing pH data in the parameterization is discussed.

II. PHENOMENOLOGICAL EQUATIONS

The theory of calculating multiphase equilibria at fixed temperature and pressure is based on the Gibbs free energy minimization principle (Callen (1960)). The solution to the following minimization problem is required.

$$\text{Minimize} \qquad G = \sum_{i=1}^{N} n_i \mu_i \quad . \tag{1a}$$

$$\text{subject to} \qquad \sum_{i=1}^{N} n_i c_{ij} = b_j \qquad j = 1, M+P_E \tag{1b}$$

$$n_i \geq 0 \qquad i = 1, N$$

In Eq. (1), G is the Gibbs free energy for the system; n_i is the number of moles of species i; μ_i is the chemical potential for species i; b_j is the number of moles of component j; c_{ij} are the coefficients in the linear mass and charge balance equations; N is the total number of species; P_E is the number of possible electrolyte aqueous and solid solution phases; and M is the total number of components. All the variables in Eq. (1) are adequately defined except the chemical potentials, which depend upon the macroscopic chemical properties of the system. Since it is currently impossible to calculate these properties ab initio, a phenomenological description of these functions must be provided.

It is conventional to define the activities of the species, a_i, in electrolyte solutions by the following equation:

$$\frac{\partial G}{\partial n_i} = \mu_i = \mu_i^o + RT \ln a_i \quad , \tag{2a}$$

where μ_i^o is the standard chemical potential for species i . The

activity and osmotic coefficients are defined by

$$\ell n\ a_i = \ell n\ \gamma_i m_i \tag{2b}$$

for each solute species i and,

$$\ell n\ a_{H_2O} = -\frac{W}{1000}\left\{\sum_i m_i\right\}\phi \tag{2c}$$

for the solvent. γ_i and m_i are the activity coefficient and molality of the solute species. The osmotic coefficient, ϕ, is related to the activity of the solvent by Eq. (2c) where W is the molecular weight of water (18.016). (The sum over i in Eq. (2c) represents the sum over all solutes: cations, anions and neutrals.)

The chemical potentials for pure phases, such as minerals, are constants at fixed temperature and pressure. For gases, the fugacity of a gas phase species, f_i, is defined by the equation,

$$\frac{\mu_i}{RT} = \frac{\mu_i^0}{RT} + \ell n\ f_i \tag{2d}$$

For many gases below one atm., the fugacity nearly equals the partial pressure, P_i.

The remaining variables lacking explicit definition in the theory are the excess functions, γ_i and $(\phi-1)$. We use the semiempirical equations of Pitzer (1973) and co-workers to model these functions. These functions have been rewritten in Eqs. (3), and resemble those of HW except for the addition of terms for neutral species. The neutral species terms include new parameters, λ , which account for the interactions between neutral species and ionic species in the solution (see Pitzer and Silvester (1976)). In the carbonate system, the inclusion of neutral species (e.g. $CO_2(aq)$) is

required to describe observed solution behavior.

$$\sum_i m_i\,(\phi-1) = 2\left(-A^{\phi} I^{3/2}/(1+1.2I^{1/2}) + \sum_{c=1}^{N_c}\sum_{a=1}^{N_a} m_c m_a (B^{\phi}_{ca} + ZC_{ca}) + \sum_{c=1}^{N_c-1}\sum_{c'=c+1}^{N_c} m_c m_{c'} (\Phi^{\phi}_{cc'} + \sum_{a=1}^{N_a} m_a \psi_{cc'a}) + \sum_{a=1}^{N_a-1}\sum_{a'=a+1}^{N_a} m_a m_{a'} (\Phi^{\phi}_{aa'} + \sum_{c=1}^{N_c} m_c \psi_{aa'c}) + \sum_{n=1}^{N_n}\sum_{a=1}^{N_a} m_n m_a \lambda_{na} + \sum_{n=1}^{N_n}\sum_{c=1}^{N_c} m_n m_c \lambda_{nc}\right) \qquad (3a)$$

$$\ln \gamma_M = z_M^2 F + \sum_{a=1}^{N_a} m_a (2B_{Ma} + ZC_{Ma}) + \sum_{c=1}^{N_c} m_c (2\phi_{Mc} + \sum_{a=1}^{N_a} m_a \psi_{Mca}) + \sum_{a=1}^{N_a-1}\sum_{a'=a+1}^{N_a} m_a m_{a'} \psi_{aa'M} + |z_M| \sum_{c=1}^{N_c}\sum_{a=1}^{N_a} m_c m_a C_{ca} + \sum_{n=1}^{N_n} m_n (2\lambda_{nM}) \qquad (3b)$$

$$\ln \gamma_X = z_X^2 F + \sum_{c=1}^{N_c} m_c (2B_{cX} + ZC_{cX}) + \sum_{a=1}^{N_a} m_a (2\Phi_{Xa} + \sum_{c=1}^{N_c} m_c \psi_{Xac}) + \sum_{c=1}^{N_c-1}\sum_{c'=c+1}^{N_c} m_c m_{c'} \psi_{cc'X} + |z_X| \sum_{c=1}^{N_c}\sum_{a=1}^{N_a} m_c m_a C_{ca} + \sum_{n=1}^{N_n} m_n (2\lambda_{nX}) \qquad (3c)$$

$$\ell n\ \gamma_N = \sum_{c=1}^{N_c} m_c(2\lambda_{Nc}) + \sum_{a=1}^{N_a} m_a(2\lambda_{Na}) \qquad (3d)$$

In Eqs. (3) m_c and z_c are the molality and charge of cation c. N_c is the total number of cations. Similar definitions apply for anions, a, and neutrals, n. The subscripts M, X and N refer to cations, anions, and neutrals, respectively. For use in Eqs. (3), the following terms are defined.

$$F = -A^{\phi}\left(\frac{I^{\frac{1}{2}}}{1 + 1.2I^{\frac{1}{2}}} + \frac{2}{1.2}\ell n(1 + 1.2I^{\frac{1}{2}})\right) + \sum_{c=1}^{N_c}\sum_{a=1}^{N_a} m_c m_a B'_{ca}$$
$$+ \sum_{c=1}^{N_c-1}\sum_{c'=c+1}^{N_c} m_c m_{c'} \Phi'_{cc'} + \sum_{a=1}^{N_a-1}\sum_{a'=a+1}^{N_a} m_a m_{a'} \Phi'_{aa'} \quad , \qquad (4a)$$

$$C_{MX} = C^{\phi}_{MX}/2|z_M z_X|^{\frac{1}{2}} \quad , \qquad \text{and} \qquad (4b)$$

$$Z = \sum_i |z_i| m_i \quad . \qquad (4c)$$

A^{ϕ} is one third the Debye-Hückel limiting slope and equal to .392 at 25°C.

Eqs. (3b) and (3c) are ion activity coefficients which have been defined by convention. In general, the thermodynamic properties of a system do not depend upon the value of any single ion activity (Guggenheim (1929, 1930a)). Consequently, single ion activity cannot be measured, and Eqs. (3)should not be interpreted as having special physical significance. As

written, Eqs. (3b) and (3c) are symmetric for anions and cations, and satisfy Maxwell relationships among all the species in solution. When these equations are used to calculate mean activity coefficients, or any linear combination, $\sum \nu_i \ln a_i$, for which $\sum \nu_i z_i = 0$, solubilities, they are equivalent to the equations given by Pitzer and co-workers.

The second virial coefficients, B, in Eqs. (3) are given the following ionic strength dependence. (See Pitzer (1973)).

$$B^{\phi}_{MX} = \beta^{(0)}_{MX} + \beta^{(1)}_{MX}\, e^{-\alpha_{MX}\sqrt{I}} + \beta^{(2)}_{MX}\, e^{-12\sqrt{I}} \tag{5a}$$

$$B_{MX} = \beta^{(0)}_{MX} + \beta^{(1)}_{MX}\, g(\alpha_{MX}\sqrt{I}) + \beta^{(2)}_{MX}\, g(12\sqrt{I}) \tag{5b}$$

$$B'_{MX} = \beta^{(1)}_{MX}\, g'(\alpha_{MX}\sqrt{I})/I + \beta^{(2)}_{MX}\, g'(12\sqrt{I})/I \quad . \tag{5c}$$

The functions, g and g', are defined by the equations,

$$g(x) = 2(1-(1+x)e^{-x})/x^2 \tag{5d}$$

$$g'(x) = -2(1-(1+x+\frac{x^2}{2})e^{-x})/x^2 \tag{5e}$$

with $x = \alpha_{MX}\sqrt{I}$ or $12\sqrt{I}$. When either cation M or anion X is univalent $\alpha_{MX} = 2.0$. For 2-2 or higher valence pairs $\alpha_{MX} = 1.4$. In most cases $\beta^{(2)}$ equals zero for univalent type pairs. For 2-2 electrolytes a non-zero $\beta^{(2)}$ is more common. The addition of a $\beta^{(2)}$ term for univalent electrolytes represents a minor modification of the original Pitzer approach. This term has primarily been utilized to describe small negative deviations from the limiting law which are observed for certain

pairs of ions. A more detailed discussion is given in Section III.

The second virial coefficients, Φ, which depend on ionic strength, are given the following form (see Pitzer (1975)).

$$\Phi^{\phi}_{ij} = \Theta_{ij} + {}^{E}\Theta_{ij}(I) + I\,{}^{E}\Theta'_{ij}(I) \tag{6a}$$

$$\Phi_{ij} = \Theta_{ij} + {}^{E}\Theta_{ij}(I) \tag{6b}$$

$$\Phi'_{ij} = {}^{E}\Theta'_{ij}(I) \tag{6c}$$

The functions, ${}^{E}\Theta_{ij}(I)$ and ${}^{E}\Theta'_{ij}(I)$ are functions only of ionic strength and the electrolyte pair type. Integrals defining these terms are given by Pitzer (1975) and are summarized in the Appendix of HW. The interested reader is referred to Appendix B of this paper for a useful numerical method for calculating these functions. The constant, θ_{ij}, is a parameter of the model.

The second virial coefficients, λ_{ni}, representing the interactions between ions and neutral species are assumed to be constant. The form of Eqs. (3) for neutral species follows very closely the treatment of Pitzer and Silvester (1976). We refer the reader to this article for details concerning the derivation of these equations.

The third virial coefficients, C^{ϕ}_{MX} and ψ_{ijk}, are also assumed to be independent of ionic strength. C^{ϕ}_{MX} is a single electrolyte parameter which is related to C_{MX} in Eqs. (3) by Eq. (4b). ψ_{ijk} are mixed electrolyte parameters which are defined when the indices i, j, and k do not all correspond to ions of the same sign. By convention, the first two subscripts are chosen as the like charged ions and the last subscript is

chosen as the oppositely charged ion.

The complete set of parameters defining the model for the nonideal behavior of electrolyte solutions are $\beta^{(0)}_{MX}$, $\beta^{(1)}_{MX}$, $\beta^{(2)}_{MX}$ and C^{ϕ}_{MX} for each cation-anion pair, MX; θ_{ij} for each cation-cation and anion-anion pair; ψ_{ijk} for each cation-cation-anion and anion-anion-cation triplet; and λ_{ni} for ion-neutral pairs. Given a set of mole numbers which satisfy charge balance (Eq. (1b)), the molalities and, consequently, the functions I, Z, g, g', $^{E}\theta$, and $^{E}\theta'$ can be calculated. The functions $B^{\phi}_{MX}(I)$, $B_{MX}(I)$, $B'_{MX}(I)$, $\phi^{\phi}_{ij}(I)$, $\Phi_{ij}(I)$, $\Phi'_{ij}(I)$ and then F may be calculated using their defining equations. All of these numbers may be substituted into Eqs. (3) to obtain the activity and osmotic coefficients. Finally, the chemical potentials for each of the species are calculated using Eqs. (2), and the parameters, μ^{0}_{i}/RT. Equilibrium conditions are defined when the assumed set of n_i, minimizes the free energy, Eqs. (1). Mathematical procedures for adjusting the values for the n_i so that the free energy is minimized are discussed elsewhere (HW). The parameters which completely define the model for the Na-K-Mg-Ca-H-Cl-SO_4-HCO_3-CO_3-OH-CO_2-H_2O system are given in Table 1, 2, 3 and 4. The process of determining these parameters is discussed in some detail in section V. As written in Eqs. (5), the phenomena associated with ion pairing is often described via the $\beta^{(2)}$ contribution. When strong complexing is evident in the data, ion complex reactions are included explicitly in the model. This is discussed in detail in the next section. When an ion complex species is assumed, the activity coefficient for this species is also given by Eqs. (3).

III. THE PHENOMENOLOGICAL DESCRIPTION OF AQUEOUS ELECTROLYTE SOLUTIONS - ION ASSOCIATION AND IONIC STRENGTH DEPENDENT VIRIAL COEFFICIENTS.

A specific interaction model based on a virial expansion with ionic strength dependent virial coefficients correctly represent the thermodynamic behavior of many mixed electrolyte solutions to high concentration. With this type of model the explicit definition of ion complex species is not normally required. However, the observed concentration dependence of solution properties for certain electrolytes which exhibit strong attractive interactions can only be described with the use of ion complex species (e.g. HCO_3^-). The dilute solution behavior may indicate when complex species are required in a model. We believe that a virial expansion model which includes strongly bound ion complex species is both convenient and sufficiently general to accurately describe the observed behavior of most multicomponent electrolyte solutions to high concentration.

Many aqueous solution models have relied exclusively on ion pairing to account for the thermodynamic behavior resulting from the specific interactions among the dissolved ions in solution. In such models ion complexes, such as $NaSO_4^-$ or $NaHCO_3$, are defined explicitly and the component activities are calculated from the activity coefficients and the equilibrium distributions of mass among the various species. Characteristically, the activity coefficients for all solute species are defined to be universal functions of ionic strength, and therefore, do not depend explicitly on the relative concentrations of the various species in solution. The dependence of the component activities on the solute composition is described totally in terms of the association equilibria and the resulting decrease in the apparent ionic strength. While this model can be accurate in dilute solutions, or over a limited solute concentration range, it cannot be extended to concentrated

electrolyte solutions of arbitrary composition. The failure of this ion pairing model stems from the use of activity coefficients which depend only on ionic strength. It is an experimental fact that above the dilute range, the activity coefficients depend on the relative concentrations of the major solutes present in solution. The upper two curves in Fig. 1 illustrate that the mean activity coefficient for HCl, $\gamma^{\pm}_{HCl}$, depends strongly on whether the major solute is HCl or KCl (the $\gamma^{\pm 0}_{HCl}$ or $\gamma^{\pm tr}_{HCl}$ curve). Similar plots of $\gamma^{\pm}_{HCl}$ measured in other electrolyte solutions (see Harned and Owen (1958) Fig. 14-22) also reveal this compositional dependence. Under the reasonable assumption that HCl, KCl, NaCl, etc, are highly dissociated in solution, a model activity coefficient for HCl which depends only on ionic strength cannot explain this behavior. (See Harvie (1981) for details concerning the significant problems in fitting the data in Fig. 1 when HCl or KCl are assumed to be strongly associating electrolytes.)

Advances in electrolyte solution theory have suggested new phenomenological approaches which emphasize an excess free energy virial expansion with ionic strength dependent virial coefficients. This form of expansion is obtained from the statistical mechanical treatment of electrolyte solutions given by Mayer (1950), and is incorporated into the semi-empirical approach of Pitzer (1973), described in Section II. The success of this approach is illustrated in the following simplified example related to Fig. 1. Neglecting typically less important terms proportional to Φ_{HK}, C_{HCl}, C_{KCl} and ψ_{HKCl}, Eqs. (3) for $\gamma^{\pm}_{HCl}$ and $\gamma^{\pm}_{KCl}$ are simplified to give

$$\ln \gamma^{\pm}_{HCl} = \ln \gamma_{DH}(I) + B_{HCl}(I)m_H + B_{KCl}(I)m_K + B_{HCl}(I)m_{Cl} \quad (7a)$$

$$\ln \gamma^{\pm}_{KCl} = \ln \gamma_{DH}(I) + B_{HCl}(I)m_H + B_{KCl}(I)m_K + B_{KCl}(I)m_{Cl}. \quad (7b)$$

$\ell n\ \gamma_{DH}$ represents an extended Debye-Hückel function common to all ions (i.e., Eq. (4a) when terms proportional to B' and Φ' are also neglected). B_{HCl} and B_{KCl} are the ionic strength dependent second virial coefficients. In a HCl-H_2O solution all terms in Eq. (7a) reflect the HCl interaction. However, in a KCl-H_2O solution with trace amounts of HCl, the HCl and KCl interaction terms are weighted equally. In the KCl solutions, solvated hydrogen ions are surrounded by solvated chlorine ions, while the solvated chlorine ions are surrounded by solvated potassium ions.

The ionic strength dependent interaction functions, B_{HCl} and B_{KCl}, may be evaluated from the data in the single electrolyte solutions, HCl-H_2O and KCl-H_2O. The following formulae,which are obtained from Eqs. (7), apply to these single electrolyte solutions:

$$B_{HCl}(I) = \frac{\ell n\ \gamma_{HCl}^{\pm 0}(I) - \ell n\ \gamma_{DH}(I)}{2I} \qquad (8a)$$

$$B_{KCl}(I) = \frac{\ell n\ \gamma_{KCl}^{\pm 0}(I) - \ell n\ \gamma_{DH}(I)}{2I} \qquad (8b)$$

The superscript zero denotes the experimental mean activity coefficients in single electrolyte solutions (e.g. HCl-H_2O or KCl-H_2O). Since no ion association is assumed, I equals the total concentration of the electrolytes in the respective solutions. Eqs. (8) define the B's at given values of the solution ionic strength. The B's are assumed independent of solution compositions and therefore are the same in all solutions of the same ionic strength. Substituting Eqs. (8) for B_{HCl} and B_{KCl} in Eq. (7a), the expression for the trace activity coefficient of HCl in a KCl-H_2O solution is,

$$\ell n\ \gamma_{HCl}^{\pm tr} = \frac{\ell n\ \gamma_{HCl}^{\pm 0}(I) + \ell n\ \gamma_{KCl}^{\pm 0}(I)}{2} \quad , \qquad (9)$$

where the ionic strength in this example equals the molality of KCl.

Eq. (9) gives a relationship between the independently observable values of $\gamma^{\pm tr}_{HCl}$, $\gamma^{\pm 0}_{HCl}$, and $\gamma^{\pm 0}_{KCl}$ (at the same ionic strength) which is in good agreement with the experimental data (Fig. (1), dashed line).

In this article, our use of ion complex species is dictated by their importance in representing the experimentally determined thermodynamic properties. The virial expansion approach accurately represents the compositional dependence of the thermodynamic properties in most multicomponent electrolyte solutions to high ionic strengths. When an accurate description of the data is possible without the addition of ion complex species, this model is preferred due to its computational simplicity. The complete dissociation description appears possible, when the dilute solution activity coefficients are moderately less than or exceed those given by the limiting law in dilute solutions. However, for certain strongly associating or even covalently bound pairs of ions (e.g., H and SO_4 or H and CO_3), the activity coefficients in dilute solutions are significantly smaller than those predicted by the limiting law assuming complete dissociation (i.e., $\ell n\, \gamma^{\pm} << -|z^+z^-|A\sqrt{I}$). In such cases, the observed solution behavior cannot be conveniently represented by Eqs. (3) unless ion complex species are assumed in the model (e.g., HSO_4^- and HCO_3^-). Even in these cases, it should be emphasized, the virial expansion activity coefficients are necessary for a correct representation of the thermodynamic properties at high concentration.

A hypothetical system, A^{+2}-B^--C^+-D^--H_2O, was selected for investigating the different thermodynamic behavior predicted using a virial expansion model with or without an AB^+ ion complex. Model solutions were selected evenly spaced between solutions rich in A to solutions rich in B. The salt, CD, was added to many test solutions to increase the ionic strength without

increasing the A or B concentrations. The AB_2 activity was calculated in each of test solutions using the model with the ion complex. The activities at all points were then used as data to be fit by adjusting parameters in Eq. (3) without the ion complex. A parameter in these calculations is the dissociation constant, K_d, for the ion complex. As K_d is increased the agreement between the two models improves. A critical value for K_d may be defined. For any K_d above this value the thermodynamic behavior predicted by the model with the ion complex can be fit to within some specified tolerance by the model without the ion pair. This feature is illustrated for dilute single electrolyte solutions in Fig. 2. For $K_d \geq .05$, it is always possible to fit the thermodynamic properties given by the model with the ion complex (solid lines) using Eqs. (3) $\beta^{(0)}_{AB} = \beta^{(1)}_{AB} = C^{\phi}_{AB} = 0$. For K_d somewhat below this value, the two models differ significantly, regardless of the parameter value of $\beta^{(2)}_{AB}$ chosen in Eq. (3). The critical value for K_d depends on the activity coefficient expression used. When a typical extended Debye-Hückel activity coefficient (fit to $\gamma^{\pm}_{MgCl_2}$),

$$\log \gamma_i = \frac{-z_i^2 \, A\sqrt{I}}{1+1.85\sqrt{I}} \quad , \tag{10}$$

is used to evaluate K_d from experimental data in dilute solutions, the critical value of $K_d = .05$ appears to be reliable for 2-1 electrolytes. (A similar analysis is possible for 2-2 electrolytes. Comparison of the results of Pitzer and Mayorga (1974) to that of Pitzer (1972) suggests the critical K_d value is less than .002.

Our experience in parameterizing the various subsystems of the complete model (Section V) supports the use of the ion pair model when large negative deviations from the limiting law behavior are observed. In

these cases, the dilute solution properties appear to be better represented by the ion complex form and the additional flexibility provided by the virial expansion of the ionic complex activity coefficients is generally required to fit the high concentration behavior. For example, the data in the single electrolyte system, H_2SO_4-H_2O, cannot be accurately represented using Eqs. (3) without an HSO_4^- complex. K_d for this species is about .01. The data in mixed electrolyte solutions containing H_2SO_4 can also not be fit accurately without the use of this complex. In contrast to the H_2SO_4-H_2O system, the model for $Ca(OH)_2$ does not require a $CaOH^+$ ion pair. The activity coefficients for $Ca(OH)_2$ calculated with Eqs. (3) deviate by less than 2% from the $K_d = .05$ curve depicted in Fig. 2. These calculated activity coefficients for $Ca(OH)_2$ are in good agreement with precise emf data in dilute $Ca(OH)_2$-$CaCl_2$-H_2O and $Ca(OH)_2$-KCl-H_2O solutions. Moreover, Portlandite solubilities in various mixed electrolyte solutions are accurately represented by the model (Fig. 11). The $Ca(OH)_2$ model exhibits good predictability in mixed electrolyte solutions to high ionic strengths without the $CaOH^+$ species.

In very dilute solutions, where solvated ions can be treated as point charges, electrolyte solution theory indicates that the solution activity coefficients are functions only of ionic strength. However, when the short-range part of the interaction potentials due to the finite size of the solvated ions is important this simple concentration dependence can not be expected and is not observed. In Fig. 1, for example a comparison of $\gamma_{HCl}^{\pm o}$ and $\gamma_{KCl}^{\pm o}$ in their respective HCl-H_2O and KCl-H_2O solutions of the same ionic strength provides a measure of the difference in the interaction potentials. When these values do not agree, $\gamma_{HCl}^{\pm}$ will also differ in the

two solutions. Since the activity coefficients in these two systems both exceed the limiting law behavior expected for point charges ($\ell n \gamma = -A\sqrt{I}$), the net contribution due to the short-range interaction is repulsive. The description of the variation of $\gamma^{\pm}_{HCl}$ due to different repulsive interactions in terms of ion association phenomenology seems unwarranted. For certain systems, exhibiting large negative deviations from the limiting law behavior, attractive forces exceeding those associated with the coulombic interactions can be expected. In parameterizing the model in Section V, we have first evaluated virial coefficients assuming no complex species. When, by this analysis, the virial coefficient, $B_{MX}(I)$, was found to be large and negative, an ion complex model was defined. We believe there to be a strong correlation between negative virial coefficients and the formation of ion complex species.

IV. THERMODYNAMIC INTERPRETATION OF pH

pH data constitute the only laboratory cell measurements which we have found for a few aqueous electrolyte systems. pH is one of the most common chemical measurements made in the field. It may also be the only practical cell measurement in some natural waters due to experimental difficulties (e.g. non-specificity of electrodes). Therefore, it is of interest for parameterization and for comparison to field data that a method relating pH to the thermodynamic properties of a solution be defined if possible.

The pH is a semi-quantitative indicator of the acid-base equilibrium properties of aqueous solutions. However, since the emf of a cell with a liquid junction depends on the irreversible as well as the reversible properties of the system, any interpretation of pH in terms of purely reversible (equilibrium) properties is approximate. In this section we attempt to quantitatively assess the approximations involved in equating the operational definition of pH with an equilibrium property of the system.

Consider the following cell which may be used in a pH measurement:

$$\text{Pt, } H_2 \,|\, \text{soln X} \,||\, \text{KCl(sat)} \,|\, Hg_2Cl_2, \text{Hg, Pt} \quad . \tag{A}$$

The cell potential, E, may be calculated by the equation (see Appendix A):

$$E = E_o - \frac{RT}{F} \ln a_H(X) - E_{LJ}(X) \quad . \tag{11}$$

E_o is independent of the composition of solution X and is a constant

for fixed hydrogen fugacity. $E_{LJ}(X)$ is the liquid junction potential between the KCl-saturated solution and the unknown solution, X. Since absolute single ion activities cannot be measured, a_H is a conventionally defined hydrogen ion activity in solution X. It is useful to define conventional single ion activities in terms of the measurable mean activities. Such a definition requires that one reference ion activity or ion activity coefficient is specified arbitrarily. The observable emf cannot depend upon the convention used to define the ion activities. However, each of the component terms in Eq. (11) is a function of this definition. Therefore, a different choice of convention will alter the relative magnitudes of E_o E_{LJ} and the term involving a_H, while the sum of all three terms is invarient. (Appendix A).

Operationally, the pH of solution X is defined by the equation (Bates (1973)):

$$pH(X) = pH(S) + \frac{(E_X - E_S)}{RT(\ell n\ 10)/F} \quad . \tag{12}$$

E_X and E_S are the measured emf values of the cell of type A with unknown solution X or with standard solution S, respectively. The pH, pH(s), of a standard containing chloride, can be defined in terms of a measurable mean activity, as

$$pH(S) \equiv - \log_{10} a_H(S) = - \log_{10} \left(\frac{a_{HCl}}{\gamma_{Cl}\ m_{Cl}} \right) \quad . \tag{13}$$

a_{HCl} is the mean activity for hydrochloric acid in solution S determined using a reversible cell (e.g. a cell without a liquid junction). γ_{Cl} is

a specified value for a conventional chloride ion activity coefficient in solution S. The following conventions defining chloride ion activity in a solution of a known ionic strength will be discussed in this and the next section:

$$\ln \gamma_{Cl} = \ln \gamma^{\pm 0}_{HCl}(I) \qquad \text{Hydrochloric acid convention} \qquad (14a)$$

$$\ln \gamma_{Cl} = \ln \gamma^{\pm 0}_{NaCl}(I) \qquad \text{Sodium chloride convention} \qquad (14b)$$

$$\ln \gamma_{Cl} = \ln \gamma^{\pm 0}_{KCl}(I) \qquad \text{Extended MacInnes convention} \qquad (14c)$$

$$\ln \gamma_{Cl} = -A\sqrt{I}/(1+1.5\sqrt{I}) \qquad \text{Extended Battes-Guggenheim convention} \qquad (14d)$$

For the extended MacInnes convention, $\gamma^{\pm 0}_{KCl}$ is the mean activity coefficient for KCl in a KCl-H_2O solution at the same ionic strength as the electrolyte solution in question. Similar definitions are used for the sodium-chloride and hydrochloric acid conventions. The Bates and Guggenheim (1960) convention has been utilized by Bates and co-workers in defining (by interpolation and at low I) the pH of N.B.S. standard reference solutions (Bates (1973)). In Eqs. (14d) A is the Debye-Hückel limiting slope.

In order to relate pH(X) to the thermodynamic properties of solution X, some assumption regarding the difference in the liquid junction potentials of the cells with solution X and S must be made. Substituting Eq. (11) for the cell potentials of Eq. (12), the following equation can be derived.

$$pH(X) = -\log_{10} a_H(X) - \frac{\Delta E_{LJ}(X,S)}{RT(\ln 10)/F} = -\log_{10} a_H(X) - \Delta pH \quad . \qquad (15)$$

ΔE_{LJ} represents the difference in the liquid junction potentials between a cell with solution X and a cell with solution S. In deriving Eq. (15).

the terms involving pH(S) and $a_H(S)$ exactly cancel (Eq. (13)), providing that the same ion activity convention was used in Eq. (11) as was originally used to define the pH of the standard. The value of the term ΔpH reflects this choice of convention. The usual equilibrium interpretation of pH assumes that the irreversible term, ΔE_{LJ}, is negligible; and therefore, that pH(X) is approximately equal to $-\log_{10} a_H^C(X)$. Consequently, the magnitude of ΔE_{LJ} is proportional to the error in calculating the thermodynamic property $\ell n\ a_{HCl}(X)$ by this assumption.

The magnitude of ΔE_{LJ} or ΔpH can be determined experimentally by replacing the hydrogen electrode in cell A with an electrode sensitive to the ion whose activity is defined by convention. For the case of chloride the Ag-AgCl electrode may be used in place of the hydrogen electrode. The emf for this modified cell differs from Eq. (11) in that the conventional activity for chloride appears rather than that for hydrogen and E_o differs by an additive constant. Since the liquid junction potential does not depend on the electrodes used, $E_{LJ}(X)$ is the same for both cells. The difference in the emf between two cells with the AgCl-Ag electrode, one with unknown solution X and the other with standard solution S, can be expressed as:

$$E'_X - E'_S = \frac{RT}{F} \ell n \left(\frac{\gamma_{Cl}(X)\ m_{Cl}(X)}{\gamma_{Cl}(S)\ m_{Cl}(S)} \right) - \Delta E_{LJ}(X,S) \quad . \qquad (16)$$

Eq. (16) can be used to calculate ΔE_{LJ} with respect to an assumed standard since all other terms can be measured or are defined by convention.

The four curves plotted in Fig. 3 give ΔE_{LJ} in NaCl solutions calculated from the data of Shatkay and Lerman (1969). Each curve is defined

for a different ion activity convention (also note that the values of $E_{Cl,calomel}$ reported by SL equal -E' in Eq. (16). In principle any solution could be used as a reference for calculating ΔE_{LJ}. In obtaining Fig. 3, we have defined a .01 m NaCl solution as the standard reference solution. Assuming an ideal glass electrode, this choice of standard is comparable to the ΔE_{LJ} one would expect with standardization using the NBS Scale. (Note that NBS standards contain no chloride and therefore the equation for pH is slightly more complicated than Eq. (16). Extrapolation of Eq. (16) to zero chloride in the standard solution s would provide a consistent definition for ΔE_{LJ}^{NBS}.) In Fig 3, ΔE_{LJ} is about 3mv (ΔpH = .05) using the MacInnes convention for .725 m NaCl solution. also, using the MacInnes convention, ΔE_{LJ} is computed to be about 3mv between the NBS standard and a .725 m NaCl plus .005 m $NaHCO_3$ solution (using the data of Hawley and Pytkowicz (1973)).

Fig. 3 emphasizes the conventional nature of the liquid junction. While it has long been recognized that the liquid junction potential between two different solutions cannot be measured (Guggenheim (1929)), once an ion activity convention has been defined the value of the corresponding liquid junction is also defined and measurable by experiment. Conventional ion activities can similarly be measured. From a thermodynamic point of view all ion activity conventions are equivalent and no theoretical value for an ion activity can be verified directly by experiment. That the liquid junction potential is small for a particular convention does not imply that the corresponding γ_{Cl^-} resembles in any way a real ion activity coefficient for the chloride ion. In this article we adopte the MacInnes convention and consistently report ion activities and liquid junction changes with respect to this convention. With a proper choice for ω, Eq. (A7) in Appendix A can be used to convert Eqs. (3) to this convention.

Due to the difficulties associated with the exact interpretation of the pH(X) in terms of the thermodynamic properties of a solution, we utilize reversible cell, isopiestic and solubility data in preference to pH data in the parameterization in Section V. However, pH measurements are the only cell data that we found in certain concentration ranges. In these cases, it is necessary to estimate the change in the liquid junction potential (plus any corrections due to the glass electrode asymmetry potential) using the available data.

To convert pH data into a form which is useful to a thermodynamic model, a constant ionic media assumption often provides a convenient and accurate method to eliminate the ΔpH term (see, for example, Bates (1973) and references therein). Under certain titration conditions, the activity coefficients and ΔpH are approximately constant over the entire concentration range resulting from the addition of titrant to solution. Often in such cases, the conventional ΔpH can be evaluated from the data in a narrow concentration range of the titration curve. By assuming this ΔpH value is constant, the remaining pH data can be corrected to the appropriate ion activity convention and subsequently used to evaluate mean activity coefficients or apparent equilibrium constants.

ΔpH can often be calculated using the equation,

$$\log_{10} \gamma_H^{NBS} = \log_{10} \gamma_H^{M} + \Delta pH \quad . \tag{17}$$

γ_H^{NBS} is defined by a convention equating pH^{NBS} to $-\log_{10} a_H^{NBS}$, where pH^{NBS} is determined using the NBS standardization procedure. γ_H^{NBS} can typically be calculated using data on the acid side of a titration curve (see Culberson and Pytkowicz (1973) or Hansson (1972)). γ_H^{M} is the hydrogen

activity coefficient defined within the extended MacInnes convetion and may be calculated using $\gamma^{\pm}_{HCl}$ for the same solution. Using the equation, $\gamma^{M}_{H} = \gamma^{\pm}_{HCl}/\gamma^{M}_{Cl}$, with Eq. (14c) ($\gamma^{\pm}_{HCl}$ can be measured by experiment or calculated using a suitable model.), reported values of apparent equilibrium constants, such as $K_1 = a^{NBS}_{H}\ m_{HCO_3}/m_{CO_2}$, can the be corrected to the MacInnes convention once ΔpH has been evaluated for the experiment.

V. PARAMETERIZATION AND DATA COMPARISON

In this section, we discuss the extension of our previous solubility model to include acid-base equilibria and the carbonate system at 25°C. Parameters for calculating mineral solubilities in the system Na-K-Ca-Mg-H-Cl-SO_4-OH-HCO_3-CO_3-CO_2-H_2O using the model defined in Section II are provided in Tables 1, 2, 3 and 4. Since in most cases the model is parameterized from the data in binary and common-ion ternary systems, the following comparisons to data in more complex systems generally represent predictions by the model. The agreement of the model with the data is good, the model exhibiting good predictability even in complex,mixed,electrolyte solutions. While some important qualifications are discussed in this section, we believe that the model defined here is sufficiently accurate for most geological applications. It will calculate accurately mineral solubilities over broad ranges of relative composition and to high ionic strength.

In the following discussion, the model is compared to the experimental data for each of the subsystems. The agreement with isopiestic and electromotive force data is designated by citing standard deviations. For isopiestic data the standard deviation is given in terms of the osmotic coefficient (e.g., $\phi_{exp} - \phi_{calc}$). For emf data, unless otherwise indicated, the standard deviation is given in terms of the natural logarithm of the activity coefficient for the cell. For example, the standard deviation for the data determined from a cell utilizing a hydrogen electrode and a silver-silver chloride electrode is reported in terms of $\ln \gamma_{HCl}^{\pm\ exp} - \ln \gamma_{HCl}^{\pm\ calc}$. The comparison to the solubility data is made graphically.

The parameter values for each system are determined by minimizing a weighted standard deviation of all the data for the system. In general, low weights are assigned to solubility data in comparison to the typically more accurate isopiestic and cell data. This approach represents an improvement over the methods used by HW where parameter values were determined using various graphical methods. The parameter values given in Tables 1-4, are usually cited to higher accuracy than is warranted by the data fit. The choice of different weights can change parameter values significantly. We have attempted to select weights which give the solubilities within 5% of their observed values. A brief discussion of the numerical method used to evaluate parameters is given by Harvie (1981). Many parameters in the tables are set equal to zero (denoted by dashes). For some case, these parameters are approximately redundant with other parameters (see following discussion of H_2SO_4-H_2O and Pitzer et al., 1977). In other cases, no data are available to evaluate a parameter.

In light of new data the $CaSO_4$ parameters of the original Harvie-Weare model have been revised to improve the calculated dilute solution solubility of Gypsum. Recently, Rogers (1981) fit the $CaSO_4$ system using the Pitzer model. We utilize her parameters except for the third virial coefficients which are refit to be internally consistent with our model. The revised $CaSO_4$ model has been discussed in Harvie et al. (1982) and Harvie (1981).

In Fig. (4a) the calculated solubilities of Halite, Sylvite, Bischofite, Antarcticite and $CaCl_2 \cdot 4H_2O$ in aqueous HCl solutions are plotted together with the experimental data. The experimental data usually are those summarized in Linke (1965). The data for Bischofite in hydrochloric acid solutions are given by Berecz and Bader (1973). The parameters values for $\beta^{(0)}_{H,Cl}$, $\beta^{(1)}_{H,Cl}$, and $C^{\phi}_{H,Cl}$ are given by Pitzer and Mayorga (1973). The values for $\theta_{K,H}$, $\theta_{Na,H}$, and $\psi_{Na,H,Cl}$ are taken from Pitzer and Kim (1974). The value for $\psi_{K,H,Cl}$ is adjusted slightly from the Pitzer value to improve the agreement of the model with the solubility data in the KCl-HCl-H_2O system.

The values for $\theta_{Mg,H}$ and $\psi_{Mg,H,Cl}$ are obtained by refitting the emf results of Khoo et al. (1977b) together with the solubility data for the $MgCl_2$-HCl-H_2O system. Unlike the model used by Khoo et al. the equations we use contain terms to account for electrostatic forces in unsymmetrical mixtures (Pitzer (1975)). Hence, it was necessary to re-evaluate the parameters given by Khoo et al. The standard deviation of our fit to the Khoo et al. data is σ = .0021 in $\ln \gamma^{\pm}$. When the emf results are fit without the solubility data, σ = .0016. The evaluating $\theta_{Ca,H}$ and $\psi_{Ca,H,Cl}$, a similar analysis was carried out using the emf results of Khoo, et al. (1977a) and the solubility data in the CaCl-HCl-H_2O system. The standard chemical potential of $CaCl_2 \cdot 4H_2O$ is treated as a adjustable parameter in the fit. Our standard deviation to the emf data in the $CaCl_2$-HCl-H_2O system is σ = .0027. The activity coefficients for $CaCl_2$ at high $CaCl_2$ concentrations are not in good agreement with experiment. To fit the solubility data we have made small changes in the chemical potentials for salts like Antarcticite. This would not be allowed in a more precise model. When third virial coefficients are treated as adjustable

parameters, it is possible to obtain agreement (10%) with the observed trends in solubility at high concentrations. This is probably related to the rapidly increasing activity coefficient for $CaCl_2$, in which case small changes in concentration produce pronounced changes in the activity.

Pitzer et al. (1977) have accurately fit the data for the sulfuric acid-water system, incorporating the species HSO_4^-. We found that it is not possible to accurately fit the data for the H_2SO_4-H_2O system, without a HSO_4^- ion pair, using Eqs. (3). Since we are using the unsymmetrical electrolyte theory the parameters given by Pitzer et al. are re-evaluated. This is accomplished by fitting the unsymmetrical mixing equations to the interpolated activity and osmotic coefficients given by Pitzer et al. In agreement with Pitzer et al. an approximate redundancy among the parameters is noted. For example, the standard deviation of a least squares fit when adjusting the parameters , $\beta^{(0)}_{H,SO_4}$, C^{ϕ}_{H,SO_4}, $\beta^{(0)}_{H,HSO_4}$ and $\beta^{(1)}_{H,HSO_4}$, is essentially independent of the value of $\beta^{(1)}_{H,SO_4}$. Within a broad range of $\beta^{(1)}_{H,SO_4}$ values the optimal value for any of the adjustable parameters changes but the standard deviation of the fit remains the same. Thus, the parameters for the H_2SO_4-H_2O system could not be uniquely determined. Nevertheless, the thermodynamic properties of the system are accurately described by any set of these four parameter values corresponding to a given $\beta^{(1)}_{H,SO_4}$. We have adopted Pitzer's convention of setting the redundant parameters, $\beta^{(1)}_{H,SO_4}$, C^{ϕ}_{H,HSO_4}, θ_{HSO_4,SO_4}, and $\psi_{SO_4,HSO_4,H}$, equal to zero. As should be expected, we agree with the tabulated activity and osmotic coefficients of Pitzer et al. The standard deviation of the overall fit to ϕ and $\ln \gamma^{\pm}$ is $\sigma = .0007$.

The agreement of the model with the data for the $HCl-H_2SO_4-H_2O$ system is good. The data for this system are the emf data of Nair and Nancollas (1958), Davies et al. (1952) and Storonkin et al.(1967). The first two sets of experiments are confined to low concentrations, $I<<1$. The data of Storonkin apply to systems up to ionic strengths of almost 4. The standard deviation of the Nair and the Davies data is $\sigma = .0008$ $\ell n\ \gamma^{\pm}$. For the Storonkin data, the standard deviation is $\sigma = .015$. All of the data are insensitive to reasonable variations in the parameter $\psi_{H,SO_4,Cl}$. Consequently, this parameter is set equal to zero

The parameters $\beta^{(0)}_{Na,HSO_4}$, $\beta^{(1)}_{Na,HSO_4}$, ψ_{H,Na,HSO_4}, and ψ_{Na,HSO_4,SO_4}, and the standard chemical potential for $Na_3H(SO_4)_2$ are evaluated simultaneously by a least squares fit of the emf data of Harned and Sturgis (1925), Randall and Langford (1927), and Covington et al (CDW) (1965), together with the solubility data (Linke (1965)). The parameters, ψ_{Na,H,SO_4} and C^{ϕ}_{Na,HSO_4}, are approximately redundant with the above parameters; therefore, they are set equal to zero. The standard emf, E^0, values of Randall and Covington are also treated as adjustable parameters, while the standard emf for the HS data is fixed so that the activity coefficient in 0.1 m H_2SO_4 solution agrees with Pitzer et al., (1977). As noted by Pitzer et al the interpolated E^0 value for the Randall data does not agree well with the accepted value for similar cells. As usual in fitting the parameters, the weights on the solutility data are increased until good agreement with these data is obtained. This procedure tends to minimize the standard deviation of the emf data while insuring good agreement with the solubility measurements. The resulting standard deviations are $\sigma = .018$, $\sigma = .013$, $\sigma = .006$ for the Harned, Randall and Covington data, respectively. Additional emf measurements at concentrations which will define the $Na-HSO_4$ interaction

are desirable for this system. The resulting solubility curve is given in Fig. (4b). The data defined by the closed circles are that of Foote (1919) and Luk'yanova (1953). The open circles and dashed line denote the data of Korf and Shchatrovskaya (1940). The Korf experiments observed an additional monohydrite salt separating the Thenardite, and $Na_3H(SO_4)_2$ fields. We have parameterized the equations to the Foote and Luk'anova data since these authors are in good agreement, and the $Na_3H(SO_4)_2 \cdot H_2O$ salt has not been observed above 0^oC by other authors (see Linke (1965)).

The data for the system K_2SO_4-H_2SO_4-H_2O are fit in much the same way as the corresponding sodium system, except that the parameter, ψ_{K,H,SO_4}, is allowed to vary. The cell data of Harned and Sturgis (1925) are fit with a standard deviation of .018. The calculated solubilities are compared in Fig. (4c) to the data of D'Ans (1913) (solid circles) and of Storozhenko and Shevchuk (1971) (open circles). The difference between these two sets of data is sizeable. The major difference in the parameters fit with either set of data is in the chemical potentials or the acid salts. We have parameterized the model to the D'Ans data.

A similar analysis for the $MgSO_4$-H_2SO_4-H_2O system yields a standard deviation of σ = .02 to the emf data of Harned and Sturgis (1925). The solubility data predicted in Fig. (4d) are that of Flippov and Antonova (1978).

The parameters, $\beta^{(0)}_{Ca,HSO_4}$ and $\beta^{(1)}_{Ca,HSO_4}$, are evaluated directly from the solubility data of Marshall and Jones (1966) depicted in Fig. (4e). These data are insensitive to reasonable adjustments in all other parameters for the system. Hence, ψ_{Ca,H,SO_4}, ψ_{Ca,H,HSO_4}, $\psi_{SO_4,HSO_4,Ca}$

and C^{ϕ}_{Ca,HSO_4} are all set equal to zero. In Fig. (4f) the calculated solubility of Gypsum in hydrochloric acid solutions is in good agreement with the experimental data summarized in Linke (1965).

In Figs (5a) and (5b) the calculated solubility of CO_2 in different aqueous electrolyte solutions are compared to experiment. Each curve is labelled with the salt present in the solution. As previously discussed, the parameterization includes the evaluation of a single parameter, $\lambda_{CO_2,i}$, for each ion i present in the system. Since measurements can only be made in neutral solutions, one of the parameters must be assigned arbitrarily. We use the convention of setting $\lambda_{CO_2,H}$ equal to zero. The remaining parameters, evaluated directly from the solubility data, are given in Table 3. The standard chemical potential for CO_2 (gas), given in Table 4, is that of Robie et al. (1978). $\mu^{0}_{CO_2(aq)}$ is evaluated, together with the λ's, from the solubility data. The calculated CO_2 solubility in pure water is about 3% low. This is probably the result of a deficiency of the linear theory. However, since deviations in the entire concentration range are usually within 5%, the increased complication of higher order terms for neutral species does not seem warranted. (This is particularly true in the context of the geochemical applications for which the model is intended.) The solubility data given in Figs. (5) are primarily those of Yasuniski and Yoshida (1979) and Markham and Kobe (1941). The data of Geffchen (1904) are given for the CO_2-HCl-H_2O system. The Harned and Davis (1943) data are included in the figure for the NaCl-HCl-H_2O system. The parameter, $\lambda_{CO_2,Cl}$, is determined from the data in the HCl-CO_2-H_2O system. Using this parameter,

the value of λ for each of the cations (except H^+) is obtained by fitting the data in the chloride systems. The parameter, λ_{SO_4,CO_2}, is then evaluated from the data in the Na_2SO_4-CO_2-H_2O system. Lastly, λ_{HSO_4,CO_2} is evaluated from the H_2SO_4-CO_2-H_2O system. The data in the K_2SO_4 and $MgSO_4$ systems in Fig. (5b) test the specific interaction model, since all the parameters for these systems are evaluated from other data.

The Na-OH and K-OH interaction parameters are obtained from Pitzer and Mayorga (1973). The values for $\theta_{OH,Cl}$ and $\psi_{OH,Cl,Na}$ of Pitzer and Kim (1974) are retained, while $\psi_{OH,Cl,K}$ is slightly adjusted to improve the fit with the solubility data. The calculated solubility curves for these hydroxide systems are plotted together with the solubility data of Akerlof and Short (1937) in Figs. (6a). The parameters, θ_{OH,SO_4}, ψ_{OH,SO_4Na} and $\psi_{OH,SO_4,K}$, are evaluated solely from the solubility data in these systems. For the Na-OH-SO_4 system the data of Windmaisser and Stockl (1950) are used exclusively (Fig. 6b). For the K-OH-SO_4 system the data of D'Ans and Schreiner (1910) were used (Fig. (6d)). (It is noteworthy that the data of D'Ans and Schreiner (1910) for the Na-OH-SO_4 system are not in good agreement with that of Windmaisser (Linke (1965)).

The parameters representing the Na-HCO_3 interaction and $\theta_{HCO_3,Cl}$ are from Pitzer and Peiper (1980). (At the time of publication improved parameter values have been evaluated by Peiper and Pitzer (1981).) The chemical potential for bicarbonate is evaluated from the equilibrium constant given by Pitzer and Peiper (1980). The Na-CO_3 interaction parameters, together with $\mu^0_{CO_3}$, are evaluated from the isopiestic results of Robinson and Macaskill (1979) and the emf results of Harned and Scholes (1941). Parameters for Na, CO_3 listed in Table 2 differ from those given by Robinson and Macaskill because we account for the hydrolysis of carbonate

to bicarbonate. The standard deviation of the isopiestic data remains at σ = .002 in the osmotic coefficient. The standard deviation of the Harned and Scholes emf data equals .004.

The remainder of the $Na-CO_3-HCO_3-Cl-SO_4-OH-H_2O$ system is parameterized exclusively from solubility data in common ion systems. The chemical potentials of Nacholite and Natron are obtained from the solubility data of Hill and Bacon (1927) and Robinson and Macaskill (1979), respectively. The parameters θ_{CO_3,HCO_3} and $\psi_{CO_3,HCO_3,Na}$ and the standard chemical potential for Trona are based on the solubility data of Hill and Bacon (1927) and Freeth (1922) (Fig. (7a)). Several of the Freeth points are in poor agreement with the Hill data and the model. The parameter, $\psi_{Cl,HCO_3,Na}$, is evaluated from the data of Bogoyavlenskii and Manannikova (1955) and Freeth (1922). θ_{HCO_3,SO_4} and $\psi_{HCO_3,SO_4,Na}$ are evaluated primarily from the data of Markarov and Jakimov (1933). In the $Na-SO_4-HCO_3$ system θ_{SO_4,HCO_3} and $\psi_{SO_4,HCO_3,Na}$ are nearly redundant, hence these parameters can not be determined uniquely. Acceptable values which are in good agreement with the majority of the data in the more complex systems are given in Table 2. (See Fig. (7b)). Additional experiments are required to refine these values.

The solubility data of Freeth (1922) are used in evaluating the parameters, $\theta_{Cl,\ CO_3}$ and $\psi_{Cl,CO_3,Na}$, as well as the standard chemical potential for sodium carbonate hepahydrate (Fig. (7d)). The parameters, θ_{SO_4,CO_3} and $\psi_{SO_4,CO_3,Na}$, are evaluated primarily from the data of Makarov, and Krasnikov (1956) and Caspari (1924). Given the data available there is redundancy between these parameters. The values chosen are consistent with the data. (Figs. (7) and (8)).

The parameters, θ_{OH,HCO_3} and $\psi_{OH,HCO_3,Na}$, are unnecessary since

the concentrations of OH and HCO_3 cannot simultaneously be large. The small effects of these parameters are redundant with the more important parameters, $\theta_{CO_3,OH}$ and $\psi_{CO_3,OH,Na}$. The parameter, θ_{OH,HCO_3}, and all ψ's for OH,HCO_3 and a cation are set equal to zero. $\theta_{CO_3,OH}$ and $\psi_{CO_3,OH,Na}$ are evaluated from the data of Freeth (1922) and Hostalek (1956). The chemical potential of Thermonatrite is also determined from these data.

Data from more complex systems are used to test the model. The $Na-CO_3-SO_4-OH-H_2O$ system was studied by Itkina and Kokhova (1953). From their data the Burkeite chemical potential is evaluated. Comparison of our solubility calculations with these experimental data is given in Fig. (9a). In general the agreement is quite good. With the exception of Burkeite, 70% of the calculated activity products for each salt at each of the points (Fig. (8b)) are within 5% of the corresponding equilibrium constant. 90% of the activity products are within 10% of the equilibrium constant. An exception is the Natron-$Na_2CO_3 \cdot 7H_2O$-Burkeite point which appears from calculation to be undersaturated by about 12% in the calculated equilibrium constant for Natron. In Figs (8), the Burkeite fields are assumed to be in equilibrium with the mineral having a sulfate to carbonate ration of 2 to 1. The agreement of the data with this model is somewhat surprising, since $Na_2CO_3-Na_2SO_4$ solid solutions of the Burkeite type are known to occur (see Jones (1963)). In Fig. (8f), the model activity of Na_2CO_3 in aqueous solution is plotted versus the model activity for Na_2SO_4 in aqueous solution. Each point represents the Na_2CO_3 and Na_2SO_4 activities calculated for each solution composition reported by Itkina and Kokhova (1953) to be in equilibrium with a Burkeite phase. A curve resembling that of a $Na_2CO_3 \cdot 2Na_2SO_4$ mineral (solid curve) is suggested. In contrast, an ideal solid solution would satisfy linear behavior (e.g.

dashed curve). The mineral approximation for the Burkeite phase gives relatively good results. The Na_2CO_3-Na_2SO_4 diagram indicates that Burkeite is only slightly unstable at 25°C in this system. This is consistent with the 25.5°C invariant point for Burkeite-Natron-Mirabilite-solution coexistence in Na_2CO_3-Na_2SO_4-H_2O solution (Makarov and Bleiden (1938)).

Further comparisons of the model with experiment are given for the Na-CO_3-Cl-OH-H_2O, Na-CO_3-Cl-SO_4-H_2O, Na-CO_3-HCO_3-Cl-H_2O and Na-CO_3-HCO_3-SO_4-H_2O systems (Fig. (8)). With the exception of the Na-CO_3-SO_4-Cl-H_2O data of Makarov and Bleiden (1938), all of the calculated diagrams are in good agreement with the experiments. In the Na-CO_3-SO_4-Cl system (Fig. (8e)) the experimental Natron-Mirabilite-Burkeite invariant point (triangle) is not in good agreement with the model or the experimental 25.5°C invariant point on the CO_3-SO_4 edge.

In Table 5, the calculated activities of water and the equilibrium carbon dioxide partial pressures are compared to the experimental determinations of Hatch (1972) and Eugster (1966) in the Na-CO_3-HCO_3-Cl-H_2O system. These experiments were performed by saturating aqueous solutions with the various minerals listed in Table 5 and measuring the activity of water and/or carbon dioxide pressure. Agreement with the activity of water measurements is within 3% and often better. The calculated CO_2 pressures are within the scatter of the data for the Eugster measurements, and within about 10% of the Hatch measurements.

The data available for the K-CO_3-HCO_3-OH-Cl-SO_4-H_2O system are more sparse than for the corresponding sodium system. In particular, emf data in the moderate concentrations appear to be absent. Consequently, a parameterization procedure using more complicated data is used. The value for $\beta^{(1)}_{K,HCO_3}$ is estimated by Pitzer and Peiper (1980). $\beta^{(1)}_{K,CO_3}$ is estimated

from the data of MacInnes and Belcher (1933). The extensive solubility data in the Na-K-CO_3-HCO_3-H_2O system are used in a nonlinear least square evaluation of the parameters: $\beta^{(0)}_{K,HCO_3}$, $\beta^{(0)}_{K,CO_3}$, C^{ϕ}_{K,HCO_3}, C^{ϕ}_{K,CO_3}, ψ_{Na,K,HCO_3}, ψ_{Na,K,CO_3}, and ψ_{HCO_3,CO_3K}. The standard chemical potentials for the carbonate salts with potassium are also adjusted in an eleven parameter fit. The data used are those of Hill and Hill (1927) for the $KHCO_3$-K_2CO_3-H_2O system; Hill and Miller (1927) for the K_2CO_3-Na_2CO_3-H_2O system; Hill and Smith (1929) and Oglesby (1929) for the $KHCO_3$-$NaHCO_3$-H_2O system; and Hill and Smith (1929) and Hill (1930) for the reciprocal system (Fig. (10)). The agreement between the model and the above experimental data is generally good (see Figs. (9) and (10)), except for the Nacholite data of Oglesby (1929) at P_{CO_2} = 1 atm. (Fig. (9a)). However in Fig. (9a), calculation does agree well with the experimental value for the Nacholite-$KHCO_3$ invariant point of Hill and Smith (1929) (square point in Fig. (9a)), and the $KHCO_3$ solubility data of Oglesby. We suspect that the Hill and Smith invariant point is probably correct, since the Nacholite-$KHCO_3$ coexistence data of Hill plotted in Fig. (10) extrapolate to this value. The 13% discrepancy between the Hill and Oglesby data must be resolved experimentally.

The "mineral", $KNaCO_3 \cdot 6H_2O$, is an approximation for the solid solution $(K,Na)CO_3 \cdot 6H_2O$ (Hill (1930)) (Fig. (9e). As was the case with the Burkeite phase, data giving the solid phase composition in equilibrium with an aqueous solution are required to model the solid solution behavior. Nevertheless, the experimental aqueous solution concentrations in equilibrium with the solid solution are adequately calculated using the mineral approximation. (See Figs. (9) and (10)). The data for this solid solution

are not used in the fit of the potassium carbonate parameters.

The data for the chloride system of potassium carbonate and bicarbonate are sparse. The parameters, $\psi_{Cl,CO_3,K}$ and ψ_{Cl,HCO_3K}, are evaluated from the solubility data of Blasdale (1923) and Bayliss and Koch (1952). The agreement of the model with the emf data of MacInnes and Belcher (1933) is good. The standard deviation of the fit to these authors' potassium bicarbonate data is σ = .006 in $\ell n(\gamma_{Cl}/\gamma_{HCO_3})$ and the standard deviation to their potassium carbonate-bicarbonate data is σ = .014 in $\ell n\ \gamma^{\pm}_{HCl}$. The conditions of the MacInnes and Belcher experiments are analogous to the Harned emf experiments in the sodium system. The fit to the Blasdale (1923) solubility data is good, with the exception of several Natron points which correlated quite well the sodium carbonate heptahydrate salt. Blasdale also does not observe the heptahydrate in the $NaCO_3$-NaCl-H_2O ternary system. The single point in the K_2CO_3-KCl diagram (Fig. (9d)) is the $K_2CO_3 \cdot \frac{3}{2} H_2O$-KCl coexistence point of Blasdale (1923). The data for the $KHCO_3$-KCl system are those of Bayliss and Koch (1952) for Sylvite-$KHCO_3$ coexistence.

The value of the parameter, $\psi_{SO_4,CO_3,K}$, is based on the data of Hill and Moskowitz (1929) in the K_2CO_3-K_2SO_4-H_2O system (Fig. (9f)). No data are found which are sensitive to the parameter, $\psi_{SO_4HCO_3K}$. Consequently, this parameter is set equal to zero until data becomes available. In disagreement with the data of Blasdale (1923) the calculated reciprocal diagram Na-K-SO_4-CO_3 displays different, perhaps more stable, mineral coexistences than those reported. In particular, Aphthitalite appears to occupy a large portion of the phase diagram where a $NaKCO_3 \cdot 6H_2O$ -Aphthitalite-Arcanite invariant point is stable. Also, a stable zone for Burkeite between the Aphthitalite-Mirabilite and Natron fields may be present.

The KOH-K_2CO_3 data (Fig. (9c)) used to fit $\psi_{OH,CO_3,K}$ are that of

Lang and Sukava (1958) (circles) and Klebanov and Pinchuk (1967) (squares). These two set of data are not in good agreement with each other and an average of the two sets is taken.

A $CaOH^+$ ion pair is not explicitly included in our model (section III). The aqueous solution parameters for the $Ca(OH)_2$-H_2O system have been evaluated from the emf data of Bates et al. (1959) and the solubility data of Millikan (1918) in the $Ca(OH)_2$-$CaCl_2$-H_2O system. In Fig. (11) the calculated solubilities for $Ca(OH)_2$ and other oxychloride salts are plotted vs. experiment. Since the parameterization is based only on the Bates and Millikan data the calculated solubilities in the $Ca(OH)_2$-NaCl, $Ca(OH)_2$-KCl, $Ca(OH)_2$-NaOH and $Ca(OH)_2$-KOH aqueous solutions are checks on the model (Figs. (11c)-(11f)). The agreement is for the most part excellent. The data denoted by squares in Fig. (11c) and (11d) are those of Fratini (1949) at 20°C. The analytical values of Fratini are consistently higher than the model and higher then the data of other authors in $Ca(OH)_2$-H_2O solutions (circles in the same figures). An increased chemical potential for Portlandite brings all of the Fratini data in good agreement with the model. The data in the NaCl and KCl solutions are those of Johnston and Grove (1931) and Yeatts and Marshall (1957). The $CaSO_4$-$Ca(OH)_2$ data are those of Cameron and Bell (1906) and Jones (1939). The Bates data are for dilute $Ca(OH)_2$-KCl and $Ca(OH)_2$-$CaCl_2$ solutions. The measurements are at concentrations where significant ion association should be present, yet we did not need to include a $CaOH^+$ species to obtain good agreement with the data. The standard deviation of the model to the data is σ = .003.

In Fig. (12b)-(12f) the calculated solubilities of Calcite (solid curves) in water and NaCl solutions are compared to experiment. The solubilities of Aragonite (dashed curves) are also plotted. The experimental

data in the $CaCO_3$-H_2O-CO_2 system (Fig. (12a)) are those summarized by Jacobson and Langmuir (1974) to 1 atm. and those of Miller (1952) (below the curve) and Mitchell (1923) (above the curve) at higher pressure. For CO_2 pressures somewhat greater than 1 atm. the fugacity was calculated from the CO_2 pressure using the real gas virial coefficient summarized in Angus et al. (1976). Fig. (12a) compares the calculated and measured solubilities of Calcite in pure water as a function of the fugacity of CO_2 in the vapor phase. (The lowest and right hand scales depict the lower pressure range, whereas the upper and left hand scales are for higher CO_2 fugacities). The calcium carbonate interaction parameters and the chemical potentials for Calcite and Aragonite are evaluated from these data. μ^0 for Aragonite is evaluated from the data of Backstrom (1921).

A neutral ion complex, $CaCO_3^0$, was defined for this system, since the parameter, $\beta^{(2)}_{CaCO_3}$, was extremely large and negative (~ -200) when the pH data of Reardon and Langmuir (1974) are fit without this complex. We suspect that the model with the ion complex is the better model for this system. This is consistent with the conclusions drawn in section III for 2-1 electrolytes. This conclusion is admittedly based on a relatively sparse set of pH data. With or without $CaCO_3$, the resulting model is found to be consistent with the $CaCO_3$-H_2O-CO_2 solubility data when the Ca-HCO_3 second virial coefficient parameters are adjusted to fit the data.

Jacobson and Langmuir (1974) showed that the CO_2 pressure dependence of the solubility of Calcite in water is not consistent with a $Ca(HCO_3)^+$ ion pair. Our calculations agree with this result. Since these solubility data, plotted in Fig. (12), are reproducible and ion pair is not assumed. Positive coefficients, which are inconsistent with strong association, are obtained when these data are fit without the

ion pair, $CaHCO_3^+$. The value for $\beta^{(0)}_{CaHCO_3}$ is selected within a range of possible values consistent with the data. $\beta^{(1)}_{CaHCO_3}$ is fit to the data given this choice of $\beta^{(0)}_{CaHCO_3}$.

In Figs. (12b)-(12f), the predicted solubility of Calcite in NaCl solutions is plotted together with the available data. At 0.97 atm. the data are those of Shternina and Frolova (1952, 1962), Frear and Johnston (1929) and Cameron, et al. (1907). At lower pressures, the data are primarily those of Shternina and Frolova (1952). In Fig. (12f), the results of Cameron and Seidell (1902) are plotted. The Shternina data are consistently designated by circles. All of the data are reported for Calcite solubility.

The calculated behavior for the solubility of Calcite is constrained by the data in other systems. For $P_{CO_2} \geq .06$ atm. the concentrations of CO_3^{-2} and $CaCO_3^0$ are negligible compared to the solubility of Calcite. Consequently, the dominant reaction determining the Calcite solubility is:

$$CaCO_3 + H_2O + CO_2(gas) = Ca^{+2} + 2HCO_3^- \quad ,$$

and the solubility may be calculated to good approximation by the following equation:

$$K = \frac{a_{Ca}\left(a_{HCO_3}\right)^2}{a_{H_2O}\,P_{CO_2}} \simeq 4\,\frac{\left(\gamma^{\pm}_{Ca(HCO_3)_2}\right)^3 m^3}{a_{H_2O}\,P_{CO_2}} \quad . \qquad (18)$$

In the above equation m is the solubility of Calcite. Since the solubility is small, the thermodynamic mean activity coefficient for $Ca(HCO_3)_2$ may be approximated by the trace activity coefficient for $Ca(HCO_3)_2$ in NaCl

solutions. This activity coefficient is related to the trace activity coefficients in the $CaCl_2$-NaCl-H_2O and $NaHCO_3$-H_2O systems by the equation,

$$\gamma^{\pm tr}_{Ca(HCO_2)_2} = \gamma^{\pm tr}_{CaCl_2} \left(\gamma^{tr}_{HCO_3} / \gamma_{Cl} \right)^{2/3} \quad . \tag{19}$$

$\gamma^{\pm tr}_{CaCl_2}$ may be determined from the isopiestic data of Robinson and Bower (1966) or from the solubility data of Gypsum or Portlandite in NaCl solutions. The activity coefficient ratio ($\gamma^{tr}_{HCO_3^-}/\gamma_{Cl^-}$) is measured directly by the emf experiments of Harned and Bonner (1945) to 1.0 molal NaCl. Our model is in good agreement with all the above data. Substituting Eq. (19) into Eq. (18), the following equation is obtained :

$$m = \left(\frac{K\, a_{H_2O}}{4 \left(\gamma^{\pm tr}_{CaCl_2} \right)^3 \left(\gamma^{\pm tr}_{HCO_3} / \gamma_{Cl} \right)^2} \right)^{1/3} P_{CO_2}^{1/3} \quad . \tag{20}$$

For relatively large NaCl concentrations the ionic strength, a_{H_2O} and the trace activity coefficients are fixed and the solubility of Calcite should depend roughly on the CO_2 pressure to the 1/3 power. As noted by Shternina and Frolova (1952), this behavior is satisfied by the data.

Since the solubility of Calcite is not negligible, Eqs. (20) is approximate due to the neglect of the Ca-HCO_3 interaction. From other data we have an independent determination of $\gamma^{\pm tr}_{Ca(HCO_3)_2}$ and we can, therefore, calculate the effects due to this interaction. When the Ca-HCO_3 interaction is positive the observed solubility will be less than that predicted by Eq. (20), as is the case below 1 m NaCl and for Calcite in pure water. When the interaction is negative (e.g. ion association) the opposite behavior should be observed. This is consistently the case above 1 m NaCl.

However, there exists an inconsistency between a strong negative interaction and a 1/3 power law in the solubility. At 2 m NaCl and P_{CO_2} = .97 atm. the calculated solubility is about 85% of the experimental value. A $Ca(HCO_3)^+$ ion pair might be introduced to improve the agreement at this pressure and NaCl concentration. However, such a model is inconsistent with other data at lower NaCl concentrations. Furthermore, calculations verify that while agreement can be improved at any given pressure with a $CaHCO_3^+$ ion pair, it is not possible to fit the observed pressure dependence of Shternina and Frolova (1952) with such a model. As the pressure is reduced, the concentration and the degree of association are also reduced. Further data are needed to understand these discrepencies.

The pH data of Stock and Davies (1948) are used to evaluate the chemical potential for the $MgOH^+$ ion pair which is found to have a pK_d value of 2.19. A liquid junction plus asymmetry potential of .23 pH units is obtained from the acidic region of the titration curve reported by these authors (Table II of SD). While this value is large, our K_d is also in good agreement with that determined by McGee and Hostetler (1975) from pH data. With the McGee and Hostetler data, however, the model deviations trend from -.029 at pH = 10.03 to .005 at pH = 10.39. The change in the solution composition for this range is small. If this trend is significant there may be a problem with an $MgOH^+$ model. A detailed reversible cell study of the $Mg(OH)_2$ - $MgCl_2$ - H_2O system would be useful in precisely characterizing the interactions in this system. Higher concentrations of $MgCl_2$ should be possible owing to the increasing solubility of Brucite. This study would also be useful due to the importance of the Mg-OH interaction in determining pK_w in seawater. There is also some

evidence that the precipitation of a magnesium oxychloride buffers highly concentrated $MgCl_2$ evaporite solutions (Bodine (1976)). Our preliminary calculations support this result.

The solubility data for Brucite and Magnesium oxychloride in $MgCl_2$ solutions are plotted in Fig. (13). Brucite is denoted by the circles and the Oxychloride is denoted by squares. Closed points correspond to the data of Robinson and Waggaman (1909). Open points are those of D'Ans and Katz (1941) and D'Ans. et al. (1955) at $20^{o}C$. It is difficult to obtain any definitive information from these data. We, therefore, estimate the intermediate concentration behavior of $MgOH^{+}$ from the Culberson and Pytkowicz (1973) measurements of pK_w in artificial seawater. Adjustments in the third virial coefficients, $\psi_{Mg,MgOH,Cl}$, are then made so the DBF data are fit at high concentration. We select these over the other data in Fig. (13) since the model fit to the dilute solution and seawater system approximately without the third virial coefficient predicts these data. We also require that the Brucite-Oxychloride invariant point is less than 2M $MgCl_2$ since Bodine (1976) observes conversion of Brucite to Oxychloride slightly above this concentration. The chemical potential for Brucite is evaluated from the equilibrium constant given by McGee and Hostetler (1973).

In fitting the model to the Culberson and Pytkowicz (1973) data, the composition of the artificial seawater used in the experiments is also used in the calculations, except that NaF is replaced by NaCl. The presence of F in solution should cause a decrease in the total (stoichiometric) activity coefficient for H due to HF association. The experimentally determined apparent equilibrium constant, $K_w' = m_H^T m_{OH}^T$, should therefore be larger in solutions with traces of fluorine than in solutions without fluorine.

However, Hansson (1972) has determined K_w in the absence of F, and his values are larger than those in the fluorine containing solutions when corrected to the same units as CP. Our calculations indicate that the difference cannot be explained by the concentration differences of the artificial seawater used in the different studies. For the above reasons, we make no corrections for this effect. The fitted results are compared to the data in Table 6. Values for ΔpH (Eq. (17)) calculated from these data and the activity coefficient for H (in molality units) are also given.

The $Mg\text{-}HCO_3$ and $Mg\text{-}CO_3$ interaction parameters are estimated from the Hansson (1973) data for K_1' and K_2' in seawater together with the high pressure Nesquehonite solubility data of Mitchell (1923) and the $P_{CO_2} \sim 1$ atm result of Kline (1929). The high pressure (1-10 atm) trend for the solubility has been reproduced at a number of different temperatures and the .97 atm result is in agreement with these determinations as well as the smoothed temperature dependence (See Linke (1965) and Langmuir (1965)). In fitting the high pressure results the fugacity-pressure correction is made as in the $CaCO_3$ system.

In Table 7, reported pK_1' and pK_2' values are compared to those calculated. The total hydrogen activity coefficients (in NBS convention), determined by Mehrback et al. (1973) may be used with the calculated activity coefficients in the MacInnes convention to evaluate the liquid junction potential contribution, ΔpH, using Eq. (17) (Section IV). The resulting values differ from those calculated with the Culberson and Pythowicz (1973) data by about .02 pH units (see Table 6). Since the differences in the concentration are small (as

comparison of the calculated γ_H^M suggests), this would appear to reflect a changing liquid junction potential. (Mehrbach et al. (1973) observe a .011 pH change between "identical" reference electrodes.)

There appear to be some problems with the lower pressure results of Kline (1929). A solubility product for Nesquehonite of 3.5×10^{-5} is consistent with the Kline Brucite-Nesquehonite equilibrium P_{CO_2} (.00038 atm.) and the McGee and Hostetler (1973) Brucite solubility product. Using the 3.5×10^{-5} value and the analytic concentrations of Mg and HCO_3 cited by Kline, $\gamma^{\pm}_{Mg(HCO_3)_2}$ is calculated to be greater than one at lower pressures. Assuming the solubility product of 1.1×10^{-5} cited by Kline, $\gamma^{\pm}_{Mg(HCO_3)_2}$ = .76 at P_{CO_2} = .000511. The limiting law value of $\gamma^{\pm}_{Mg(HCO_3)_2}$ is .59. To fit this difference with an extended Debye-Hückel equation requires a very large ionic radius of about 10 Å (for a model without ion pairs). Furthermore, this 10 Å Debye-Huckel model is not consistent with the reproducible (see above) solubility data of Nesquehonite at $P_{CO_2} \simeq 1$ atm.

Assuming that the Kline Nesquehonite data are accurate, a $K_{sp} = 1.2 \times 10^{-4}$ may be determined from the Mg and HCO_3 concentrations at low pressures assuming limiting law activity coefficients. To explain the high carbonate concentrations at low pressures a $MgCO_3^o$ ion pair (or large negative $MgCO_3$ interaction parameters) may be defined. This model, however, cannot account for the rapidly decreasing total CO_3 concentration observed by Kline at high pressure. (The $MgCO_3^o$ concentration is fixed when in equilibrium with Nesquehonite (neglecting small changes in a_{H_2O}) and the concentration determined from the low pressure data is significantly larger than the total CO_3 observed at high pressure.)

To explain the Kline data, we must assume that enormous changes in the interactions occur over a very small concentration range. We could not fit the Kline data, using a number of conventional electrolyte solution models including those with and without $MgHCO_3$, etc. type ion pairs.

Kline points to some problems with his HCO_3^- determination. Also, his solutions may not have equilibrated with the low P_{CO_2} atmospheres in 3 to 5 days. As Nesquehonite dissolves, CO_2 is depleted from solution. If CO_2 were not sufficiently replenished from the atmosphere, the apparent CO_2 pressure could be significantly reduced and Brucite would precipitate. This might explain Kline's observation of Nesquehonite to Brucite conversion at a seemingly high P_{CO_2}. Using our model derived from data other than Kline's we calculate the total Mg concentration at Nesquehonite-Brucite equilibrium to be .0140. This is in agreement with the value of .0136 which Kline extrapolated from his alkalinity measurements, but our calculated transition pressure is 7.6×10^{-5} atm. as compared to Kline's value of 3.8×10^{-4} atm. Further data for this system are needed.

After establishing the parameters β^0 and $\beta^{(1)}$ for the $MgHCO_3$ and $MgCO_3$ systems, the parameters ψ_{mg,HCO_3,SO_4} and $\psi_{Mg,HCO_3,Cl}$ were obtained from the Nesquehonite solubility data of Trendafelov et al. (1981). The low concentration end of this data places a rather strong constraint on the acceptable values of $\beta^{(1)}$ and $\beta^{(0)}$. The predicted solubilities of the model for these systems are compared to experimental data in Fig. (14).

In Fig. (15), the pH for 35‰ salinity seawater in equilibrium with Calcite is plotted versus the carbonate alkalinity. The data are those of Morse et al.(1980). These authors determine the Calcium concentration, pH, and carbonate alkalinity, A_c. Calcite equilibrium is approached from supersaturation and undersaturation in a closed apparatus. The supersaturation experiments are performed by adding Calcite to natural seawater. For these experiments the relationship, $2m_{Ca}-A_C - Q$, (where Q is a constant for seawater), is approximately satisfied by their data. The curve corresponding to the data from supersaturation is calculated using seawater with composition given in Table 8. In Table 8, the molal concentration of 35‰ salinity seawater are given together with

the calculated total MacInnes ion activity coefficients. The seawater concentrations are derived from the Appendix Table 2 in Riley and Skirrow (1975).

Starting with natural seawater, in contact with calcite crystals, calcite will precipitate from solution under atmospheric conditions. Specification of one additional variable, such as pH, P_{CO_2} or A_c is sufficient to completely define chemical equilibrium. For a given value of Ac, the pH and P_{CO_2} can be calculated from equilibrium conditions using a model. The data and calculated curve in Fig. 15 represent the dependence of the equilibrium pH as a function of A_c. The apparent P_{CO_2} also varies along the curve. By virtue of electrical neutrality constants, the function is independent of the equilibrium values of P_{CO_2}, pH or A_c. For unmodified seawater Q =.018 eq/kgSW.

To approach calcite equilibrium from undersaturation, Morse et al. add a small amount of HCl to undersaturate the natural seawater with respect to Calcite. From the average value of Q calculated for the data from undersaturation, the quantity of HCl added has been estimated and added to the synthetic seawater in Table 8. This modified seawater solution was then used to calculate the curve corresponding to the undersaturation approach to equilibrium (leftmost curve in Fig.15).

The solid curves in Fig. 15 correspond to the calculated "pH" using the conventional hydrogen activity for the MacInnes convention. The two dashed curves are calculated assuming that ΔpH for the Morse et al. apparatus equals .03 (Table 6) or .05 (Table 7). The .05 curve is generally above the undersaturated data points and below the supersaturation points. There appears to be little trend in the data with equilibration times or the small variations in Q. Morse et al. also report no statistically significant variation in the solubility with the solid Calcite to solution ratio.

The increased solubility due to the precipitation of Magnesium-Calcite surface layers has recently received careful consideration (Wollast et al. (1980); Schoonmaker (1981). The measurements from supersaturation of Morse

et al. should presumably be sensitive to this effect although undersaturated experiments should not. With the uncertainty due to the liquid junction and the potential formation of Magnesium Calcite surface layers, it is not possible to make an exact comparison to the data of Morse et al. Pessimistically, the calculation is within 10% of the true solubility. If pH = .05 and the data represent true Calcite equilibrium the agreement is much better. Using the model, a value of $K'_{Calcite} = m^T_{Ca}\ m^T_{CO_3} = 4.98 \times 10^{-7} (molal)^2$ is obtained. $(4.65 \times 10^{-7}\ (moles/kgSW)^2)$.

VI. DISCUSSION

In the previous section, we have utilized, for the most part, data in binary and ternary systems to parameterize the solution model. We have tested the model by calculating mineral solubilities in different, more complex systems. For example, in Fig. 15, the predicted relationship between the pH and carbonate alkalinity of 35% salinity seawater in equilibrium with calcite is shown to be in good agreement with experiment.

The general agreement of these predictions with the available data demonstrates the value of the Pitzer approach in modeling natural systems. The thermodynamic properties of rather complex and possibly concentrated multicomponent solutions can be accurately predicted from a knowledge of the thermodynamics of relatively simple component solutions.

The chemistry of seawater has been well measured. While this system provides an excellent test of the model, there are other models which can accurately produce these data over a limited range of composition and concentration. The model, used in calculating Fig. (15), also accurately predicts thermodynamic properties to very high concentration for systems of composition very different from seawater. This capability is unique. Since many natural systems differ considerably from seawater (e.g., formational waters in oil fields, evaporite interstitial waters, estuarine brines, etc.) this is an important generalization. To illustrate this flexibility, the predicted halite-saturated Jänecke projection for the $Na-K-Cl-SO_4-CO_3-H_2O$ quinary system is compared to experimental data in Fig. (16a).

The calculations and data depicted in Fig. (16a) are confined to a closed system, where CO_3 bearing minerals are dissolved in water and CO_2 transfer between the atmosphere and solution is prevented. For many natural waters, the aqueous CO_2 activity or the effective equilibrium P_{CO_2} is controlled by reaction with the atmosphere, photosynthesis, water-rock reactions, etc. Fig. (16b) and (16c) depict the change in the phase equilibria from that shown in Fig. (16a) when the solutions are allowed to equilibrate with a gas phase of constant P_{CO_2} (3.3×10^{-4} and 3.3×10^{-3} atm., respectively).

Comparison of Fig.s (16a), (16b) and (16c) illustrates the strong P_{CO_2} dependence of the stable mineral equilibria. It is known that the aqueous CO_2 activity is an important indicator of the chemical processes leading to the formation and subsequent diagenetic evolution of carbonate sediments. However, quantitative interpretation of carbonate sediments in terms of this CO_2 variable has not generally been possible due to the lack of data or of a sufficiently accurate model. The model described here enables accurate prediction of the CO_2 activity for arbitrary fluid composition in the eight-component system. This allows improved analysis of mineral stabilities and directions of diagenetic reactions in carbonate mineral systems by quantitative equilibrium and ion activity product calculations.

It is apparent that we have relied on a diverse set of data, much of which is over half a century old, in our effort to obtain a complete model for the system $Na-K-Ca-Mg-H-Cl-SO_4-OH-HCO_3-CO_3-CO_2-H_2O$. We have attempted to identify compositional ranges where data would significantly improve the accuracy of the model. For many systems, it was necessary to estimate parameter values from limited and often unreproduced data. We believe that an increased effort to experimentally characterize the chemical interactions between the various aqueous species by examining the thermodynamics of binary and ternary systems in detail

will lead to a significant improvement in the quantitative understanding of the thermodynamics of carbonate natural waters.

We have utilized earlier versions of the Pitzer parameters, some of which have more recently been improved (see Downes and Pitzer (1976); Pieper and Pitzer (1981)). In the future, as refinements of the model are made, we will attempt to incorporate the currently accepted parameter values into the solubility model. The reader is cautioned, however, from modifying parameters in the present model without extensive checking of the calculated solubilities, since the parameters are quite interdependent.

The most important limitation of the application of this and similar models to natural systems is the inherent equilibrium nature of the predictions. Most natural systems constantly evolve due to various environmental and biological factors and therefore are never in a state of total equilibrium. The uses of such models must therefore be directed toward identifying and understanding the chemical processes by which natural systems change. In the study of surface waters and interstitial fluids, the calculated mineral saturation states are commonly utilized to infer possible chemical processes which influence the evolution of a given formation. In more specific studies of closed-basin systems, simple hydrological models which utilize an equilibrium assumption can be used to place constraints on the inflow composition, and to calculate approximate mineral precipitation sequences and lake water compositions (see Eugster and Jones (1979)). Such calculations can provide additional guidelines useful in constructing a model for the evolution of a given natural system. Recently, we have used this model to compare the evolution of seawater in natural evaporation processes with the predictions of chemical equilibrium. The agreement between the results of the equilibrium models and the measured field results

is remarkable, emphasizing the value of equilibrium evaporation paths as guidelines for understanding evaporite evolution (Møller-Weare et al., in preparation).

Many natural systems evolve through chemical reactions with aqueous solutions. The principle transport mechanisms include convention and diffusion within the interstitial pores of a rock medium. When the important processes are sufficiently slow (in particular from diffusion) local chemical equilibrium between the fluid and the porous medium can be established. Local equilibrium is commonly observed in a number of geological environments (Korzkinskii (1959), Thompson (1959)). Recent evidence indicates that local equilibrium is established for some minerals in lake beds and oceanic sediments. The data of Emerson et al. (1980) and Sayles (1981) suggest that Calcite equilibrium is maintained in some seawater sediments. A similar calculation using the model described here has indicated that Gypsum saturation is maintained at various depths in the sediments of the Great Salt Lake (Spencer (1980)). When local equilibrium conditions are maintained, the time-dependent features of geochemical evolution may be treated by incorporating equilibrium models into a hydrodynamic flow model (Weare et al. (1976)).

Acknowledgement

We gratefully acknowledge many fruitful discussions with Hans P. Eugster and the help of J. P. Greenberg with the parameterization in the $MgCO_3$ system. The manuscript was improved through comments by Andrew Dickson. Work was supported by the Petroleum Research Fund, PRF # 12692-AC5, Department of Energy, ATO3-81SF-11563 and 4X29-935M-1 and the National Science Foundation, OCE82-08482.

REFERENCES

ÄKERLOF, G., SHORT, O. (1937) Solubility of sodium and potassium chlorides in corresponding hydroxide solutions at 25°C. J. Amer. Chem. Soc. 59, 1912-1915.

ANGUS, S., ARMSTRONG, B., REACH, K. M. (1976) International Thermo-Dynamics Tables of Fluid State Carbon Dioxide, Pergamon Press, Oxford.

BACKSTROM, H. L. J. (1921) Über die Afinität der Aragonite-calcite-Umwandlung. Z. Phys. Chem. 97, 179-222.

BATES, R. G. (1973) Determination of pH-Theory and Practice, John Wiley and Sons, Inc. (Second Edition).

BATES, R. G., BOWER, V. E., CANHAM, R. G., PRUE, J. E. (1959) The dissociation constant of $CaOH^+$ from 0° to 40°C. Trans. Faraday Soc. 55, 2062-2068.

BATES, R. G., GUGGENHEIM, E. A. (1960) Report on the Standardization of pH and Related Terminology. Pure and Appl. Chem. 1, 163-168.

BAYLISS, N. S., KOCH, D. F. A. (1952) Investigation of the Engel-Precht Method for the Production of Potassium Carbonate. Aust. J. Appl. Sci. 3, 237-251.

BERECZ, E., BADER, I. (1973) Physiochemical study of ternary aqueous electrolyte solutions VII. Viscosities and densities of the $MgCl_2$-HCl-H_2O system and the solubility of $MgCl_2$. Acta Chim. Acad. Sci. Hung. 77,

BLASDALE, W. C. (1923) Equilibrium in solutions containing mixtures of Salts III. The system, water and the chlorides and carbonates of sodium and potassium at 25°C. IV. The system, water and the sulfates and carbonates of sodium and potassium at 25°C. J. Amer. Chem. Soc. 45, 2935-2946.

BODINE, M. W. JR. (1976) Magnesium hydrochloride: A possible pH buffer in marine evaporites. Geology 4, 76-80.

BOGOYAVLENSKII, P. S., Manannikova, A. S. (1955) The system NaCl-$NaHCO_3$-H_2O at 25°C. Zh. Prikl. Khim. 18, 325-328.

BONNER, F. T. (1944) Ph.D. Dissertation Yale University, New Haven, CT. June 1944.

BOWEN, N. L. (1928) The Evolution of Igneous Rocks, Princeton Univ. Press.

BRIGGS, C. C. (1978) Ph.D. Thesis, University of Sheffield, Sheffield, England.

CALLEN, H. B. (1960) Thermodynamics, John Wiley and Sons, New York.

CAMERON, F. K., BELL, J. M. (1906) The system lime, gypsum, water at 25°C. J. Amer. Chem. Soc. 28, 1220-1222.

CAMERON, F. K., BELL, I.M., ROBINSON, W. O. (1907) The solubility of certain salt present in alkali soils, J. Phys. Chem. 11, 396-420.

CAMERON, F. K., SEIDELL, A. (1902) Solubility of calcium carbonate in aqueous solutions containing certain electrolytes in equilibrium with atmospheric air, J. Phys. Chem. 6, 50-56.

CASPARI, W. A. (1924) The system sodium-carbonate-sodium sulfate-water. J. Chem. Soc. 125, 2381-2387.

COVINGTON, A. K., DOBSON, J. V., WYNNE-JONES, W. F. K. (1965) Dissociation constant of the bisulfate ion at 25°C. Trans. Faraday Soc. 61, 2057-2062.

CULBERSON, C. H., PYTKOWICZ, R. M. (1973) Ionization of Water in Seawater Mar. Chem. 1, 309-316.

D'ANS, J. (1913) Acid sulfates and pyrosulfates of sodium potassium and ammonium Z. Anorg. Chem. 90, 235-245.

D'ANS J. (1933) Die Losungsgleichgewichte der Systeme der Salze Ozeanischer Salzblagerungen. Kail-Forschungsanstalt, Berlin.

D'ANS, J., BUSSE, W., FREUND, H. (1955) Über Basische Magnesiumchloride, Kali U. Steinsaltz 8, 3-7.

D'ANS, J. KATZ, W. (1941) Magnesiumhydroxyd-Loslichkeiten, pH-zahlen und Pufferung im System H_2O-M_gCl_2-$Mg(OH)_2$, Kali 35, 37-41.

D'ANS, J., SCHREINER, O. (1910) Z. Anorg. Chem. 67, 437.

DAVIES, C. W., JONES, H. W., MONK, C. B. (1952) E.M.F. studies of electrolytic dissociation, Part I - sulfuric acid in water.

DOWNES, C. J., PITZER, K. S. (1976) Thermodynamics of Electrolytes. Binary Mixtures Formed from Aqueous NaCl, Na_2SO_4, $CaCl_2$ and $CaSO_4$ at 25°C. J. Soln Chem. 5, 389-398.

EMERSON, S., JAHNKE, R., BENDER, M., FROELICH, P., KLINKHAMMER, G., BOWSER, C., SETLOCK, G. (1980) Early diagenesis in sediments from the eastern equatorial Pacific I. Pore water nutrient and carbonate results. Earth Planet. Sci. Lett. 49, 57-80.

EUGSTER, H. P. (1966) Sodium carbonate-bicarbonate-minerals as indicators of P_{CO_2} J. Geophys. Research 71, 3369-3379.

EUGSTER, H. P., HARVIE, C. E., WEARE, J. H. (1980) Mineral equilibria in a six-component seawater system, Na-K-Mg-Ca-SO_4-Cl-H_2O, at 25°C. Geochim. Cosmochim. Acta 44, 1335-1347.

EUGSTER, H. P., JONES, B. F. (1979) Behavior of major solutes during closed-basin brine evolution. Amer. J. Sci. 279, 609-631.

FILIPPOV, V. K., ANTONOVA, V. A. (1978) The thermodynamic study of the $MgSO_4$-H_2SO_4-H_2O ternary system. Zh. Prikl. Khim. 51, 251-255 (trans.)

FOOTE, H. W. (1919) Ind. Eng. Chem. 11, 629-631.

FRATINI, N. (1949) Ann. Chim. Applicata. 39, 616-620.

FREAR, G. L., JOHNSTON, J. (1929) The solubility of calcium carbonate (calcite) in certain aqueous solutions at 25°C. J. Amer. Chem. Soc. 51, 2082-2093.

FREETH, F. A. (1922) II. The system Na_2O-CO_2-NaCl-H_2O considered as two four-component solutions, Royal Soc. London Phil. Trans. Ser. A, 223, 35-87.

GARRELS, R. M., THOMPSON, M. E. (1962) A chemical model for seawater at 25°C and one atmosphere total pressure, Amer. Jour. Sci. 260, 57-66.

GEFFCHEN, G. (1904) Z. Physik Chem. 49, 271-296.

GUGGENHEIM, E. A. (1929) The conception of electrical potential difference between two phases and the individual activity of ions. J. Phys. Chem. 33, 842-849.

GUGGENHEIM, E. A. (1930a) On the conception of electrical potential difference between two phases, II. J. Phys. Chem. 34, 1541-1543.

GUGGENHEIM, E. A. (1930b) Studies of cells with liquid-liquid junctions, Part II. Thermodynamic significance and relationship to activity coefficients, J. Phys. Chem. 34, 1758-1766.

GUGGENHEIM, E. A. (1960) Thermodynamics, North-Holland Publishing Co., John Wiley and Sons (5th edition).

HAASE, R. (1963) Thermodynamics of Irreversible Processes. Addison-Wesley Publishing Co.

HANSSON, I. (1972) An analytic approach to the carbonate system in seawater. Thesis, University of Goteborg, Goteborg, Germany.

HANSSON, I. (1973) A new set of acidity constants for carbonic acid and boric acid in seawater. Deep Sea Research 20, 461.

HARNED, H. S., BONNER, F. T. (1945) The first ionization of carbonic acid in aqueous solutions of sodium chloride. J. Amer. Chem. Soc. 67, 1026-1031; also see Bonner (1944).

HARNED, H. S., DAVIS, R., JR. (1943) The ionization constant of carbonic acid in water and the solubility of carbon dioxide in water and aqueous salt solutions from 0° to 50°C, J. Amer. Chem. Soc. 65, 2030-2037.

HARNED, H. S., OWEN, B. B. (1958) The Physical Chemistry of Electrolyte Solutions, Reinhold (3rd Edition).

HARNED, H. S., SCHOLES, S. R., JR. (1941) The ionization constant of HCO_3 from 0° to 50°, J. Amer. Chem. Soc. 63, 1706-1709.

HARNED, H. S., STURGIS, R. D. (1925) The free energy of sulfuric acid in aqueous sulfate solutions, J. Amer. Chem. Soc. 47, 945-953.

HARVIE, C. E. (1981) Theoretical Investigations in Geochemistry and Atom Surface Scattering, Ph.D. Dissertation. Univ. Microfilm, Int., Ann Arbor, MI #AAD82-03026.

HARVIE, C. E., WEARE, J. H. (1980) The prediction of mineral solubilities in natural waters: The Na-K-Mg-Ca-Cl-SO_4-H_2O systems from zero to high concentration at 25°C, Geochim. Cosmochim. Acta 44, 981-997.

HARVIE, C. E., EUGSTER, H. P., WEARE, J. H. (1982) Mineral Equilibria in the six-component seawater system, Na-K-Mg-Ca-SO_4-Cl-H_2O at 25°C. II. Compositions of the saturated solutions, accepted for publication Geochim. Cosmochim Acta (Oct. 1982).

HARVIE, C. E., WEARE, J. H., EUGSTER, H. P., HARDIE, L. A. (1980) Evaporation of seawater: calculated mineral sequence, Science 208, 498.

HATCH, J. R. (1972) Phase relationships in part of the system sodium carbonate-calcium carbonate-carbon dioxide-water at one atmosphere pressure, Ph.D. Thesis, University of Illinois, Urbana, Illinois.

HAWLEY, J. D., PYTKOWICZ, R. M. (1973) Interpretation of pH measurements in concentrated electrolyte solutions, Mar. Chem. 1, 245-250.

HELGESON, H. C. (1978) Amer. J. Sci., 278A, and references therein.

HILL, A. E. (1930) Double salt formation among the carbonates and bicarbonates of sodium and potassium. J. Amer. Chem. Soc. 52, 3813-3817; Hydrated potassium sesquicarbonate $K_2CO_3 \cdot 2KHCO_3 \cdot 3/2\ H_2O$, J. Amer. Chem. 52, 3817-3825.

HILL, A. E., BACON, L. R. (1927) Ternary systems VI. Sodium carbonate, sodium bicarbonate and water, J. Amer. Chem. Soc. 49, 2487-2495.

HILL, A. E., HILL, D. G. (1927) Ternary systems V. Potassium bicarbonate, potassium carbonate and water, J. Amer. Chem. Soc. 49, 967-969.

HILL, A. E., MILLER, F. W., JR. (1927) Ternary Systems IV. Potassium carbonate, sodium carbonate, and water, J. Amer. Chem. Soc. 49, 669-686.

HILL, A. E., MOSKOWITZ, S. (1929) Ternary Systems VIII. Potassium carbonate, potassium sulfate and water, J. Amer. Chem. Soc. 51, 2396-2398.

HILL, A. E., SMITH, S. F. (1929) Equilibrium between the carbonates and bicarbonates of sodium and potassium, J. Amer. Chem. Soc. 51, 1626-1636.

HOSTALEK, Z. (1956) Chem. Listy 50, 716-720, 981-983.

ITKINA, L. S., KOKHOVA, F. S. (1953) Izv. Sktora Fix Khim. Analiza Inst. Obschch Neorgan Khim. Akad. Nauk SSR 23, 284-299.

JACOBSON, R. L., LANGMUIR, D. (1974) Dissociation constants of calcite and $CaHCO_3^+$ from 0^o to 50^oC, Geochim. Cosmochim. Acta 38, 301-318.

JOHNSTON, J., GROVE, C. (1931) The solubility of calcium hydroxide in aqueous salt solutions, J. Amer. Chem. Soc. 53, 3976-3991.

JONES, B. F. (1963) Hydrology and mineralogy of Deep Springs Lake, Inyo County, California, Ph.D. Thesis, The Johns Hopkins University, Baltimore, MD.

JONES, F. E. (1939)

JONES, H. W., MONK, C. B. (1952) E.M.F. studies of electrolytic dissociation, Part 2. Magnesium and lanthanum sulphates in water, Trans. Faraday. Soc. 48, 929-933.

KERRISK, J. F. (1981) Chemical equilibrium calculations for aqueous geothermal brines. LA-8851-MS. Los Alamos Sci. Lab., Los Alamos, NM. 87545.

KHOO, K. H., CHAN, C., LIM, T. K. (1977a) Thermodynamics of electrolyte solutions. The system $HCl+CaCl_2+H_2O$ at 298.15^oK, J. Soln. Chem. 6, 651-662.

KHOO, K. H., CHAN, C., LIM, T. K. (1977b) Activity coefficients in binary electrolyte mixtures HCl-$MgCl_2$-H_2O at 209.15°K, J. Soln. Chem. 6, 855-864.

KLEBANOV, G. S., PINCHUK, G. YA (1967) The solubility of system KI-KOH-H_2CO_3-H_2O, Zh. Prinkl. Khim. 40, 2426-2431.

KLINE, W. D. (1929) The solubility of magnesium carbonate (Nesquehonite) in water at 25°C and pressures of carbon dioxide up to 1 atm. J. Amer. Chem. Soc. 51, 2093-2097.

KORF, D. M., SHCHATROVSKAYA, L. P. (1940) Zh. Obshch. Khim. 10, 1231-1235.

KORZHINSKII, D. S. (1959) Physicochemical basis of the analysis of the paragenesis of minerals, New York Consultants Bur. 152p.; (1970) Theory of metasomatic zoning, London, Oxford University Press.

LANG, A. A., SUKAVA, A. J. (1958) The system KOH-K_2CO_3-H_2O at low temperatures, Can. J. Chem. 36, 1064-1069.

LANGMUIR, D. (1965) Stabilities of carbonates in the system MgO-CO_2-H_2O, Jour. Geol. 73, 730-753.

LINKE, W. F. (1965) Solubilities of Inorganic and Metal Organic Compounds, Am. Chem. Soc.

LUK'YANOVA, E. E. (1953)

MACINNES, P. D. (1961) Principles of Electrochemistry, Dover Publications, Inc.

MACINNES, D. A., BELCHER, D. (1933) The thermodynamic ionization constants of carbonic acid, J. Amer. Chem. Soc. 55, 2630-2646.

MAKAROV, S. Z., BLEIDEN, V. P. (1938) The polytherm of the quaternary system Na_2CO_3-Na_2SO_4-NaCl-H_2O and solid solutions of the Burkeite type, Izv. Akad. Nauk. SSSR Ser. Kim., 865-892. (English summary).

MAKAROV, S. Z., KRASNIKOV, S. N. (1956) A study of solid solution transformations in the $Na_2SO_4Na_2CO_3$ system. Izv. Sektora Fiz-Khim. Anal. Inst. Obshch. Neorg. Chim. Akad. Nauk. SSSR 27, 367-379.

MAKAROV, S. Z., JAKIMOV, M. N. (1933) Zh. Obschch. Khim. 3, 990-997.

MARKHAM, A. E., Kobe, J. A. (1941) The solubility of carbon dioxide and nitrous oxide in aqueous salt solutions, J. Am. Chem. Soc. 63, 449-454.

MARKHAM, A. E., KOBE, K. A. (1941a) The solubility of carbon dioxide in aqueous sulfuric and perchloric acids at 25°C, J. Amer. Chem. Soc. 63, 1165-1166.

MARSHALL, W. L., JONES E. V. (1966) Second dissociation constant of sulfuric acid from 25°C to 350°C. Evaluated from solubilities of calcium sulfate in sulfuric acid solutions, J. Phys. Chem. 70, 4028-4037.

MAYER, J. E. (1950) The theory of ionic solutions, J. Chem. Phys. 18, 1426-1436.

MCGEE, K. A. HOSTETLER, P. B. (1973) Stability constants for $M_g OH^+$ and Brucite below 100°C, Am. Geophys. Union Trans. 54, 487.

MCGEE, K. A., HOSTETLER, P. B. (1975) Studies in the system $MgO-SiO_2-CO_2-H_2O$. IV. The stability of $MgOH^+$ from 10^oC to 90^oC, Amer. J. Sci. 275, 304-317.

MEHRBACH, C. CULBERSON, C. H., HAWLEY, J. E., PYTOKOWICZ, R. M. (1973) Measurements of the apparent dissociation constants of carbonic acid in seawater at atmospheric pressure, Limnol. Oceanogr. 18, 897-907.

MILLIKAN, J. (1918) Die oxyhaloide der alkalischen erden. Gleichgewichte in ternaren systemen II. Z. Physik. Chem. 92, 496-520.

MILLER, J. P. (1952) A portion of the system calcium carbonate-carbon dioxide-water with geological implications, Amer. Jour. Sci. 250, 161-203.

MITCHELL, A. E. (1923) Studies on the Dolomite system, Part II. J. Chem. Soc. 123, 1887-1904.

MORSE, J. W., MUCCI, A., MILLERO, F. J. (1980) The solubility of calcite and aragonite in seawater of 35% salinity at 25^oC and atmospheric pressure, Geochim. Cosmochim. Acta 44, 85-94.

NAIR, V. S. K., NANCOLLAS, G. H. (1958) Thermodynamics of ion association, Part V. Dissociation of the bisulphate ion, J. Chem. Soc. __, 4144-4147.

NORDSTROM, P. K., PLUMMER, L. N., WIGLEY, T. M. L., WOLERY, T. J., BALL, J. W., JENNE, E. A., BASSETT, R. L., CRERAR, D. A., FLORENCE, T. M., FRITZ, B., HOFFMAN, M., HOLDREN, G. R., JR., LAFON, G. M., MATTIGOD, S. V., MCDUFF, R. E., MOREL, F., REDDY M. M., SPOSITO, G., THRAILKILL, J. (1979) A comparison of computerized chemical models for equilibrium calculation in aqueous systems, Symp. Series Amer. Chem. Soc.

OGLESBY, N. E. (1929) A study of the system sodium bicarbonate-potassium bicarbonate-water, J. Amer. Chem. Soc. 51, 2352-2362.

PEIPER, J. C., PITZER, K. S. (1981) Thermodynamics of aqueous carbonate solutions including mixtures of sodium carbonate, bicarbonate and chloride (in preparation).

PITZER, K. S. (1972) Thermodynamic properties of aqueous solutions of bivalent sulphates, J. Chem. Soc., Faraday Trans. II, 68, 101-113.

PITZER, K. S. (1973) Thermodynamics of Electrolytes I: Theoretical basis and general equations, J. Phys. Chem. 77, 268-277.

PITZER, K. S. (1975) Thermodynamics of Electrolytes V: Effects ofhigher order electrostatic terms, J. Solution. Chem. 4, 249-265.

PITZER, K. S., KIM, J. (1974) Thermodynamics of Electrolytes IV: Activity and osmotic coefficients for mixed electrolytes, J. Am. Chem. Soc. 96, 5701-5707.

PITZER, K. S., MAYORGA, G. (1973) Thermodynamics of Electrolytes II: Activity and osmotic coefficients for strong electrolytes with one or both ions univalent, J. Phys. Chem. 77, 2300-2308.

PITZER, K. S., MAYORGA, C. (1974) Thermodynamics of Electrolytes III: Activity and osmotic coefficients for 2-2 electrolytes. J. Soln. Chem. 3, 539-546.

PITZER, K. S., PEIPER, J. C. (1980) The activity coefficient of aqueous $NaHCO_3$, J. Phys. Chem. 84, 2396-2398.

PITZER, K. S., ROY, R. N., SILVESTER, L. F. (1977) Thermodynamucs of electrolytes 7. Sulfuric acid, J. Amer. Chem. Soc. 99, 4930-4936.

PITZER, K. S., SILVESTER, L. F. (1976) Thermodynamics of electrolytes VI. Weak Electrolytes including H_3PO_4, J. Soln. Chem. 5, 269-277.

RANDALL, M., LANGFORD, C. T. (1927) The activity coefficient of sulfuric acid in aqueous solutions with sodium sulfate at 25°C, J. Amer. Chem. Soc. 49, 1445-1450.

REARDON, E. J., LANGMUIR, D. (1974) Thermodynamic properties of the ion pairs $MgCO_3^o$ and $CaCO_3^o$ from 10°C to 50°C, Amer. Jour. Sci. 274, 599-612.

RILEY, J. P., SKIRROW, G. (1975) Chemical Oceanography, Academic Press (2nd Edition).

ROBIE, R. A., HEMINGWAY, B. S., FISCHER, J. R. (1978) Thermodynamic properties of minerals and related substances at 298.15K and 1 bar pressure and at high temperatures, U.S.G.S. Bulletin 1452.

ROBINSON, R. A., BOWER, V. E. (1966) J. Res. Nat. Bur. Stand. Sect. A 70, 313.

ROBINSON, R. A., MACASKILL, J. B. (1979) Osmotic coefficients of aqueous sodium carbonate solutions at 25°C, J. Soln. Chem. 8, 35-40.

ROBINSON, R. A., STOKES, R. H. (1968) Electrolyte Solutions, Butterworths.

ROBINSON, W. O., WAGGAMAN, W. H. (1909) Basic Magnesium Chlorides, J. Phys. Chem. 13, 673-678.

ROGERS, P. S. K. (1981) Thermodynamics of Geothermal Fluids, Ph.D. Thesis, Univ. of California, Berkeley.

SAYLES, F. L. (1981) The composition and diagenesis of interstitial solutions II. Fluxes and diagenesis at the water-sediment interface in the high latitude North and South Atlantic, Geochim. Cosmochim. Acta 45, 1061-1086.

SCHOONMAKER, J. E. (1981) Magnesian Calcite-Seawater Reactions, Solubility and Recrystallization Behavior. Ph.D. Thesis, Northwestern University, Evanston, Illinois.

SHATKAY, A., LERMAN, A. (1969) Individual Activities of Sodium and Chloride Ions in Aqueous Solutions of Sodium Chloride. Anal. Chem. 41, 514-517.

SHTERNINA, E. B., FROLOVA, E. V. (1952) The solubility of calcite in the presence of CO_2 and NaCl, Iz. Sek. Fiz. Khim. Anal. Inst. Ob. Neorg. Khim. Akad. Nauk SSSR 21, 271-287. (English translation: associated Tech. Services, New Jersey, USA)

SHTERNINA, E. B., FROLOVA, E. V. (1962) Extraction of Ballast Carbonates from Kara-Tau Phosphorite Ore, Zh. Prikl. Khim. 35, 751-756. (Tr. J. Chem. USSR 35, (1962), 729-733).

SPENCER, R. S. (1980) Personal communication.

STOCK, D. I., DAVIES, C. W. (1948) The second dissociation constant of Magnesium hydroxide. Trans. Faraday Soc. 44, 856-859.

STORONKIN, A. V., SHUL'ts, M. M., LANGUNOV, M. D., OKATOV, M. A. (1967) Aqueous solutions of strong electrolytes IV. Activity of hydrogen chloride in the hydrochloric acid-sulfuric acid-water system and of sodium chloride in the sodium chloride-sodium sulfate-water system, Russ. J. Phys. Chem. 41, 541-543.

STOROZHENKO, V. A., SHEVCHUK, V. G. (1971) The K_2SO_4-H_2SO_4-H_2O system at 25°C, Russ. J. Inorg. Chem. 16 (1), 121-124.

TAYLOR, P. B. (1927) Electromotive force with transference and theory of interdiffusion of electrolytes, J. Phys. Chem. 31, 1478-1500.

TEEPLE, J. E. (1929) The industrial development of Searles Lake brines with equilibrium data, Amer. Chem. Soc. Mono. Ser.

THOMPSON, J. B. (1959) Local equilibrium in metasomatic processes. In: Abelson, P. H. (ed.) Researches in Geochemistry V. 2, New York, John Wiley and Sons, 427-457.

TRENDAFELOV, D., MARKOV, L. and BALAREV, Kh. (1981) Phase equilibria in the $MgCO_3$-$MgSO_4$-H_2O and $MgCO_3$-$MgCl_2$-H_2O systems at 25°C in a CO_2 atmosphere, Russ. J. Inorg. Chem. 26 (6), 907-909.

VAN'T HOFF, J. H. (1912) Untersuchungen uber die Bildungsterhaltnisse der Ozeanischen Salzablagerungen, insobesondere das Stassfurter Salzlagers. Leipzig (and references therein).

WEARE, J. H., STEPHENS, J. R., EUGSTER, H. P. (1976) Diffusion metasomatism and mineral reaction zones. General principles and applications to feldspar alteration, Amer. Jour. Sci. 276, 767-816.

WINDMAISSER, F., STOCKL, F. (1950) Monatsb. 81, 543-550.

WOLLAST, R., GARRELS, R. M., MACKENZIE, F. T. (1980) Calcite-Seawater

YASUNISKI, A., YOSHIDA, F. (1979) Solubility of carbon dioxide in awueous electrolyte solutions, J. Chem. Eng. Data 24, 11-14.

YEATTS, L. B., MARSHALL, W. L. (1957) Aqueous systems at high temperatures, XVIII. Activity coefficient behavior of calcium hydroxide in aqueous sodium nitrate to the critical temperature of water, J. Phys. Chem. 71, 2641-2650.

Appendix A

As has been discussed in detail by Guggenheim (1929; 1930a) an ion activity or ion chemical potential cannot be measured by experiment; e.g., emf, phase equilibria, diffusion rates or reaction rates. However, ion activities may be defined by convention. In the following discussion, we demonstrate that the emf for a cell with a liquid junction can be calculated using any convention for the ion activities. Similar analyses implying the following results are discussed elsewhere (Bates (1973), Guggenheim (1960) and MacInnes (1961)).

Consider the electrochemical cell, discussed in section IV,

$$Pt,H_2|\text{soln X}||KCl(sat)|Hg_2Cl_2,Hg|Pt \quad . \qquad (A)$$

The emf of the cell is not an equilibrium property of the system. In addition to the reversible electrode potential, the electomotive force, E, of the cell depends on the electro-potential difference between solution, X, and the KCl-saturated solution. This liquid junction potential develops because of ionic diffusion between the two solution phases, and therefore, depends upon the relative mobilities of the various ionic species in solution. Using the principles of irreversible thermodynamics (see Haase (1963) for a general derivation), the following equation is obtained for the emf of cell A:

$$E = E^* - \frac{RT}{F}\left(\ell n\ a_H(X) + \ell n\ a_{Cl}(KCl) + \int_X^{KCl} \sum_k \frac{t_k}{z_k}\ d\ \ell n\ a_k \right) . \qquad (A1)$$

E^* is given by,

$$E^* = \frac{1}{2F}\left(\mu^0_{H_2} + RT\,\ell n\, f_{H_2} + \mu^0_{Hg_2Cl_2} - 2\mu^0_{Hg} - 2\mu^0_{H} - 2\mu^0_{Cl}\right) . \qquad (A2)$$

In Eq. (A1), t_k is the reduced Hittof transference number of ion k, and z_k is the charge on ion k. By definition, the transference numbers satisfy the relationship,

$$\sum_k t_k = 1 \quad . \qquad (A3)$$

The sum in Eqs. (A1) and (A3) includes all ionic species in the solution. The integration in Eq. (A1) extends over the transition region from solution X to the KCl saturated solution. The ionic activities in Eqs. (A1) are theoretically defined by a derivative in the free energy (i.e., Eq. (2a) in Section II).

Any arbitrary function of composition, $\omega(x)$, satisfies the equation,

$$\ell n\, \omega(KCl) - \ell n\, \omega(X) = \int_X^{KCl} d\, \ell n\, \omega = \int_X^{KCl} \sum_k \frac{t_k}{z_k}\, d\,(z_k\, \ell n\, \omega), \qquad (A4)$$

where Eq. (A3) has been used to obtain the last identity. Adding this equality to Eqs. (A1) and collecting similar terms, the following equation, identical to Eq. (A1) is obtained

$$E = E^* - \frac{RT}{F}\left[\ell n\, a_H(X) + z_H\, \ell n\, \omega(X) + \ell n\, a_{Cl}(KCl) + z_{Cl}\, \ell n\, \omega(KCl) + \int_X^{KCl} \sum_k \frac{t_k}{z_k}\, d\left(\ell n\, a_k + z_k\, \ell n\, \omega\right)\right] . \qquad (A5)$$

The cell emf is independent of the arbitrary function, ω.

The activity coefficient for ion k is defined by the familiar equation,

$$a_k = \gamma_k m_k \quad . \tag{A6}$$

Consider the conventional definition for the ion activity coefficients given by the equation,

$$\gamma_k^C = \gamma_k \omega^{z_k} \quad , \tag{A7}$$

where ω is chosen common to all ions in a particular solution. The conventional ion activity coefficients so defined are consistent with the measurable mean activity coefficients since,

$$(\gamma_M^C)^{\nu_M} (\gamma_X^C)^{\nu_X} = (\gamma_M)^{\nu_M} (\gamma_X)^{\nu_X} \omega^{(z_M\nu_M + z_M\nu_X)} = (\gamma_M)^{\nu_M} (\gamma_X)^{\nu_X} = (\gamma_{MX}^{\pm})^{\nu} \tag{A8}$$

In obtaining Eq. (A8), the identities $z_M\nu_M + z_X\nu_X = 0$ and $\nu_M + \nu_X = \nu$ have been used. Using the definition for ion activity coefficients in Eqs. (A6), conventional ion activities are calculated by the equation,

$$a_k^C = \gamma_k^C m_k = \gamma_k m_k \omega^{z_k} = a_k \omega^{z_k} \quad . \tag{A9}$$

Substituting the natural logarithm of Eq. (A9) for terms like $\ell n\ a_k + z_k\ \ell n\ \omega$ in Eq. (A5), the following equation for the cell emf in terms of the conventional ion activities is obtained:

$$E = E^* - \frac{RT}{F}\left[\ell n\ a_H^C(X) + \ell n\ a_{Cl}^C(KCl) + \int_X^{KCl} \sum_k \frac{t_k}{z_k}\ d\ \ell n\ a_k^C\right] . \qquad (A10)$$

Comparison of Eq. (A1) and (A10) indicates that any conventional ion activities defined by Eq. (A9) may be substituted for the theoretical ion activities in calculating the emf by Eq. (A1) without making any approximation. Therefore, it is impossible to distinguish between the various conventional or the theoretical ion activities using the measured values of the emf. Consequently, it is not possible to utilize such data to unambiguously obtain any information regarding real ion activities. This is a general result (Taylor (1927), Guggenheim (1929, 1930a)).

For convenience, Eq. (A10) may be written as :

$$E = E_O^C - \frac{RT}{F}\ \ell n\ a_H^C(X) - E_{LJ}^C(X) \quad . \qquad (A11)$$

E_O^C and E_{LJ}^C are defined by the equations,

$$E_O^C = E^* - \frac{RT}{F}\ \ell n\ a_{Cl}^C(KCl) \qquad \text{and} \qquad (A12)$$

$$E_{LJ}^C(X) = \frac{RT}{F}\int_X^{KCl} \sum_k \frac{t_k}{z_k}\ d\ \ell n\ a_k^C = \frac{RT}{F}\left[\int_X^{KCl} \sum_k \frac{t_k}{z_k}\ d\ \ell n\ a_k + \ell n\ \frac{\omega(KCl)}{\omega(X)}\right] \quad . \qquad (A13)$$

In Eqs. (A11) and (A13), the nomenclature representing the liquid junction potential explicitly denotes the dependence of this term on the composition of solution X. E_{LJ}^C also depends on the KCl reference solution and the

nature of the liquid junction. The last equality in Eq. (A13) illustrates that the liquid junction potential depends on the ion activity coefficient conventions chosen in solution X and the reference solution. While the observed emf of the cell is not dependent upon the conventional definition of the ion activities, each of the separate terms in Eq. (A11) is a function of the convention. In particular, it is demonstrated in Fig. (3) (Section IV), that the magnitude of the liquid conventional liquid junction term is a strong function of the convention specified for solution X.

The general definition of an ion activity coefficient convention is given by Eq. (A7). These equations are defined in terms of absolute ion activity coefficients which cannot be measured and consequently are not known. It is, therefore, necessary to specify an alternate procedure for calculating the conventional ion activities. The arbitrary nature of ω in Eq. (A9) permits specifying the conventional value of any ion activity coefficient in a given solution. Defining the value of γ_k^C for a particular ion k implicitly defines the value for ω by Eq. (A7). It is common practice to define the ion activity coefficient for Cl^- by convention when interpreting the data from cell A (Bates, Guggenheim (1960)). It has been demonstrated in this appendix that the interpretation of the data from a cell utilizing a liquid junction in terms of an ion activity (e.g. $\ell n\ a_{H^+}$) requires the specification of a convention. Once a convention is specified (e.g., γ_{Cl}^C is designated by an arbitrary value), the conventional ion activities are unambiguously defined in terms of the mean activities of the solution by Eq. (A8). Therefore, since mean activities can be obtained using equilibrium measurements (i.e. cells without liquid junctions), it is, in principle, unnecessary to utilize cells with liquid junctions to obtain conventional ion activities. Of course, this fact does not preclude the use of

cells with liquid junctions when experimental difficulties exclude the equilibrium approach. However, the interpretation of such data in terms of the equilibrium properties of the system without the use of the cumbersome theory of irreversible thermodynamics is approximate. Fig. (3) illustrates such an approach may lead to non-negligible errors in the reported values of the thermodynamic properties for a system when these values are derived from pH data.

Appendix B

In this section, the equations which we utilize for calculation of the mixing functions, E_θ and $E_{\theta'}$ are presented for the convenience of potential users of the model.

Numerically integrated values for $J_0(x)$ (see Appendix A of HW) and its derivative are given in Table 1. We believe these are significant to the full accuracy cited.

The calculation of $J_0(x)$ and its derivative by numerical integration is difficult and computationally slow. We have, therefore, fit $J_0(x)$ with polynomial approximations. The domain of the argument x has been split into two regions. The appropriate equations specific for these regions are given below

Region I. $x \leq 1$

$$z = 4\, x^{1/5} - 2 \tag{B1}$$

$$\frac{dz}{dx} = \frac{4}{5}\, x^{-4/5} \tag{B2}$$

$$b_k = z\, b_{k+1} - b_{k+2} + a_k^I \tag{B3}$$

$$d_k = b_{k+1} + z\, d_{k+1} - d_{k+2} \qquad k = 0,\ 20 \tag{B4}$$

Region II. $x > 1$

$$z = \frac{40}{9}\, x^{-1/10} - \frac{22}{9} \tag{B5}$$

$$\frac{dz}{dx} = -\frac{40}{90}\, x^{-11/10} \tag{B6}$$

$$\left.\begin{aligned} b_k &= z\, b_{k+1} - b_{k+2} + a_k^{II} \\ d_k &= b_{k+1} + z\, d_{k+1} - d_{k+2} \end{aligned}\right\} \quad k = 0,\ 20 \tag{B7, B8}$$

Using the calculated values for the b_k and the d_k $J_o(x)$ and $J_1(x)$ listed in the appendix of HW can be calculated from the following formulae:

$$J_0(x) = \frac{1}{4}x - 1 + \tfrac{1}{2}(b_0 - b_2) \tag{B9}$$

$$J_0'(x) = \frac{dJ_0(x)}{dx} = \tfrac{1}{4} + \tfrac{1}{2}\frac{dz}{dx}(d_0 - d_2) \tag{B10}$$

$$J_1(x) = x\, J_0'(x) \quad . \tag{B11}$$

With regard to the calculation of the arrays, b_k and d_k, the coefficients a_k^I and a_k^{II}, are given in Table 9. By definition, $b_{21} = b_{22} = d_{21} = d_{22} = 0$. Therefore, by using Eq. (B3) or (B7) the numbers, bb, can be generated in decreasing sequence. Similar calculations are used to obtain the array, d. The resulting calculated values for J and J' are in exact agreement with the tabulated values.

Figure Captions

Fig. 1: The mean activity coefficient of HCL ($\gamma^{\pm 0}_{HCl}$), is an HCl-H_2O system, the mean activity coefficient of HCL in a KCl-H_2O system ($\gamma^{\pm tr}_{HCl}$), and the mean activity coefficient for KCl in a KCl-H_2O solution ($\gamma^{\pm 0}_{KCl}$) versus the stoichiomtric ionic strength (I_s). The data points are from Robinson and Stokes (1968) and Harned and Owen (1958). The dashed curve is calculated from the literature data using Eq. (9). The solid curves are calculated using Eq. (3).

Fig. 2: The calculated dilute solution behavior of the thermodynamic mean activity coefficient for a hypothetical 2-1 electrolyte, AB_2. A typical ion pair model with activity coefficients given by Eq. (10) is used to calculate the solid curves for particular values of dissociation constant, K_d. The dashed curves are calculated using Eq. (3) with $\beta^0_{AB} = \beta^0_{AB} = C^{\phi}_{AB} = 0$, and particular values for β^2_{AB}. The results are plotted versus the square root of the total AB_2 concentration.

Fig. 3: The value for the liquid junction potential calculated from the data of Shatkey and Lerman (1969) using Eq. (16). Each curve is calculated using one of the ion activity conventions given by Eq. (14). (Curve a corresponds to convention equation (14a), etc.) .

Fig. 4: The calculated and experimental solubilities of salts in acidic solutions. The model is also in agreement with various emf and isopiestic measurements (see text). Curve a-e were used in parameterization. Curve f was predicted using fully parameterized model for acidic solutions.

Figure 5 The solubility of carbon dioxide in single electrolyte solutions. The curves in $MgSO_4$ and K_2SO_4 were predicted using the model fully parameterized from the other data.

Figure 6 The solubilities of sodium and potassium salts in hydroxide solutions. The model is also in agreement with emf data at lower concentrations

Figure 7 Salt solubilities in the $Na-Cl-SO_4-HCO_3-CO_3-OH-H_2O$ system. Closed systems.

Figure 8 Predicted Jänecke projections for ternary systems in the $Na-Cl-SO_4-HCO_3CO_3-OH-H_2O$ system. Closed systems. See text for discussion of (f). Figures predicted from fully parameterized model using solubility data in Figure 7, emf and isopiestic data.

Figure 9 Salt solubilities in potassium carbonate systems. Closed systems.

Figure 10 The reciprocal $Na-K-HCO_3-CO_3$ closed system.

Figure 11 Ca(OH) salt solubilities in various salt solutions. (a), (b) and emf data used in parameterization. c-f are predicted using fully parameterized model.

Figure 12 The solubility of calcite in water (a) and the predicted solubilities of calcite in NaCl solutions (b)-(f).

Figure 13 The preeicted solubility of Brucite and magnesium oxychloride in $Mg-OH-Cl-H_2O$ solutions versus the available data.

Figure 14: Predicted solubility of Nesquehonite in $MgSO_4$(a) and $MgCl_2$(b) solutions.

Figure 15: The predicted relationship between pH and carbonate alkalinity ($A_c = (HCO_3^-)_T + 2(CO_3^{--})_T$) for seawater at 35‰ and 25°C in equilibrium with calcite. Closed circles represent the raw data of Morse et al. (1980).

Figure 16: Predicted mineral solubilities in the Na-K-Cl-SO_4-HCO_3-CO_3-CO_2-H_2O system at 25°C. All solutions are also saturated with halite (NaCl) (a) predicted phase equilibria for the closed CO_2 system: The data denoted by closed circles are those of D'Ans (1933) and Makarov and Bleiden (1938). The open circle (Aph-Bur-Hal-Then) was interpolated between the 35°C and metastable 20°C data of Teeple (1929). The open square was extrapolated from the 35°C and 50°C data of Teeple. The open triangles were estimated from the 35°C and 50°C data of Teeple and the invariant points at 20°C where $Na_2CO_3 \cdot 7H_2O$ replaces thermonatrite. Similar estimates using the Teeple data are in good agreement with the closed circles. (b) Predicted phase equilibria at the atmospheric P_{CO_2} level of 3.3×10^{-4} atm: (c) Predicted phase equilibria at 3.3×10^{-3} P_{CO_2}, or 10 times the atmospheric P_{CO_2} level.

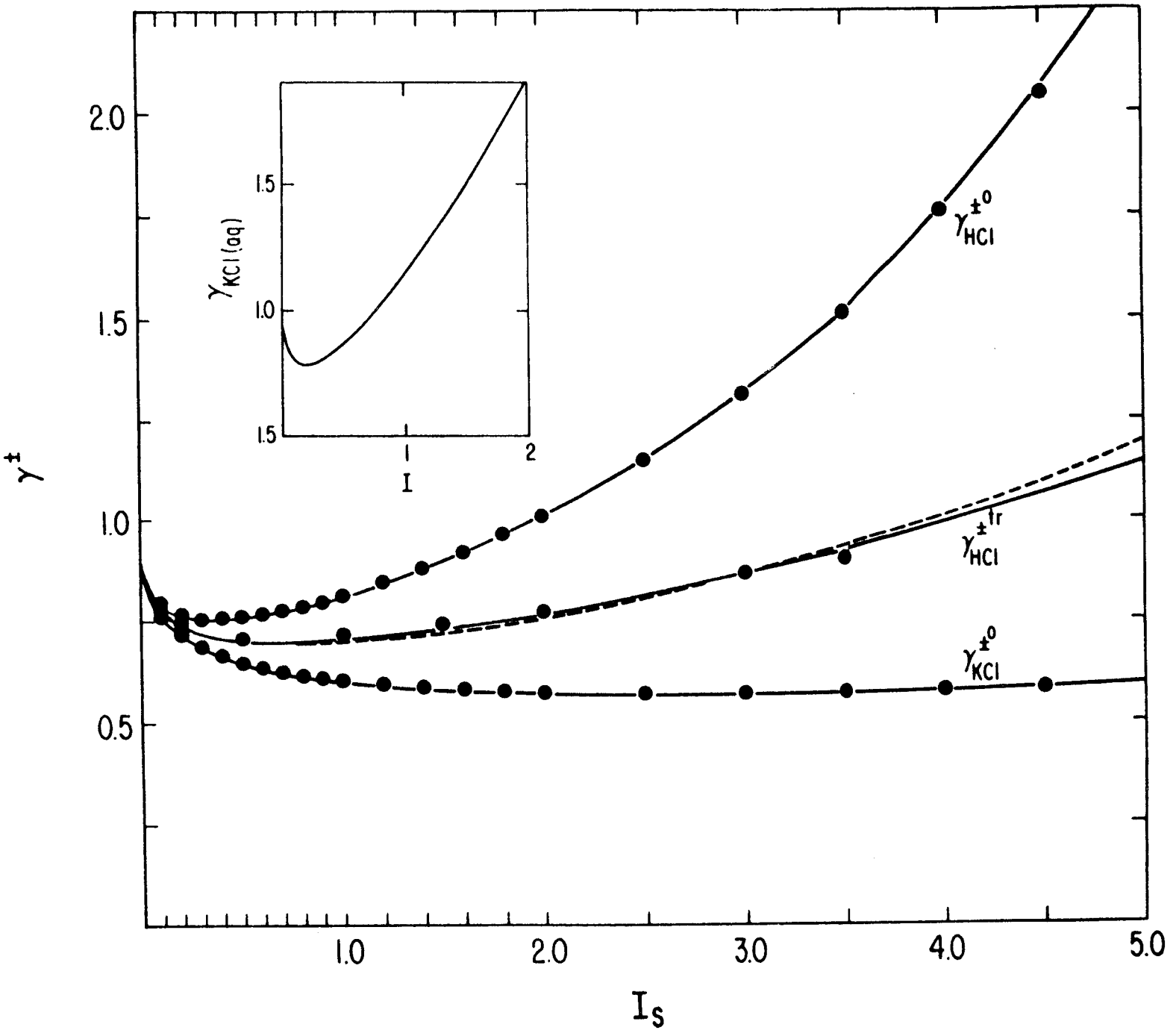
2.0
1.5
1.0
0.5
$\gamma^{\pm}$
1.0
2.0
3.0
4.0
5.0
I_S
$\gamma^{\pm 0}_{HCl}$
$\gamma^{\pm tr}_{HCl}$
$\gamma^{\pm 0}_{KCl}$
$\gamma_{KCl(aq)}$
1.5
1.0
1.5
2
I

Figure 1.

Figure 2

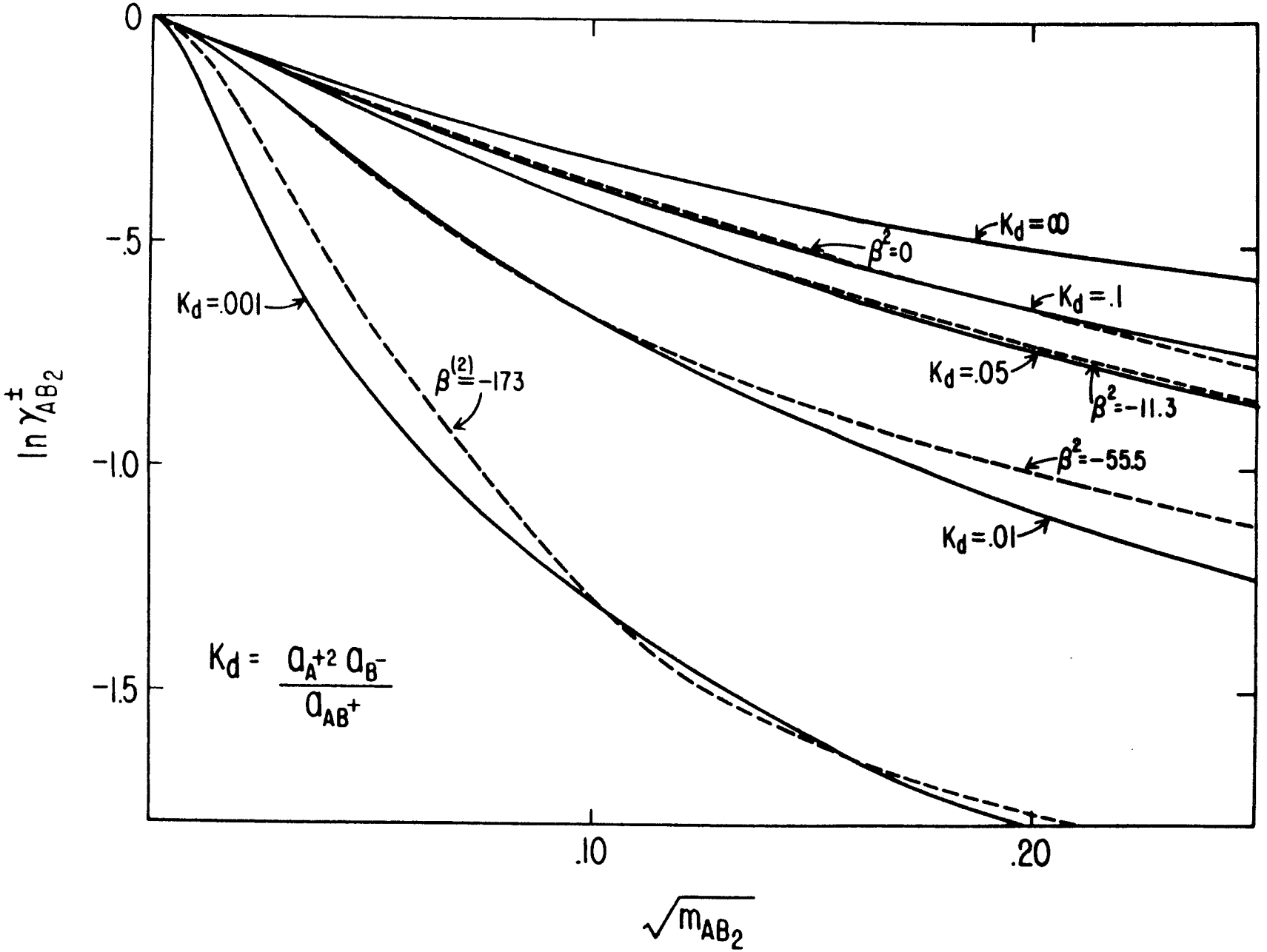
0
-.5
-1.0
-1.5
$\ln \gamma^{\pm}_{AB_2}$
$K_d = \infty$
$\beta^2 = 0$
$K_d = .1$
$K_d = .05$
$\beta^2 = -11.3$
$\beta^{(2)} = -173$
$\beta^2 = -55.5$
$K_d = .001$
$K_d = .01$
$K_d = \frac{a_{A^{+2}} a_{B^-}}{a_{AB^+}}$
.10
.20
$\sqrt{m_{AB_2}}$

Figure 3

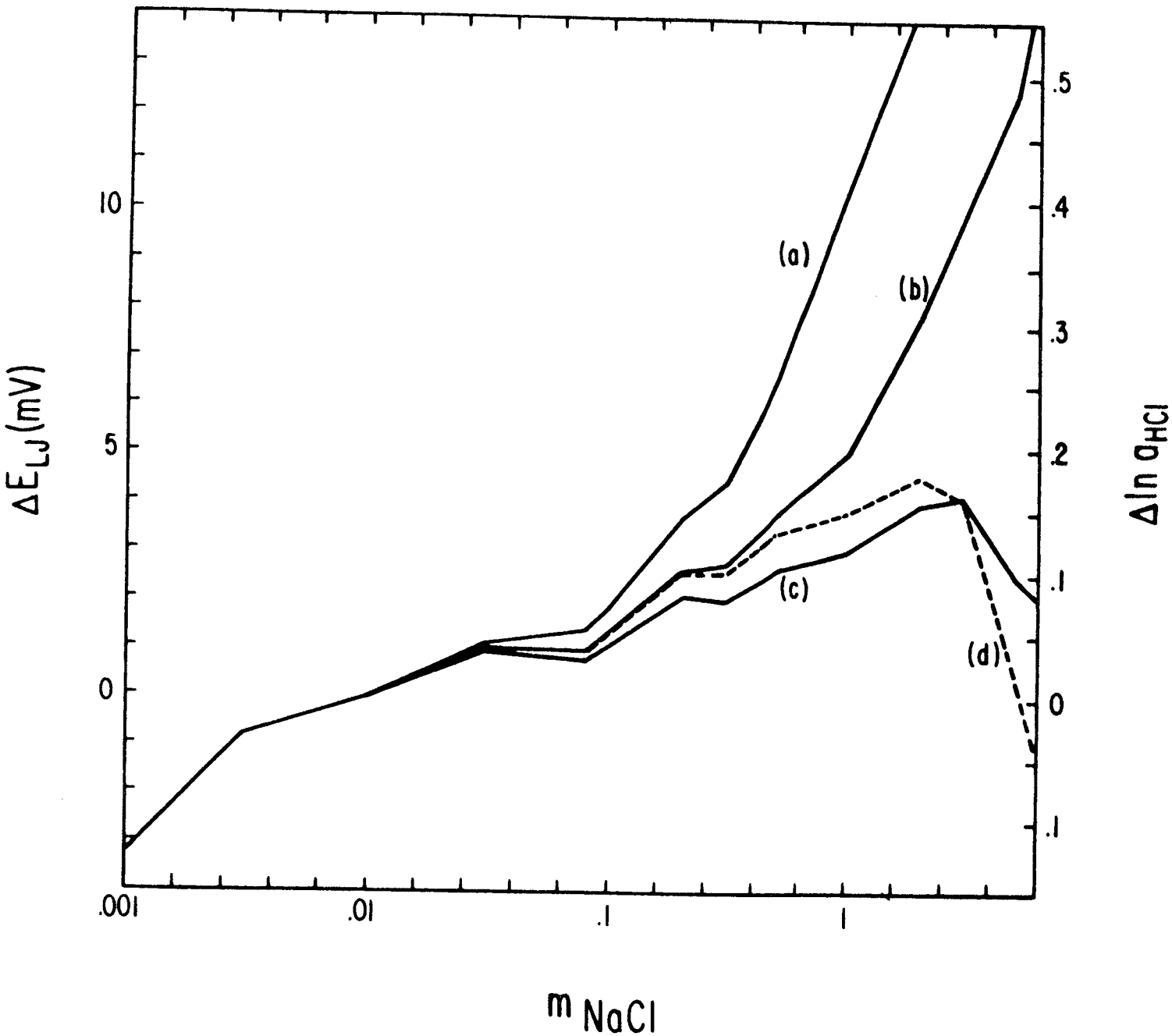

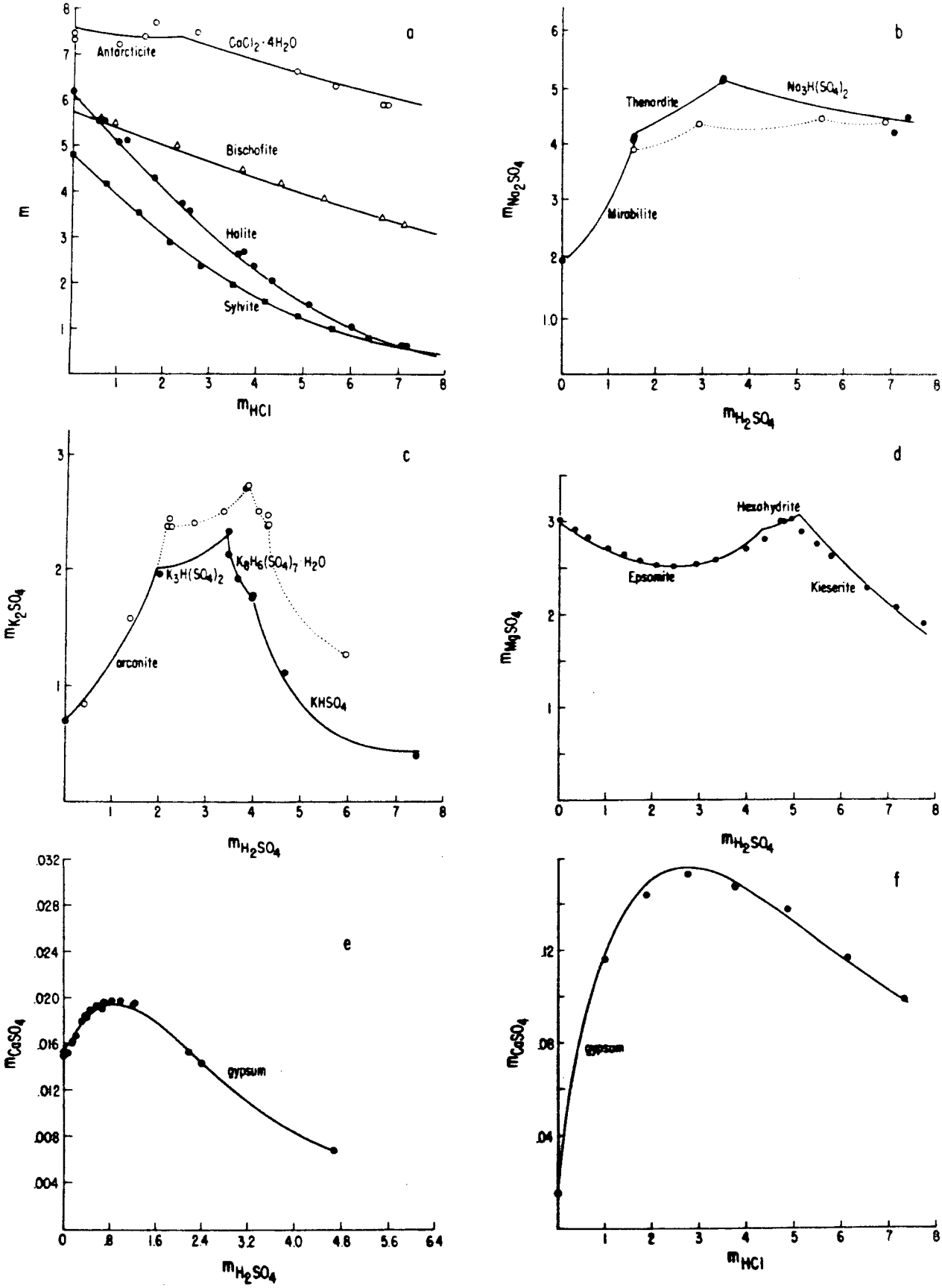
a
Antarcticite
$CaCl_2 \cdot 4H_2O$
Bischofite
Halite
Sylvite
E
m_{HCl}
b
Thenardite
$Na_3H(SO_4)_2$
Mirabilite
$m_{Na_2SO_4}$
$m_{H_2SO_4}$
c
$K_3H(SO_4)_2$
$K_8H_6(SO_4)_7 \cdot H_2O$
arcanite
$KHSO_4$
$m_{K_2SO_4}$
$m_{H_2SO_4}$
d
Hexahydrite
Epsomite
Kieserite
m_{MgSO_4}
$m_{H_2SO_4}$
e
gypsum
m_{CaSO_4}
$m_{H_2SO_4}$
f
gypsum
m_{CaSO_4}
m_{HCl}

Figure 4.

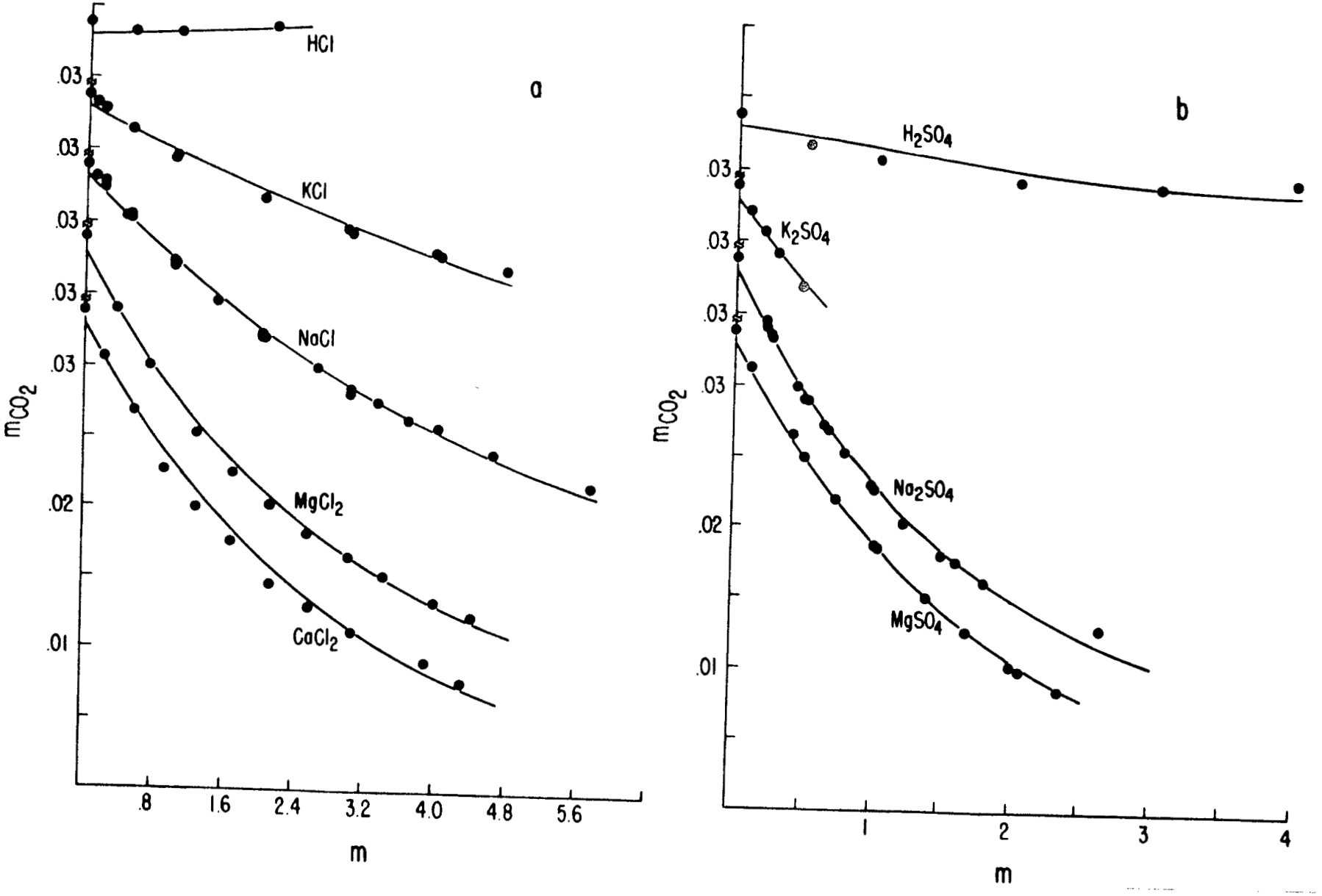
a
HCl
KCl
NaCl
MgCl2
CaCl2
mCO2
.03
.02
.01
.8
1.6
2.4
3.2
4.0
4.8
5.6
m
b
H2SO4
K2SO4
Na2SO4
MgSO4
mCO2
.03
.02
.01
1
2
3
4
m

Figure 5.

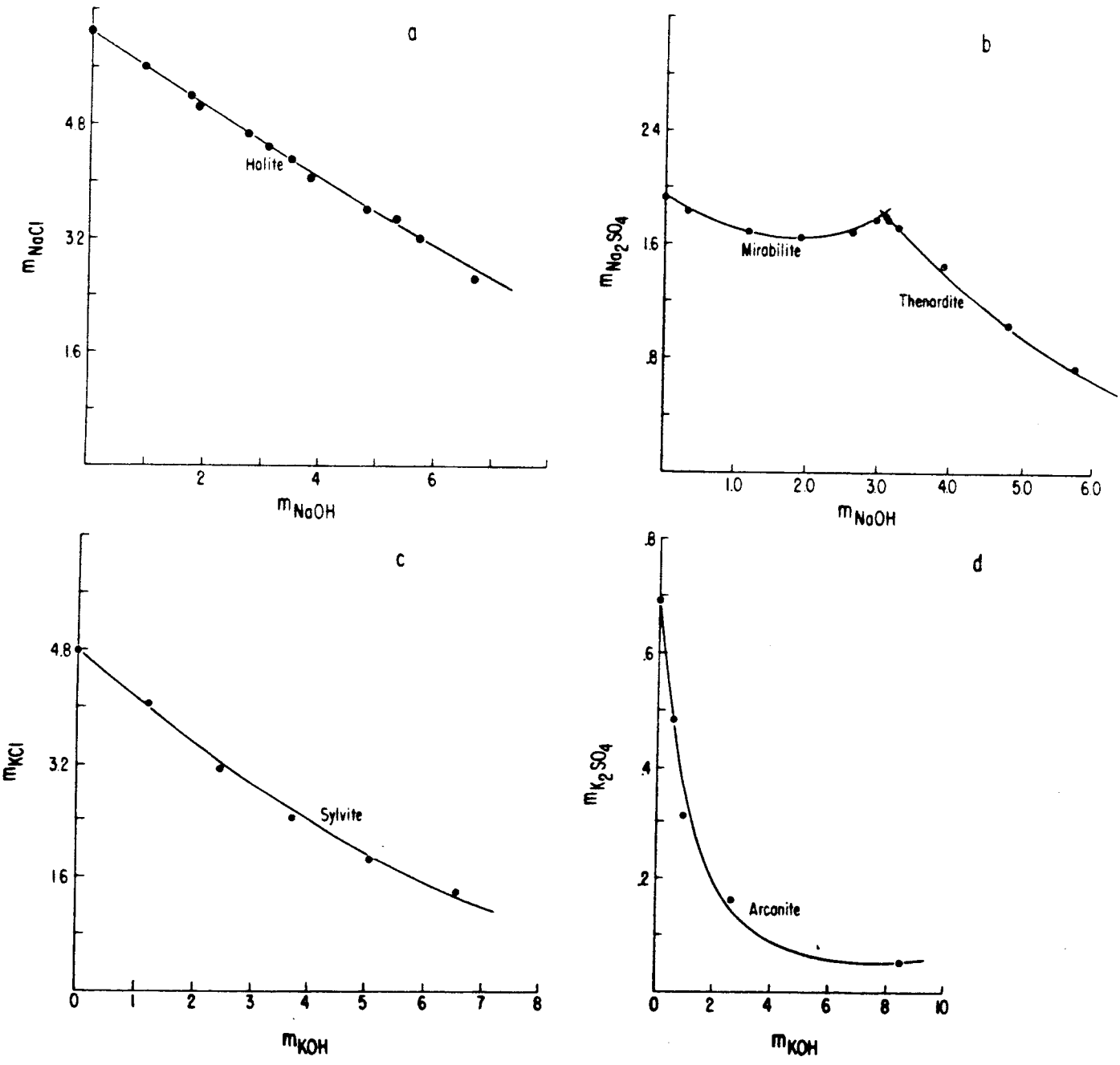
a
Halite
m_{NaCl}
4.8
3.2
1.6
2
4
6
m_{NaOH}
b
$m_{Na_2SO_4}$
2.4
1.6
.8
Mirabilite
Thenardite
1.0
2.0
3.0
4.0
5.0
6.0
m_{NaOH}
c
m_{KCl}
4.8
3.2
1.6
Sylvite
0
1
2
3
4
5
6
7
8
m_{KOH}
d
$m_{K_2SO_4}$
.8
.6
.4
.2
Arconite
0
2
4
6
8
10
m_{KOH}

Figure 6.

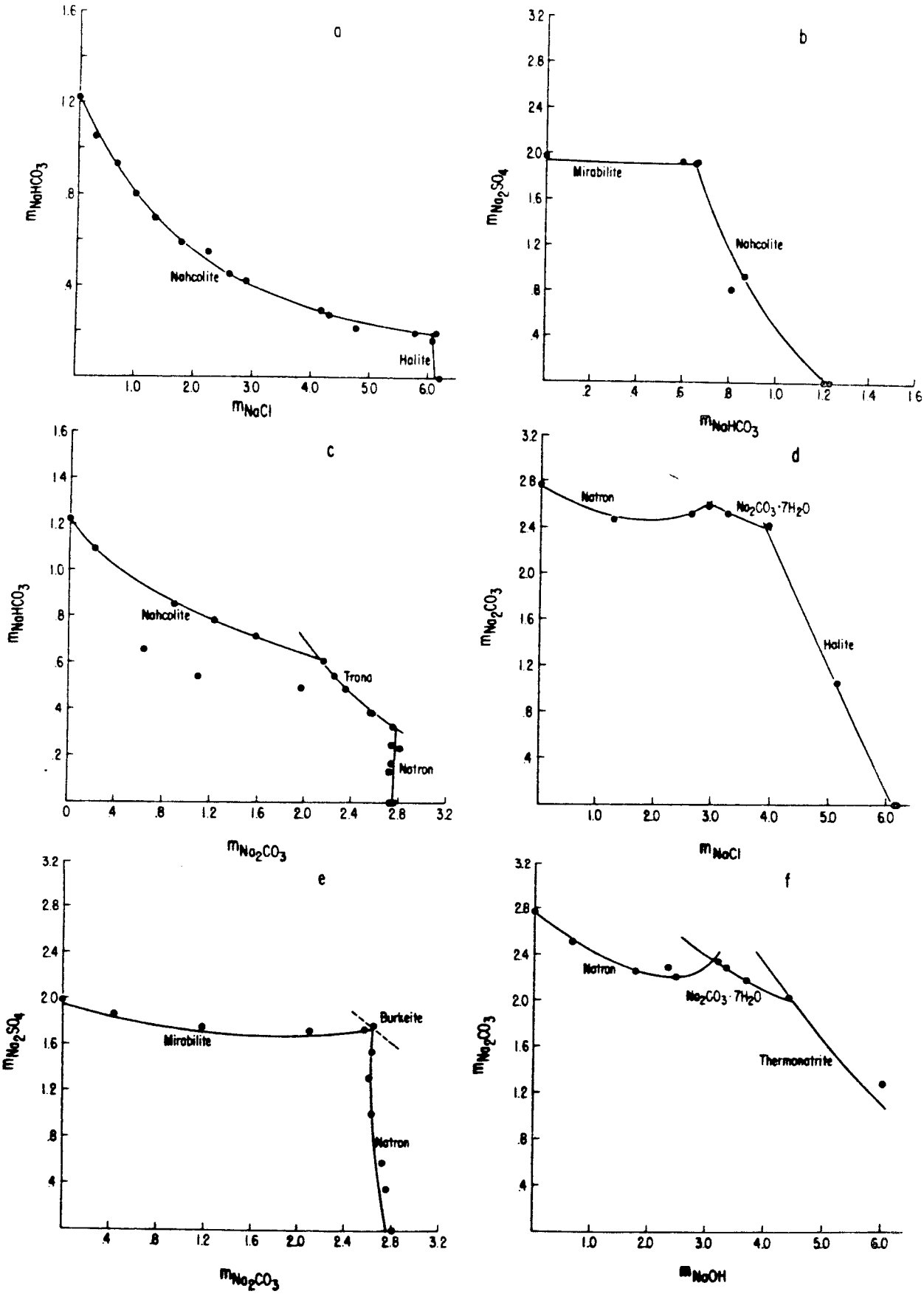
a
Nahcolite
Halite
m_{NaHCO_3}
m_{NaCl}
b
Mirabilite
Nahcolite
$m_{Na_2SO_4}$
m_{NaHCO_3}
c
Nahcolite
Trona
Natron
m_{NaHCO_3}
$m_{Na_2CO_3}$
d
Natron
$Na_2CO_3 \cdot 7H_2O$
Halite
$m_{Na_2CO_3}$
m_{NaCl}
e
Mirabilite
Burkeite
Natron
$m_{Na_2SO_4}$
$m_{Na_2CO_3}$
f
Natron
$Na_2CO_3 \cdot 7H_2O$
Thermonatrite
$m_{Na_2CO_3}$
m_{NaOH}

Figure 7.

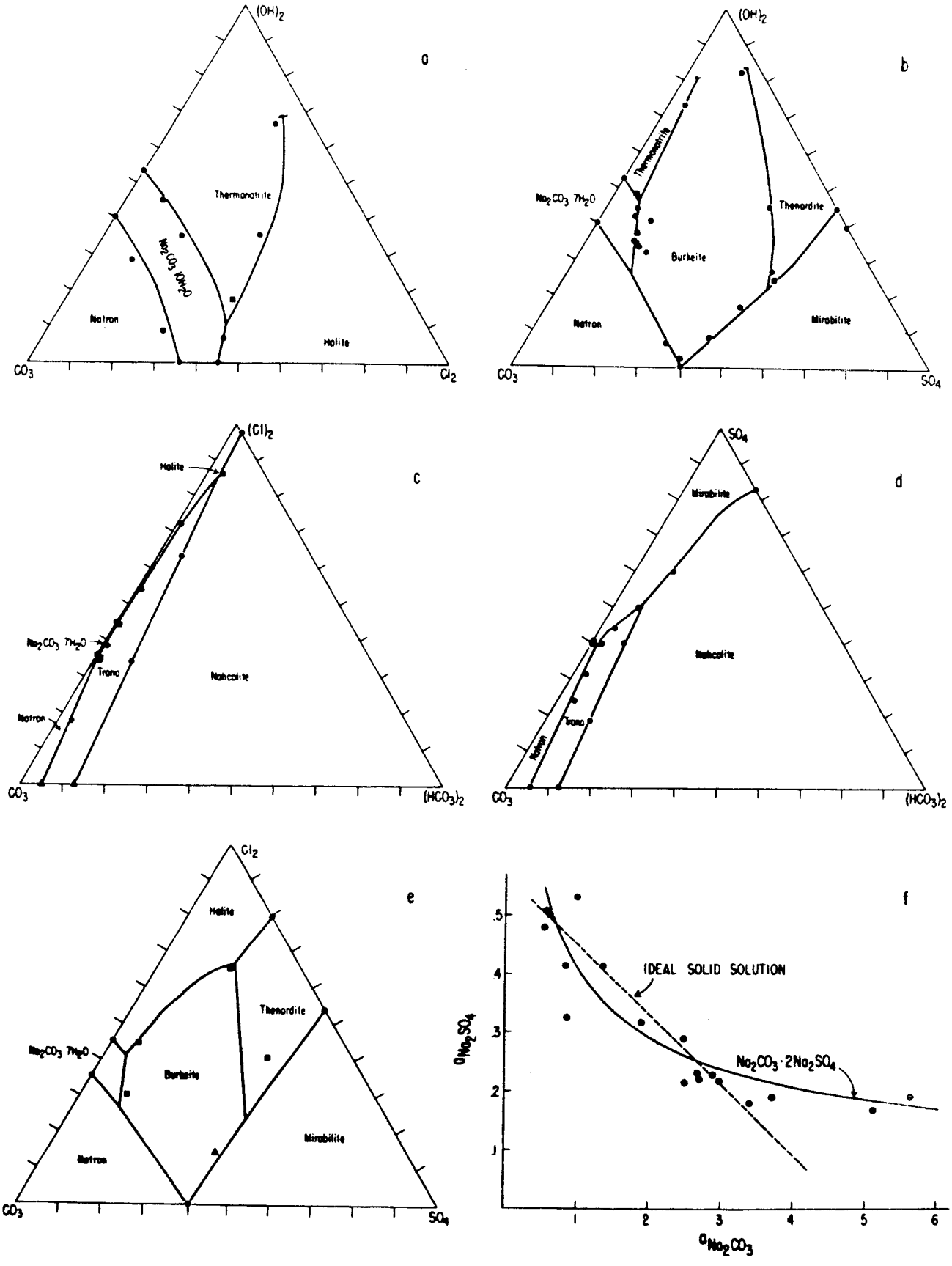
a
(OH)2
Thermonatrite
Na2CO3 1Na2O
Natron
Halite
CO3
Cl2
b
(OH)2
Thermonatrite
Na2CO3 7H2O
Thenardite
Burkeite
Natron
Mirabilite
CO3
SO4
c
(Cl)2
Halite
Na2CO3 7H2O
Trona
Nahcolite
Natron
CO3
(HCO3)2
d
SO4
Mirabilite
Nahcolite
Trona
Natron
CO3
(HCO3)2
e
Cl2
Halite
Thenardite
Na2CO3 7H2O
Burkeite
Natron
Mirabilite
CO3
SO4
f
IDEAL SOLID SOLUTION
Na2CO3·2Na2SO4
aNa2SO4
aNa2CO3
.5
.4
.3
.2
.1
1
2
3
4
5
6

Figure 8.

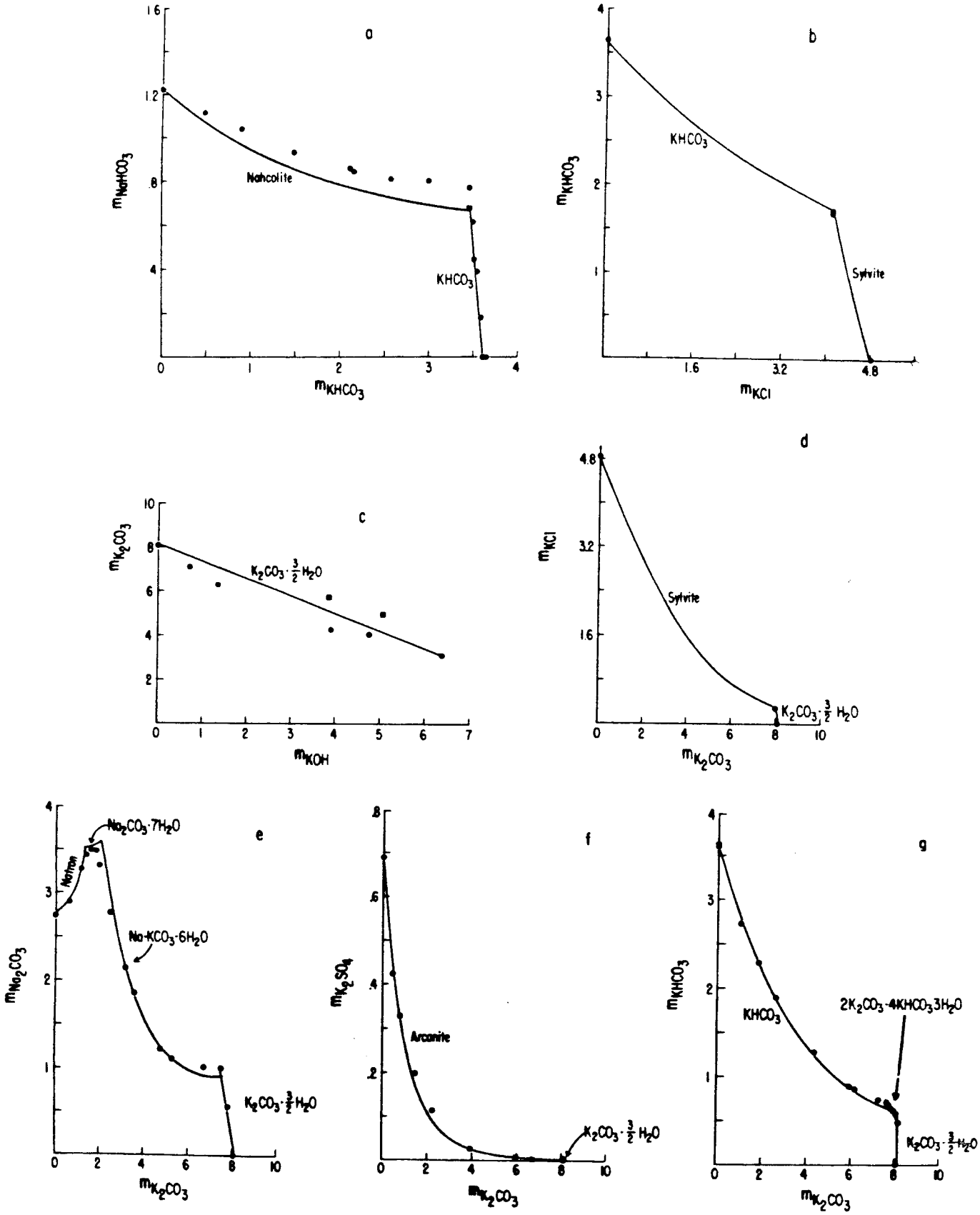
a
Nahcolite
KHCO3
mNaHCO3
mKHCO3
b
KHCO3
Sylvite
mKHCO3
mKCl
c
K2CO3·3/2H2O
mK2CO3
mKOH
d
Sylvite
K2CO3·3/2 H2O
mKCl
mK2CO3
e
Na2CO3·7H2O
Natron
Na-KCO3·6H2O
K2CO3·3/2H2O
mNa2CO3
mK2CO3
f
Arcanite
K2CO3·3/2 H2O
mK2SO4
mK2CO3
g
KHCO3
2K2CO3·4KHCO3·3H2O
K2CO3·3/2H2O
mKHCO3
mK2CO3

Figure 9.

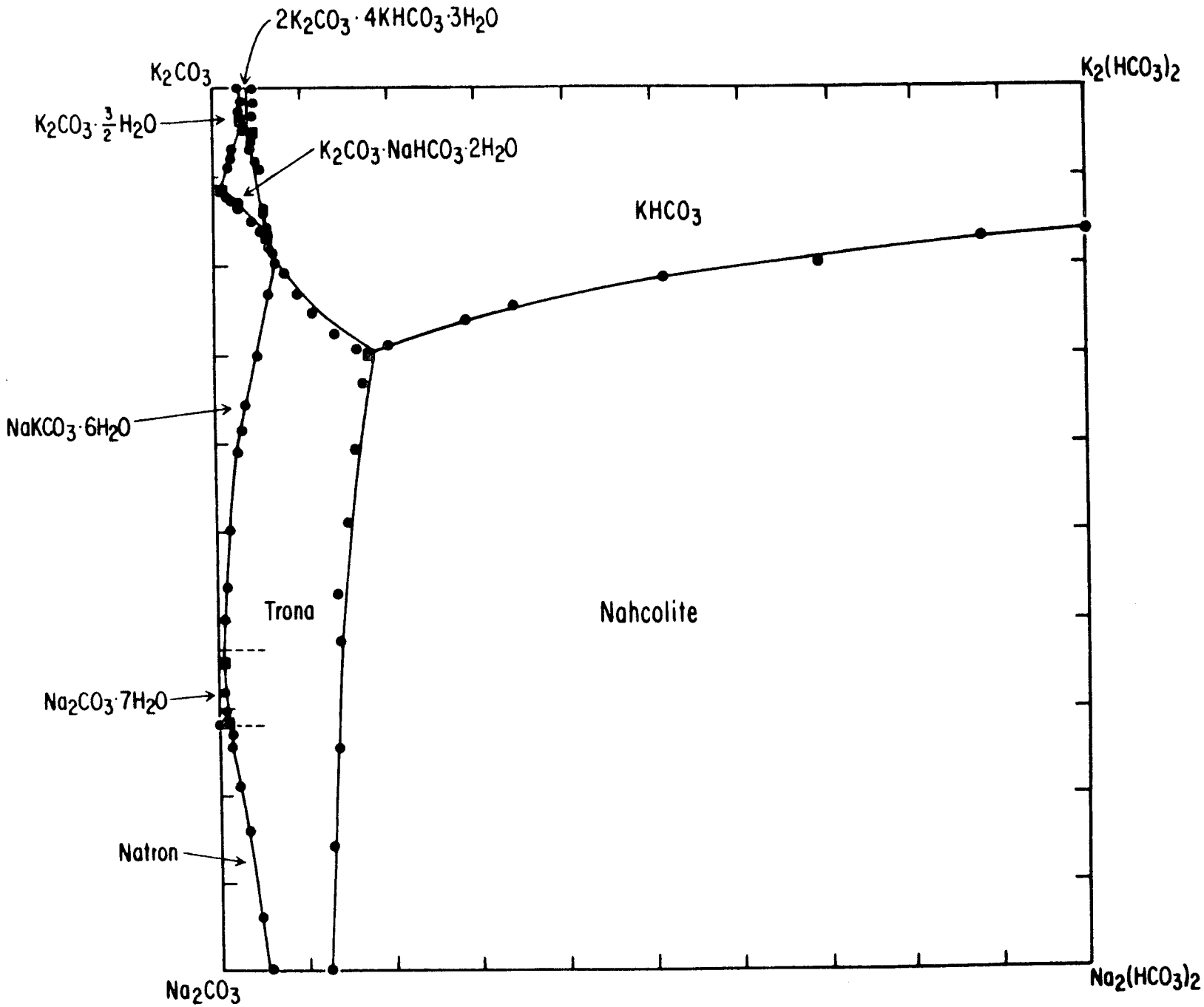
$2K_2CO_3 \cdot 4KHCO_3 \cdot 3H_2O$
K_2CO_3
$K_2(HCO_3)_2$
$K_2CO_3 \cdot \frac{3}{2}H_2O$
$K_2CO_3 \cdot NaHCO_3 \cdot 2H_2O$
$KHCO_3$
$NaKCO_3 \cdot 6H_2O$
Trona
Nahcolite
$Na_2CO_3 \cdot 7H_2O$
Natron
Na_2CO_3
$Na_2(HCO_3)_2$

Figure 10.

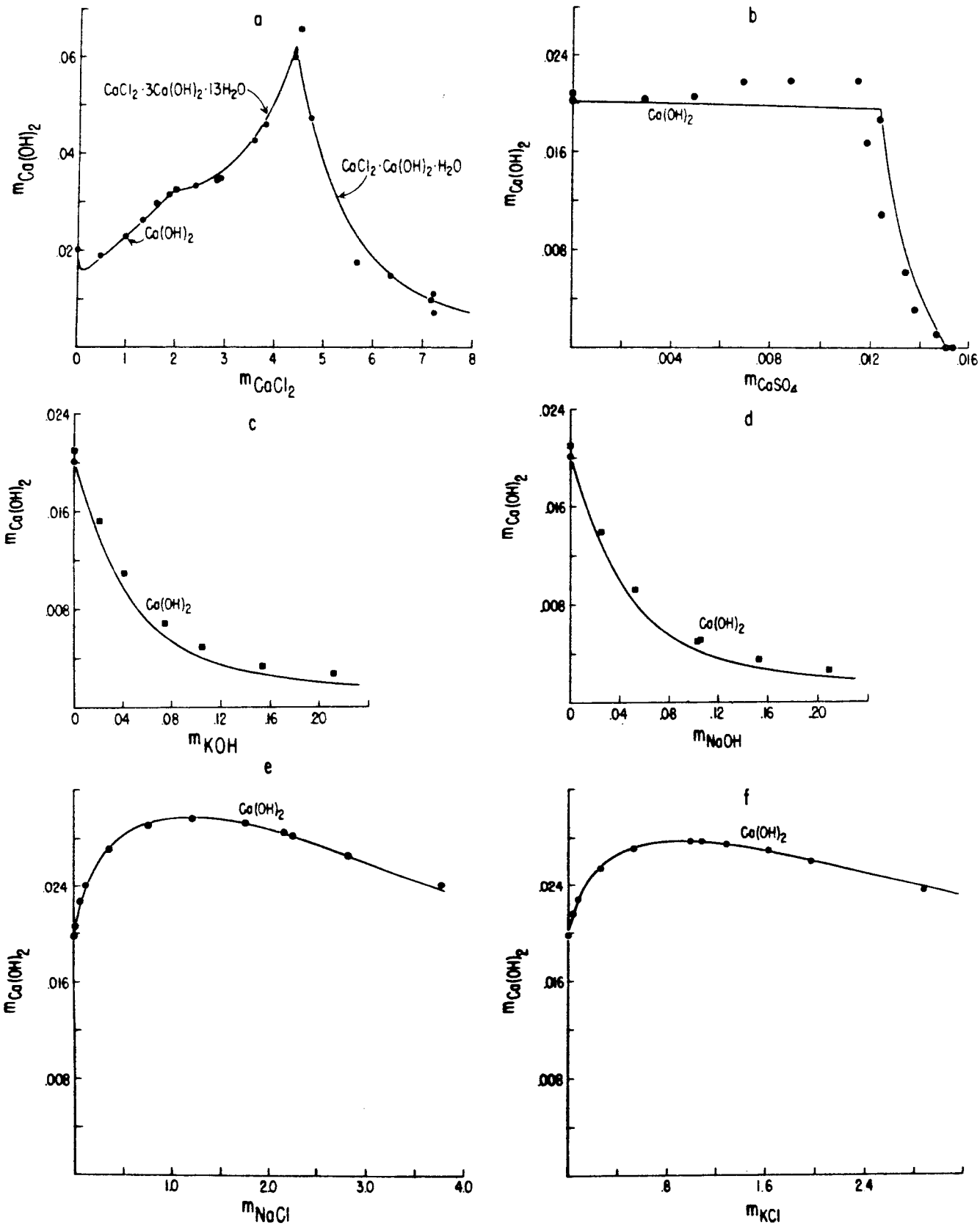
a
$CaCl_2 \cdot 3Ca(OH)_2 \cdot 13H_2O$
$CaCl_2 \cdot Ca(OH)_2 \cdot H_2O$
$Ca(OH)_2$
$m_{Ca(OH)_2}$
m_{CaCl_2}
b
$Ca(OH)_2$
$m_{Ca(OH)_2}$
m_{CaSO_4}
c
$Ca(OH)_2$
$m_{Ca(OH)_2}$
m_{KOH}
d
$Ca(OH)_2$
$m_{Ca(OH)_2}$
m_{NaOH}
e
$Ca(OH)_2$
$m_{Ca(OH)_2}$
m_{NaCl}
f
$Ca(OH)_2$
$m_{Ca(OH)_2}$
m_{KCl}

Figure 11.

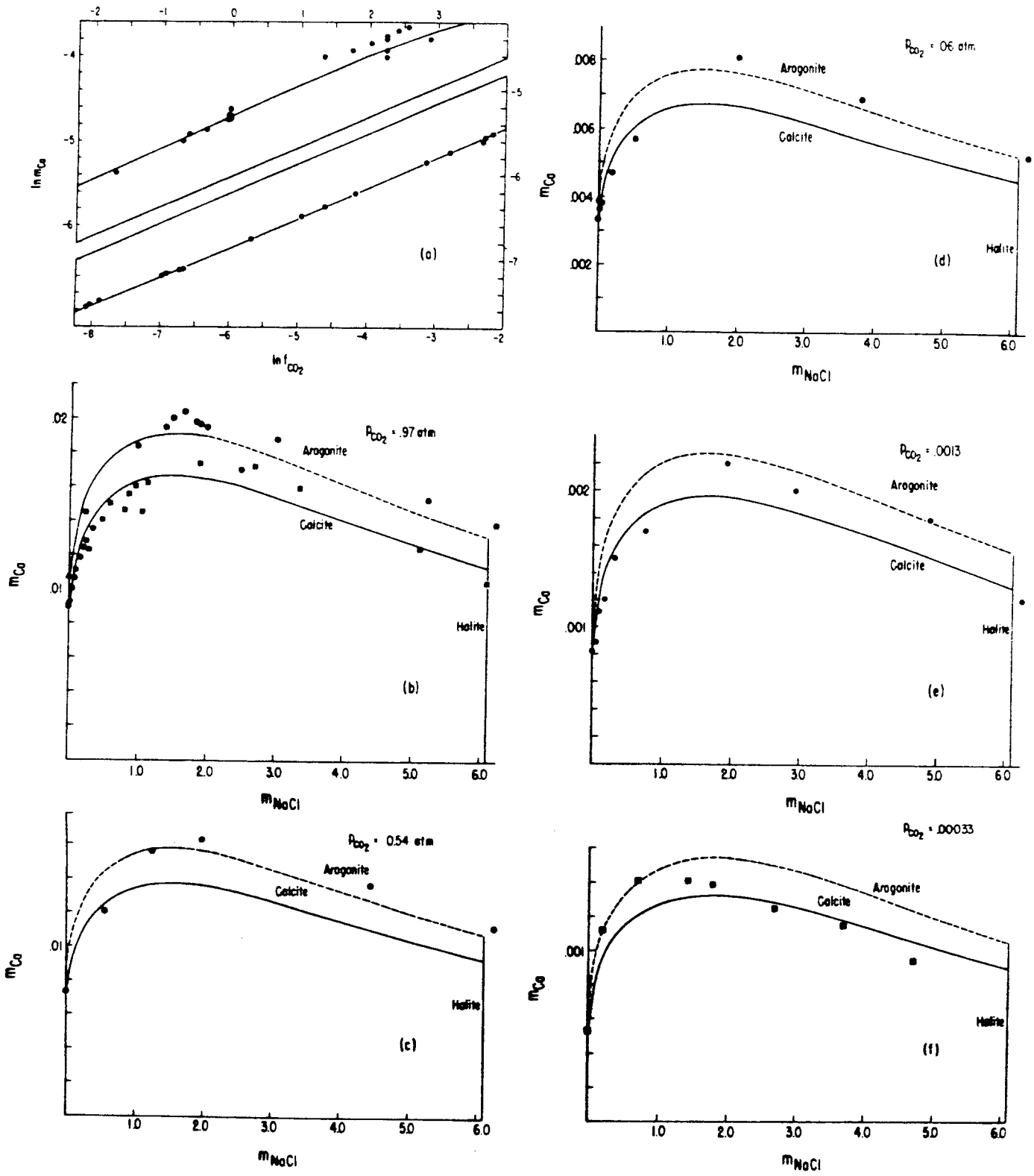
(a)
ln m_{Ca}
ln f_{CO_2}
(b)
P_{CO_2} = .97 atm
Aragonite
Calcite
Halite
m_{Ca}
m_{NaCl}
(c)
P_{CO_2} = 0.54 atm
Aragonite
Calcite
Halite
m_{Ca}
m_{NaCl}
(d)
P_{CO_2} = .06 atm
Aragonite
Calcite
Halite
m_{Ca}
m_{NaCl}
(e)
P_{CO_2} = .0013
Aragonite
Calcite
Halite
m_{Ca}
m_{NaCl}
(f)
P_{CO_2} = .00033
Aragonite
Calcite
Halite
m_{Ca}
m_{NaCl}

Figure 12.

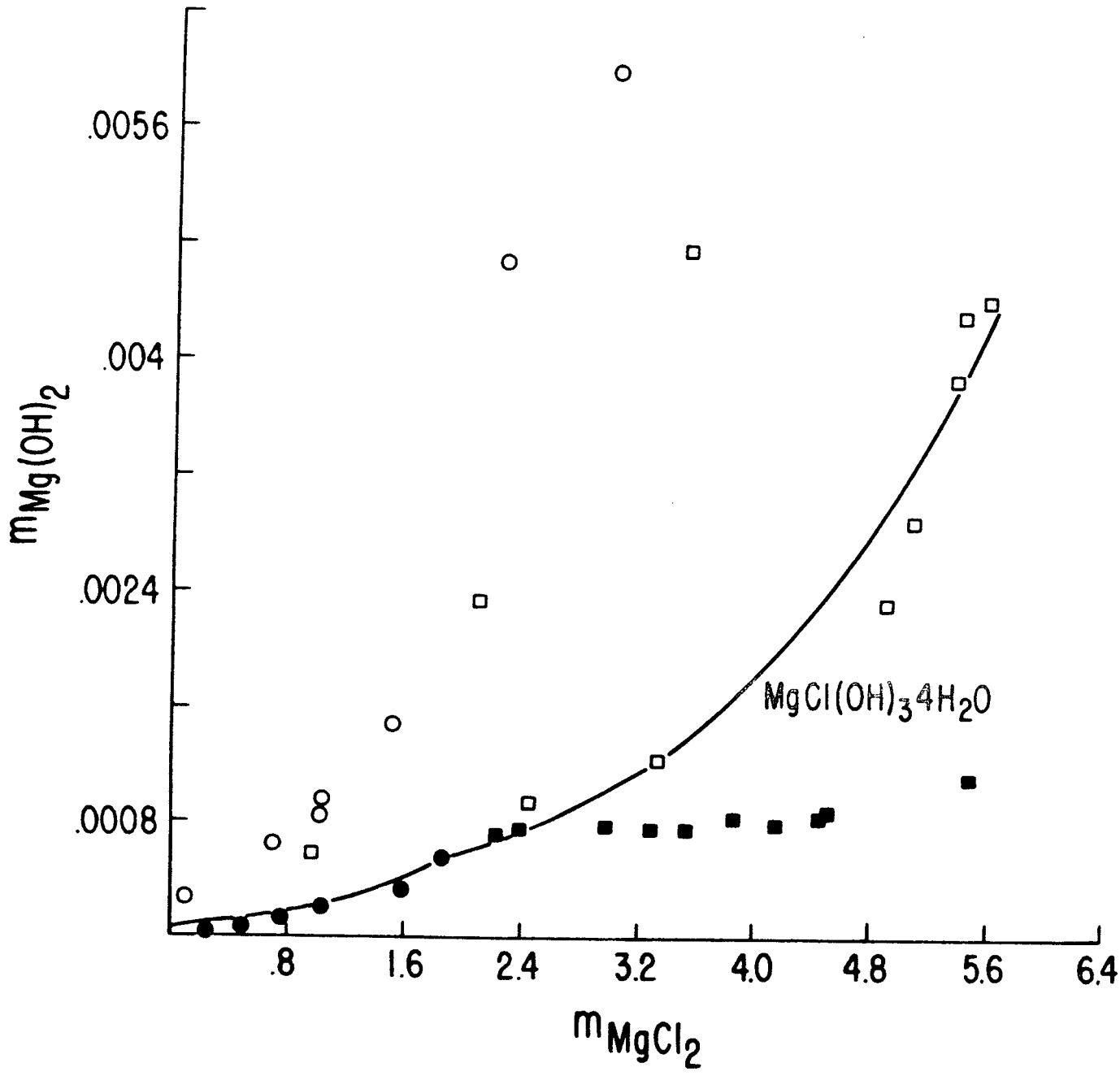
.0056
.004
.0024
.0008
$m_{Mg(OH)_2}$
$MgCl(OH)_3 4H_2O$
.8
1.6
2.4
3.2
4.0
4.8
5.6
6.4
m_{MgCl_2}

Figure 13.

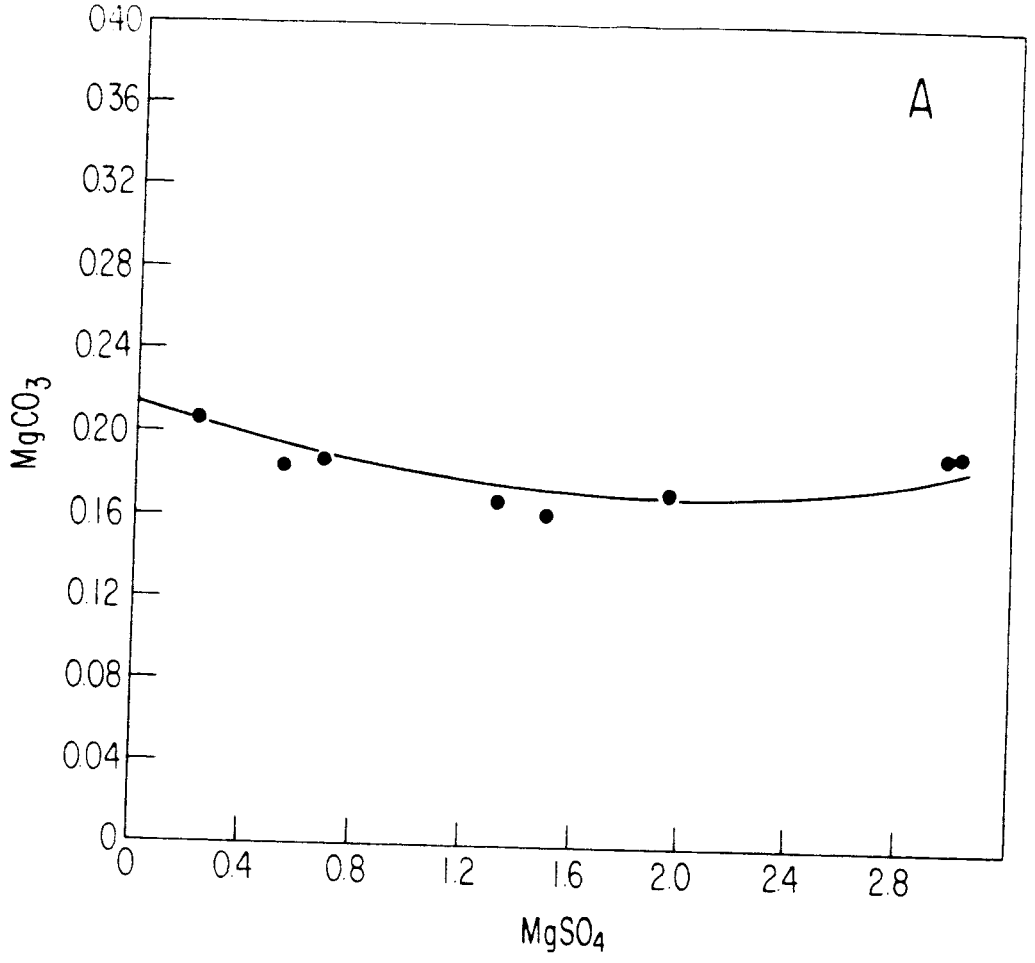
A
0.40
0.36
0.32
0.28
0.24
0.20
0.16
0.12
0.08
0.04
0
MgCO3
0
0.4
0.8
1.2
1.6
2.0
2.4
2.8
MgSO4

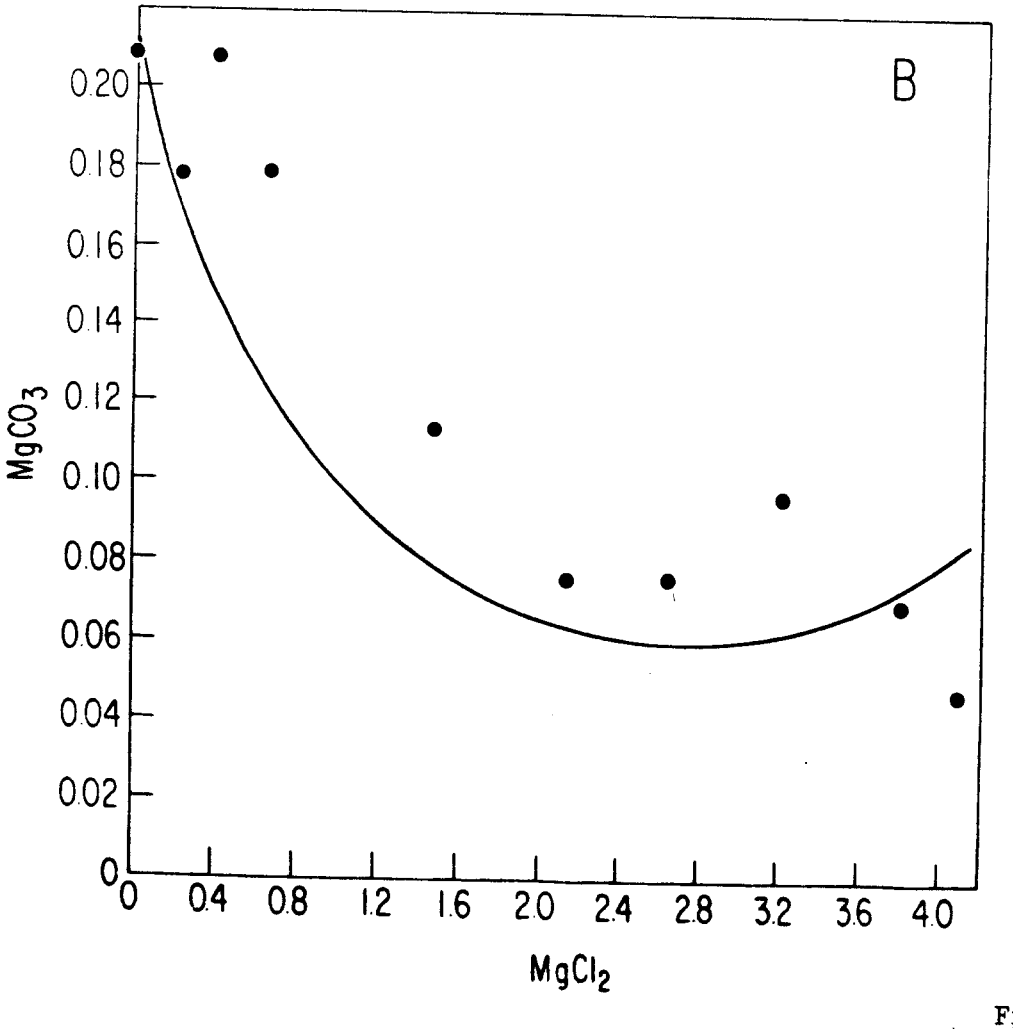
B
0.20
0.18
0.16
0.14
0.12
0.10
0.08
0.06
0.04
0.02
0
MgCO3
0
0.4
0.8
1.2
1.6
2.0
2.4
2.8
3.2
3.6
4.0
MgCl2

Figure 14.

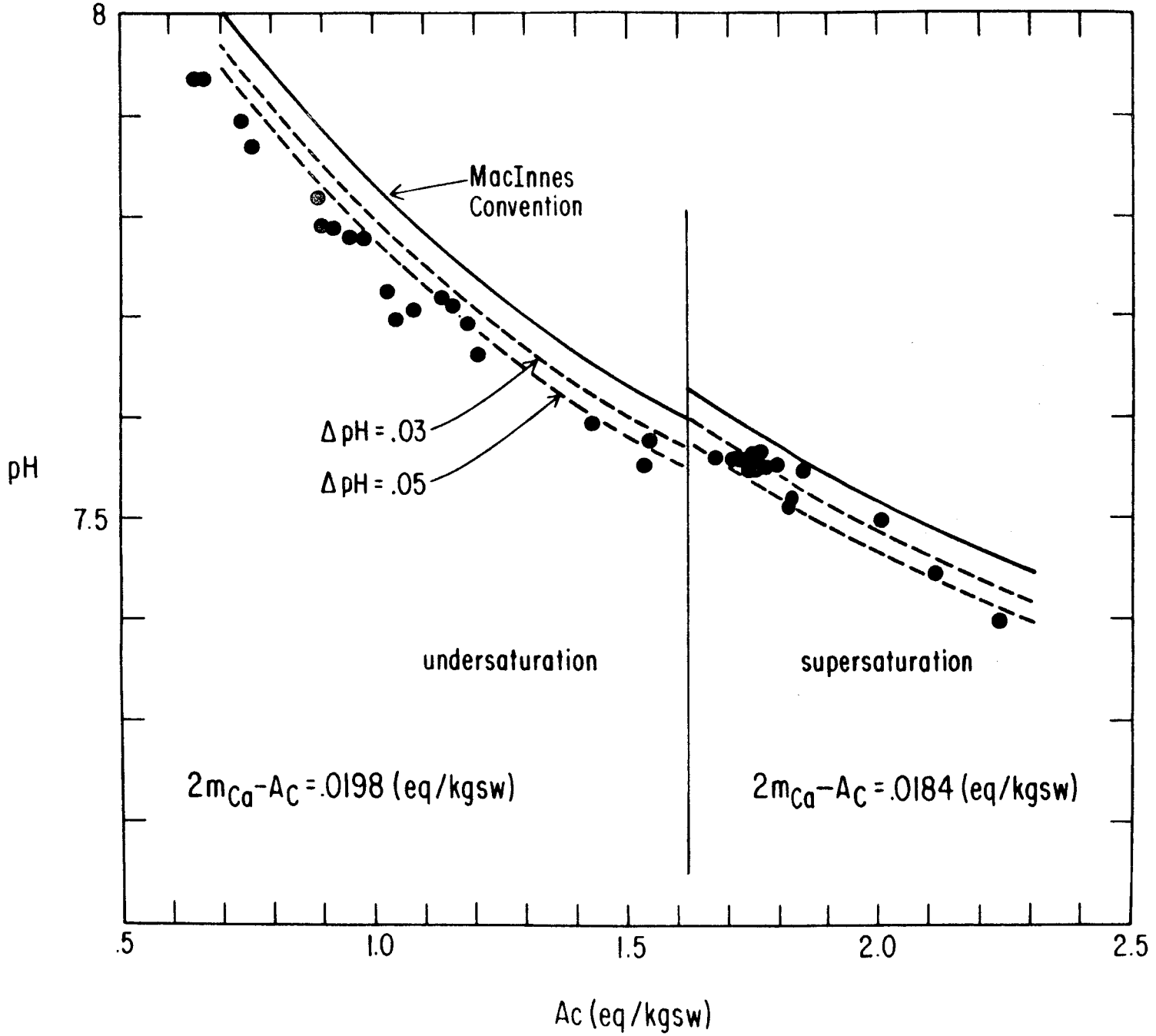
8
7.5
pH
MacInnes
Convention
Δ pH = .03
Δ pH = .05
undersaturation
supersaturation
$2m_{Ca}-A_C = .0198$ (eq/kgsw)
$2m_{Ca}-A_C = .0184$ (eq/kgsw)
.5
1.0
1.5
2.0
2.5
Ac (eq/kgsw)

Figure 15.

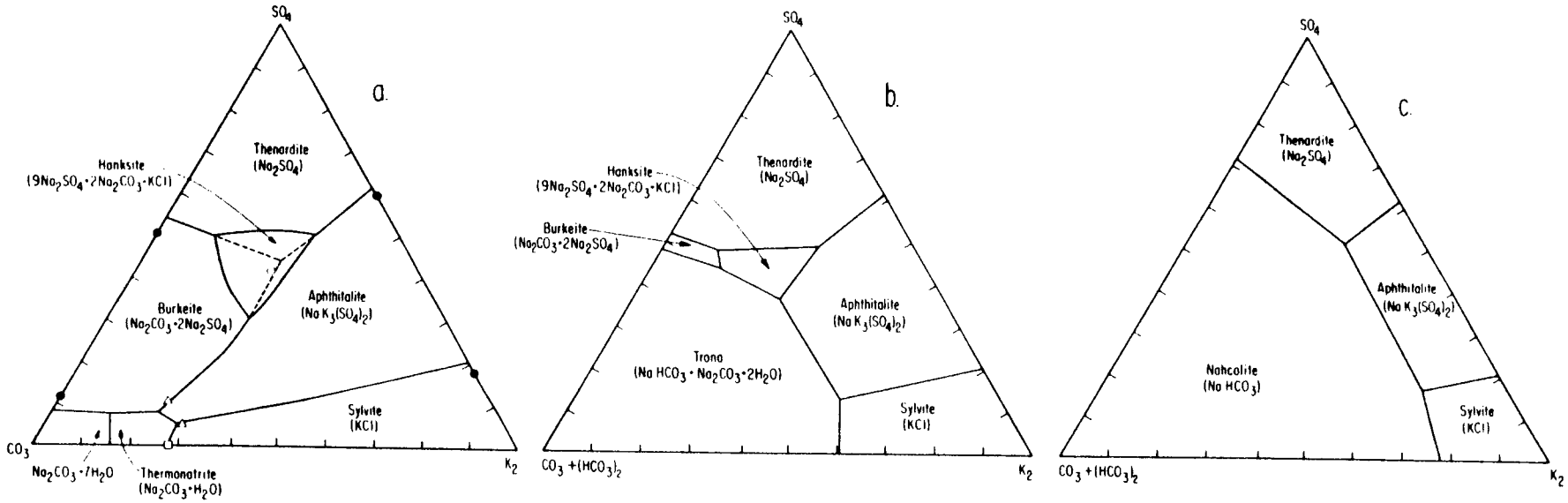
a.
SO_4
Thenardite
(Na_2SO_4)
Hanksite
($9Na_2SO_4 \cdot 2Na_2CO_3 \cdot KCl$)
Burkeite
($Na_2CO_3 \cdot 2Na_2SO_4$)
Aphthitalite
($NaK_3(SO_4)_2$)
Sylvite
(KCl)
CO_3
$Na_2CO_3 \cdot H_2O$
Thermonatrite
($Na_2CO_3 \cdot H_2O$)
K_2
b.
SO_4
Thenardite
(Na_2SO_4)
Hanksite
($9Na_2SO_4 \cdot 2Na_2CO_3 \cdot KCl$)
Burkeite
($Na_2CO_3 \cdot 2Na_2SO_4$)
Aphthitalite
($NaK_3(SO_4)_2$)
Trona
($NaHCO_3 \cdot Na_2CO_3 \cdot 2H_2O$)
Sylvite
(KCl)
$CO_3 + (HCO_3)_2$
K_2
c.
SO_4
Thenardite
(Na_2SO_4)
Aphthitalite
($NaK_3(SO_4)_2$)
Nahcolite
($NaHCO_3$)
Sylvite
(KCl)
$CO_3 + (HCO_3)_2$
K_2

Figure 16.

TABLE CAPTIONS

Table 1: Single electrolyte solution parameter values: For each cation-anion pair there are four model parameters up to three β parameters specify the ionic strength dependence of the second virial coefficients, $B_{ca}(I)$, via Eqs. (5). (Dashes indicate zeros below.) A constant third virial coefficient is used as a fourth parameter to describe the thermodynamic behavior at high concentrations, when necessary. When Eqs. (3) are simplified for single electrolyte solutions, only four model parameters for the particular cation-anion pair remain. When available, data in single electrolyte solutions are used to evaluate these parameters. (See Pitzer and Mayorga (1973, 1974) for details.)

Table 2: Common-ion two electrolyte parameter values: For each cation-cation and each anion-anion pair, a single θ parameter is specified, if necessary. (Dashes indicate zeros below.) For each anion-anion-cation and each cation-cation-anion triplet a simple ψ parameter is used to describe the high concentration behavior, when necessary. When Eqs. (3) are simplified for common-ion ternary solutions (e.g., NaCl-KCl-H_2O), only one θ and one ψ parameter (in addition to some single electrolyte parameters) remain. The θ parameter must be choosen uniquely for all solutions containing the anion-anion or cation-cation pair. When available, these parameters are evaluated from data in common-ion ternary solutions.

Table 3: Neutral-ion parameter values. For each neutral-ion pair, one model parameter is used in Eqs. (3), when necessary, to describe the experimental data.

Table 4: Values for the standard chemical potentials of the aqueous solution species and minerals: A single (unitless) parameter is specified for each model species and mineral. Many salt chemical potentials had to be evaluated in systems more complex than common-ion ternary (e.g. Polyhalite). However, the composition dependence of such a salt's solubility depends on the trends predicted by the solution model which is parameterized in simple systems. (i.e., one parameter, μ^0/RT must fit many solubility date points.) Equilibrium constants may be calculated from these data using the equation, $\ell n\ K = -\sum \nu_i (\mu_i^o/RT)$, where ν_i are the stochiometric coefficients for the reaction.

Table 5: Comparison of the calculated and experimental water activities and equilibrium P_{CO_2} pressures for solutions in equilibrium with the specified phase assemblages in the $Na\text{-}Cl\text{-}HCO_3\text{-}CO_3\text{-}CO_2\text{-}H_2O$ system at 25^oC. The data cited are those of Hatch (1972) and Eugster (1966).

Table 6: pK_w in seawater at various salinities. The data for pK_w and γ_H^{NBS} are those cited by Culberson and Pytkowicz (1973) (converted from molarity to molality units). γ_N^{NBS} is the total hydrogen ion activity coefficient defined by the convention, $pH(NBS) = -\log_{10} a_H$. γ_H^M is the hydrogen ion activity coefficient defined using the extended MacInnes convention, Eq. (14d). pH is calculated using Eq. (17).

Table 7: pK_1' and pK_2' calculated from a fit of Hansson's data[6] (all pK's are in terms of molality; γ_H is in the MacInnes convention and is in terms of molality. Mehrbach's results[7] are interpolated and corrected for HF).

Table 8: The composition of artificial 35 salinity seawater used in the calculations for this article. Also given are the total ion activity coefficients calculated with the extended MacInnes ion activity coefficient convention (Eq. (14d)). The solution given is in equilibrium with a CO_2 pressure of 3.3×10^{-4} atm. Units are in moles/kg H_2O. Neutral activity coefficients can be calculated using the formula Eq. (A8) in Appendix A, i.e. $\gamma^{\pm}_{CaCO_3} = [(.23)(.035)]^{\frac{1}{2}}$. The concentrations and activity coefficients are cited to high accuracy to facilitate program verification. See Harvie et al. (1982) for tables which are also useful in this regard.

Table 9: Numerical values of $J_0(x)$ and $J_0'(x)$ for use in the evaluation of E_θ and $E_{\theta'}$ Coefficients to be used in recursion formulae for calculating these values for arbitrary x are also given.

Table 1.

Cation	Anion	$\beta^{(0)}_{ca}$	$\beta^{(1)}_{ca}$	$\beta^{(2)}_{ca}$	C^{ϕ}_{ca}
Na	Cl	.0765	.2664	-	.00127
Na	SO_4	.01958	1.113	-	.00497
Na	HSO_4	.0454	.398	-	-
Na	OH	.0864	.253	-	.0044
Na	HCO_3	.0277	.0411	-	-
Na	CO_3	.0399	1.389	-	.0044
K	Cl	.04835	.2122	-	-.00084
K	SO_4	.04995	.7793	-	-
K	HSO_4	-.0003	.1735	-	-
K	OH	.1298	.320	-	.0041
K	HCO_3	.0296	-.013	-	-.008
K	CO_3	.1488	1.43	-	-.0015
Ca	Cl	.3159	1.614	-	-.00034
Ca	SO_4	.20	3.1973	-54.24	-
Ca	HSO_4	.2145	2.53	-	-
Ca	OH	-.1747	-.2303	-5.72	-
Ca	HCO_3	.4	2.977	-	-
Ca	CO_3	-	-	-	-
Mg	Cl	.35235	1.6815	-	.00519
Mg	SO_4	.2210	3.343	-37.23	.025
Mg	HSO_4	.4746	1.729	-	-
Mg	OH	-	-	-	-
Mg	HCO_3	.329	.6072	-	-
Mg	CO_3	-	-	-	-
MgOH	Cl	-.10	1.658	-	-
MgOH	SO_4	-	-	-	-
MgOH	HSO_4	-	-	-	-
MgOH	OH	-	-	-	-
MgOH	HCO_3	-	-	-	-
MgOH	CO_3	-	-	-	-
H	Cl	.1775	.2945	-	.0008
H	SO_4	.0298	-	-	.0438
H	HSO_4	.2065	.5556	-	-
H	OH	-	-	-	-
H	HCO_3	-	-	-	-
H	CO_3	-	-	-	-

Table 2.

c	c'	$\theta_{cc'}$	$\psi_{cc'Cl}$	$\psi_{cc'SO_4}$	$\psi_{cc'HSO_4}$	$\psi_{cc'OH}$	$\psi_{cc'HCO_3}$	$\psi_{cc'CO_3}$
Na	K	-.012	-.0018	-.010	-	-	-.003	.003
Na	Ca	.07	-.007	-.055	-	-	-	-
Na	Mg	.07	-.012	-.015	-	-	-	-
Na	MgOH	-	-	-	-	-	-	-
Na	H	.036	-.004	-	-.0129	-	-	-
K	Ca	.032	-.025	-	-	-	-	-
K	Mg	0.	-.022	-.048	-	-	-	-
K	MgOH	-	-	-	-	-	-	-
K	H	.005	-.011	.197	-.0265	-	-	-
Ca	Mg	.007	-.012	.024	-	-	-	-
Ca	MgOH	-	-	-	-	-	-	-
Ca	H	.092	-.015	-	-	-	-	-
Mg	MgOH	-	.028	-	-	-	-	-
Mg	H	.10	-.011	-	-.0178	-	-	-
MgOH	H	-	-	-	-	-	-	-

a	a'	$\theta_{aa'}$	$\psi_{aa'Na}$	$\psi_{aa'K}$	$\psi_{aa'Ca}$	$\psi_{aa'Mg}$	$\psi_{aa'MgOH}$	$\psi_{aa'H}$
Cl	SO_4	.02	.0014	-	-.018	-.004	-	-
Cl	HSO_4	-.006	-.006	-	-	-	-	.013
Cl	OH	-.050	-.006	-.006	-.025	-	-	-
Cl	HCO_3	.03	-.015	-	-	-.096	-	-
Cl	CO_3	-.02	.0085	.004	-	-	-	-
SO_4	HSO_4	-	-.0094	-.0677	-	-.0425	-	-
SO_4	OH	-.013	-.009	-.050	-	-	-	-
SO_4	HCO_3	.01	-.005	-	-	-.161	-	-
SO_4	CO_3	.02	-.005	-.009	-	-	-	-
HSO_4	OH	-	-	-	-	-	-	-
HSO_4	HCO_3	-	-	-	-	-	-	-
HSO_4	CO_3	-	-	-	-	-	-	-
OH	HCO_3	-	-	-	-	-	-	-
OH	CO_3	.10	-.017	-.01	-	-	-	-
HCO_3	CO_3	-.04	.002	.012	-	-	-	-

Table 3.

i	$\lambda_{CO_2,i}$	$\lambda_{CaCO_3,i}$	$\lambda_{MgCO_3,i}$
H	0	-	-
Na	.100	-	-
K	.051	-	-
Ca	.183	-	-
Mg	.183	-	-
MgOH	-	-	-
Cl	-.005	-	-
SO_4	.097	-	-
HSO_4	-.003	-	-
OH	-	-	-
HCO_3	-	-	-
CO_3	-	-	-

Table 4.

Species or Mineral	Chemical Formula	μ^0/RT
Water	H_2O	- 95.6635
Sodium Ion	Na	- 105.651
Potassium Ion	K^+	- 113.957
Calcium Ion	Ca^{+2}	- 223.30
Magnesium Ion	Mg^{+2}	- 183.468
Magnesium Hydroxide Ion	$MgOH^+$	- 251.94
Hydrogen Ion	H^+	0.
Chloride Ion	Cl^-	- 52.955
Sulfate Ion	SO_4^{-2}	- 300.386
Bisulfate Ion	HSO_4^-	- 304.942
Hydroxide Ion	OH^-	- 63.435
Bicarbonate Ion	HCO_3^-	- 236.751
Carbonate Ion	CO_3^{-2}	- 212.944
Aq. Calcium Carbonate	$CaCO_3^0$	- 443.5
Aq. Magnesium Carbonate	$MgCO_3^0$	- 403.155
Aq. Carbon Dioxide	CO_2^0	- 155.68
Carbon Dioxide Gas	CO_2 (gas)	- 159.092
Anhydrite	$CaSO_4$	- 533.73
Aphthitalite (Glaserite)	$NaK_3(SO_4)_2$	-1057.05
Antarcticite	$CaCl_2 \cdot 6H_2O$	- 893.65
Aragonite	$CaCO_3$	- 455.17
Arcanite	K_2SO_4	- 532.39
Bischofite	$MgCl_2 \cdot 6H_2O$	- 853.1
Bloedite	$Na_2Mg(SO_4)_2 \cdot 4H_2O$	-1383.6
Brucite	$Mg(OH)_2$	- 335.4
Burkeite	$Na_6CO_3(SO_4)_2$	-1449.4
Calcite	$CaCO_3$	- 455.6
Calcium Chloride Tetrahydrate	$CaCl_2 \cdot 4H_2O$	- 698.7
Calcium Oxychloride A	$Ca_4Cl_2(OH)_6 \cdot 13H_2O$	-2658.45
Calcium Oxychloride B	$Ca_2Cl_2(OH)_2 \cdot H_2O$	- 778.41
Carnallite	$KMgCl_3 \cdot 6H_2O$	-1020.3
Epsomite	$MgSO_4 \cdot 7H_2O$	-1157.83
Gaylussite	$CaNa_2(CO_3)_2 \cdot 5H_2O$	-1360.5
Glauberite	$Na_2Ca(SO_4)_2$	-1047.45
Gypsum	$CaSO_4 \cdot 2H_2O$	- 725.56
Halite	$NaCl$	- 154.99
Hexahydrite	$MgSO_4 \cdot 6H_2O$	-1061.60
Kainite	$KMgClSO_4 \cdot 3H_2O$	- 938.2
Kalicinite	$KHCO_3$	- 350.06
Hieserite	$MgSO_4 \cdot H_2O$	- 579.80
Labile Salt	$Na_4Ca(SO_4)_3 \cdot 2H_2O$	-1751.45
Leonite	$K_2Mg(SO_4)_2 \cdot 4H_2O$	-1403.97
Magnesite	$MgCO_3$	- 414.45
Magnesium Oxychloride	$Mg_2Cl(OH)_3 \cdot 4H_2O$	-1029.6
Mercallite	$KHSO_4$	- 417.57
Mirabilite	$Na_2SO_4 \cdot 10H_2O$	-1471.15
Misenite	$K_8H_6(SO_4)_7$	-3039.24
Nacholite	$NaHCO_3$	- 343.33
Natron	$Na_2CO_3 \cdot 10H_2O$	-1382.78
Nesquehonite	$MgCO_3 \cdot 3H_2O$	- 695.3
Picromerite (Schoenite)	$K_2Mg(SO_4)_2 \cdot 6H_2O$	-1596.1
Pirssonite	$Na_2Ca(CO_3)_2 \cdot 2H_2O$	-1073.1
Polyhalite	$K_2MgCa_2(SO_4)_4 \cdot 2H_2O$	-2282.5
Portlandite	$Ca(OH)_2$	- 362.12
Potassium Carbonate	$K_2CO_3 \cdot 3/2\ H_2O$	- 577.37
Potassium Sesquicarbonate	$K_8H_4(CO_3)_6 \cdot 3\ H_2O$	-2555.4
Potassium Sodium Carbonate	$KNaCO_3 \cdot 6H_2O$	-1006.8
Potassium Trona	$K_8NaH(CO_3)_2 \cdot 2H_2O$	- 971.74
Sesquipotassium Sulfate	$K_3H(SO_4)_2$	- 950.8
Sesquisodium Sulfate	$Na_3H(SO_4)_2$	- 919.6
Sodium Carbonate Heptahydrate	$Na_2CO_3 \cdot 7H_2O$	-1094.95
Sylvite	KCl	- 164.84
Syngenite	$K_2Ca(SO_4)_2 \cdot H_2O$	-1164.8
Tachyhydrite	$Mg_2CaCl_6 \cdot 12H_2O$	-2015.9
Thenardite	Na_2SO_4	- 512.35
Thermonatrite	$Na_2CO_3 \cdot H_2O$	- 518.8
Trona	$Na_3H(CO_3)_2 \cdot 2H_2O$	- 960.38

Table 5.

	a_{H_2O}		$P_{CO_2} \times 10^3$		
	calc	Hatch	calc	Eugster	Hatch
$Na\text{-}HCO_3\text{-}CO_3\text{-}H_2O$ + Nacholite + Trona	.906	.899-.903	1.87	1.80-1.95	2.02
$Na\text{-}HCO_3\text{-}CO_3\text{-}H_2O$ + Natron + Trona	.888	.868-.872	.37	-	.30-.34
$Na\text{-}HCO_3\text{-}CO_3\text{-}Cl\text{-}H_2O$ + Nacholite + Trona + Halite	.746	.765-.771	1.54	1.45-1.60	1.72-1.77
Solution + Natron + $Na_2CO_3 \cdot 7H_2O$	.756	.756*			
Solution + Thermonatrite + $Na_2CO_3 \cdot 7H_2O$	.697	.705*			

*Extrapolated to 25°C by Hatch

Table 6.

Salinity	19.90	26.87	34.82	44.0
pK_w^*(exp)	13.31-13.32	13.24-13.25	13.19	13.12
pK_w(calc)	13.32	13.25	13.19	13.12
γ_H^{NBS}(exp)	.695-.698	.694-.696	.702-.704	.719-.723
γ_H^M(calc)	.630	.623	.624	.632
ΔpH	.043-.044	.047-.048	.051-.052	.056-.058

$^*K_w = \bar{m}_H \bar{m}_{OH}$ (molality)^2

Table 7: pK_1' and pK_2' calculated from a fit of Hansson's data[6] (all pK's are in terms of molality; γ_H is in the MacInnes convention and is in terms of molality. Mehrbach's results[7] are interpolated and corrected for HF).

Salinity (‰)	γ_H^M	pK_1' (calc)	pK_1' (Mehrbach)	pK_1' (Hansson)	pK_2' (calc)	pK_2' (Mehrbach)	pK_2' (Hansson)
20	.631	5.893	5.920	5.921	9.133	9.130	9.117
25	.625	5.865	5.882	5.892	9.064	9.060	9.052
30	.624	5.842	5.860	5.866	9.006	9.000	8.987
35	.625	5.823	5.833	5.842	8.956	8.949	8.932
40	.629	5.808	5.810	5.831	8.911	8.896	8.883

(a) $K_1' = \frac{(H_T)(HCO_3)}{(CO_2 aq.)}$; $K_2' = \frac{(H_T)(CO_{3\ T})}{(HCO_3)}$ (concentration products) molality units

Table 8.

i	m_i	γ_i^T
Na	.48695	.706
K	.01063	.651
Ca	.01073	.229
Mg	.05516	.251
H	-	.622
Cl	.56817	.623
SO_4	.02939	.0864
OH	-	.243
HCO_3	.00185	.547
CO_3	.000276	.0346
CO_2	9.63×10^{-6}	1.13

$P_{CO_2} = 3.3 \times 10^{-4}$, $-\log_{10} a_H^M = 8.31$ $a_{H_2O} = .981$

Table 9.

x	$J_0(x)$	$J_0'(x)$	x	$J_0(x)$	$J_0'(x)$	k	a_k^I	a_k^{II}
.001	.0000011	.0019995	1.	.1164372	.1605270	0	1.925154014814667	.628023320520852
.002	.0000039	.0035423	2.	.2941608	.1906055	1	-.060076477753119	.462762985338493
.003	.0000081	.0049155	3.	.4928728	.2053288	2	-.029779077456514	.150044637187895
.004	.0000137	.0061797	4.	.7029335	.2142383	3	-.007299499690937	-.028796057604906
.005	.0000204	.0073637	5.	.9203539	.2202491	4	.000388260636404	-.036552745910311
.006	.0000284	.0084844	6.	1.1428807	.2245887	5	.000636874599598	-.001668087945272
.007	.0000374	.0095530	7.	1.3691818	.2278717	6	.000036583601823	.006519840398744
.008	.0000475	.0105773	8.	1.5983881	.2304424	7	-.000045036975204	.001130378079086
.009	.0000585	.0115631	9.	1.8298996	.2325094	8	-.000004537895710	-.000887171310131
.01	.0000706	.0125152	10.	2.0632842	.2342068	9	.000002937706971	-.000242107641309
.02	.0002385	.0207375	20.	4.4545334	.2423131	10	.000000396566462	.000087294451594
.03	.0004805	.0274726	30.	6.8936620	.2451349	11	-.000000202099617	.000034682122751
.04	.0007849	.0332963	40.	9.3526983	.2465347	12	-.000000025267769	-.000004583768938
.05	.0011443	.0384752	50.	11.8224798	.2473574	13	.000000013522610	-.000003548684306
.06	.0015528	.0431628	60.	14.2989031	.2478926	14	.000000001229405	-.000000250453880
.07	.0020062	.0474583	70.	16.7797953	.2482652	15	-.000000000821969	.000000216991779
.08	.0025009	.0514306	80.	19.2638760	.2485377	16	-.000000000050847	.000000080779570
.09	.0030339	.0551303	90.	21.7503315	.2487445	17	.000000000046333	.000000004558555
.1	.0036027	.0585959	100.	24.2386152	.2489060	18	.000000000001943	-.000000006944757
.2	.0108818	.0849528	200.	49.1709892	.2495706	19	-.000000000002563	-.000000002849257
.3	.0203209	.1028780	300.	74.1388190	.2497568	20	-.000000000010991	.000000000237816
.4	.0313124	.1163918	400.	99.1190695	.2498389			
.5	.0435081	.1271498	500.	124.1053878	.2498835			
.6	.0566797	.1360164	600.	149.0952050	.2499108			
.7	.0706657	.1435049	700.	174.0872555	.2499290			
.8	.0853459	.1499461	800.	199.0808333	.2499418			
.9	.1006276	.1555663	900.	224.0755097	.2499512			